Electrons in graphene and twisted bilayer graphene

from band structure theory to the correlated phase diagram

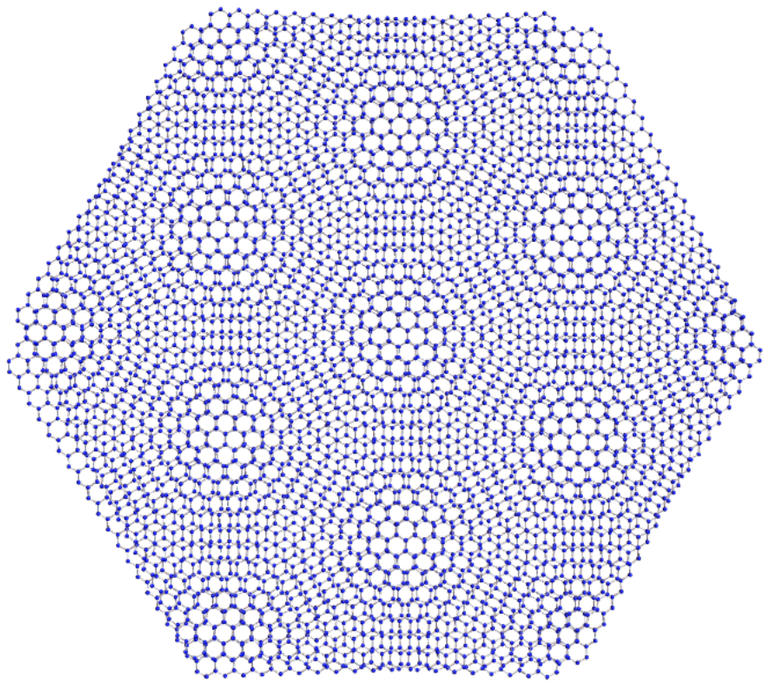

Michael M. Scherer

Institute for Theoretical Physics, Cologne University

Contents

1. Introduction and background

1.1. Solid state physics

▷ solid-state/condensed matter physics

↳ one of the most active/versatile branches of modern physics

↳ fundamental questions and technological applications

↳ general task: deal with system with many degrees of freedom

▷ Solid: atomic nuclei (ions) often arranged on regular (elastic) lattice, and of electrons:

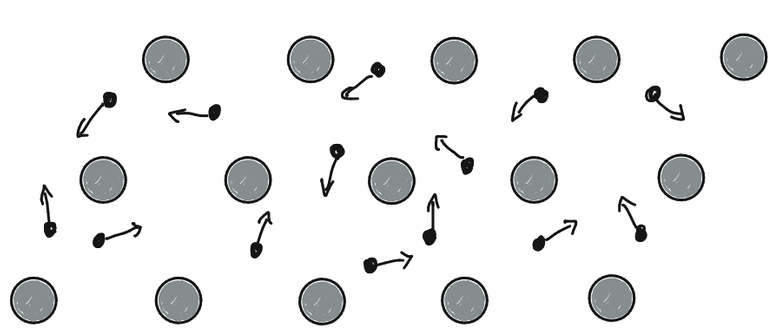

↳ description of the system via laws of quantum mechanics

↳ Hamiltonian for ions and electrons:

$$\hat{H} = \sum_i \frac{\vec{p}^2}{2m} + \frac{1}{2}\sum_{i\neq i'} \frac{e^2}{|\vec{r}_i - \vec{r}_{i'}|} + \sum_j \frac{\vec{P}_j}{2M_j} + \frac{1}{2}\sum_{j\neq j'} \frac{Z_j Z_{j'} e^2}{|\vec{R}_j - \vec{R}_{j'}|} - \sum_{i,j} \frac{Z_j e^2}{|\vec{r}_i - \vec{R}_j|} \qquad (1\text{-}1)$$

(e: elementary charge; m: free electron mass; M_j: mass of j-th nucleus)

▷ scales:

↳ microscopic length scale: Bohr radius $a_B = \frac{\hbar^2}{me^2} \approx 0.5 \cdot 10^{-10}\,m$

↳ energy scale: Hartree $\frac{e^2}{a_B} \approx 27\,eV \ll$ rest mass of electron ($\sim 0.5\,MeV$)

↳ energy scales in physics:

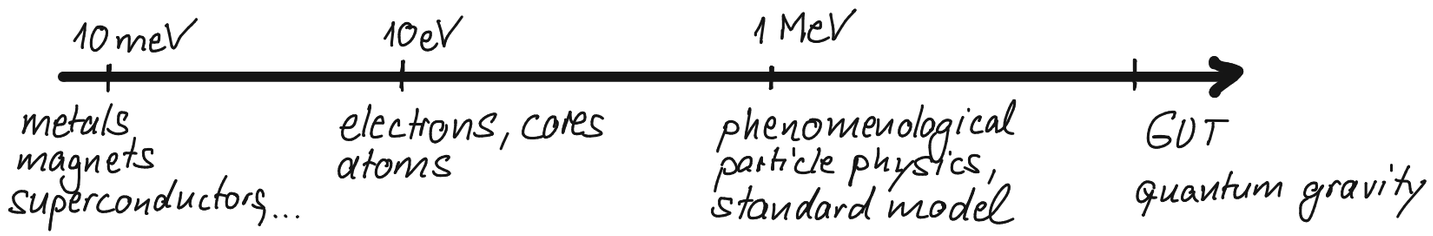

↳ in solid state physics: phenomena at room temperature ($T \sim 300K$) and below

⇝ characteristic energies: $E \sim k_B T \sim 0.03\,eV = 30\,meV \ll$ 1 Hartree

▷ goal in solid state physics: describe low-energy properties starting from eq. (1-1)

↳ rich phenomenology: metals, semiconductors, insulators, magnets, superconductors, charge ordering, quantum Hall effect(s), ...

↳ many <u>interacting</u> d.o.f. make description difficult

↳ need to understand fundamental concepts to formulate effective (reduced) theories!

1.2. Electrons in crystals

▷ many solids ⇝ periodic arrangement of atoms ⇝ crystal

↳ electrons moving in crystal feel periodic potential of ion lattice

↳ energy spectrum from delocalized eigenstates of Schrödinger equation

⇝ formation of bands of allowed energies and gaps of forbidden energies

▷ band structure theory

↳ two limiting starting points to describe band formation

(1) nearly-free electron approximation:

- free electron gas perturbed by periodic potential ⇝ breaks up continuous spectrum

(2) tight-binding approximation:

- independent atoms brought together ⇝ overlapping outer electron shells

↳ assumptions: description possible in terms of "single electron states"

⇝ electrons do not dynamically interact with other electrons, lattice vibrations, ...

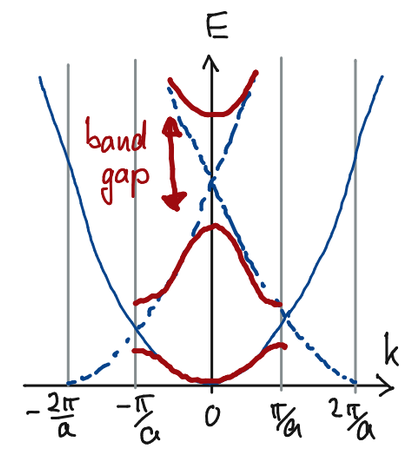

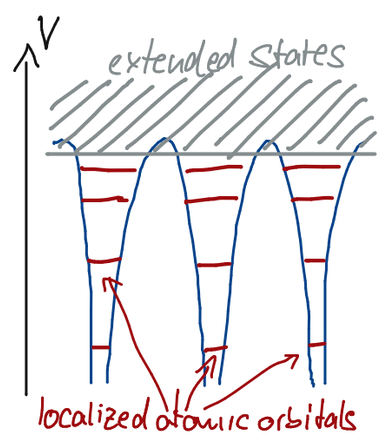

▷ filling of bands accounts for (semi-)metallic, semiconducting, (band) insulating behavior

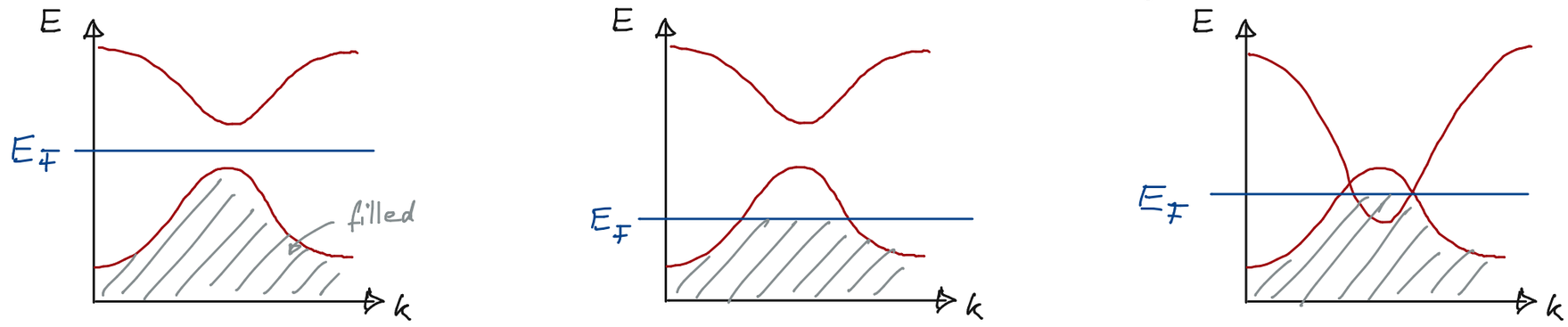

↳ successful description of many (technologically important) materials (Si, Ge, GaAs, InAs, ...)

↳ beautiful yet exotic example for successful band theory : graphene (2D crystal)

- free electron $H_{kin} \sim \frac{p^2}{2m}$ —band theory→ electron in graphene $H_{kin} \sim v_F \begin{pmatrix} \vec{\sigma}\cdot\vec{p} & 0 \\ 0 & -\sigma^*\cdot\vec{p} \end{pmatrix}$

- electrons in graphene are described by 2D Dirac-Weyl Hamiltonian

↳ justification that this still works in presence of interactions ⇝ Fermi-liquid theory

▷ band / Fermi liquid theory fails for strongly-correlated (quantum) materials

↳ such materials cannot be understood in terms of single-electron states

↳ need to take into account electron-electron interactions ⇝ difficult! interesting?

↳ beautiful yet exotic example for str.-corr. material: twisted bilayer graphene

1.3. Strongly-correlated (quantum) materials/systems

▷ electron-electron interactions important ↝ delicate interplay between

↳ kinetic energies (bands), Coulomb repulsion, crystalline lattice, Fermi statistics, ...

↳ band theory is either bad starting point or strongly renormalized

↳ qualitatively new behavior: high-T_c superconductors, exotic magnets, bad metals, ...

▷ standard paradigm: energy bands + (Coulomb) interactions

↝ Hubbard model (+ extensions)

▷ examples:

(1) high-temperature superconductors (cuprates, pnictides, ...)

(2) cold atoms as quantum simulators of correlated systems

(3) quark-gluon plasma ↝ QCD phase diagram

(4) moiré materials (twisted bilayer graphene, twisted transition metal dichalcogenides)

↑ new kid on the block!

1.3.1. High-temperature/unconventional superconductors

- first discovery in copper oxides/cuprates in 1986 by Bednorz and Müller (Nobel prize 1987)
- cuprate: layered material with CuO_2 planes separated by layers w/ La, Ba, Sr ions
- unconventional superconductivity ↝ does not conform to conventional BCS theory
  ↝ superconducting order w/ unconventional symmetry
- high-T_c cuprates:
  - ↳ starting point: magnetic insulator (not described by band theory)
  - ↳ add/remove charge carriers by doping
    - ↝ expect: poor conductor
    - ↝ observation:

      superconductivity at $T_c \sim 100K$!
  - ↳ such materials contain impurities/dirt
    - ↝ challenging to study (chemical doping, ...)

typical cuprate phase diagram

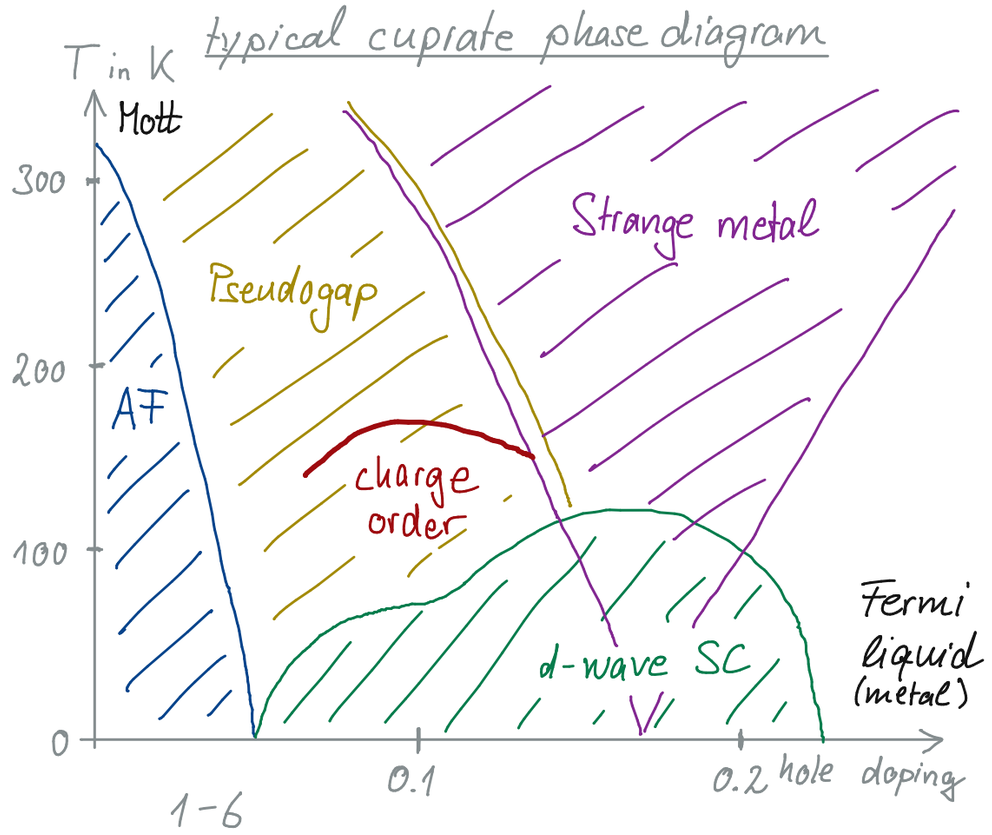

BSCCO
(used in LHC at CERN)

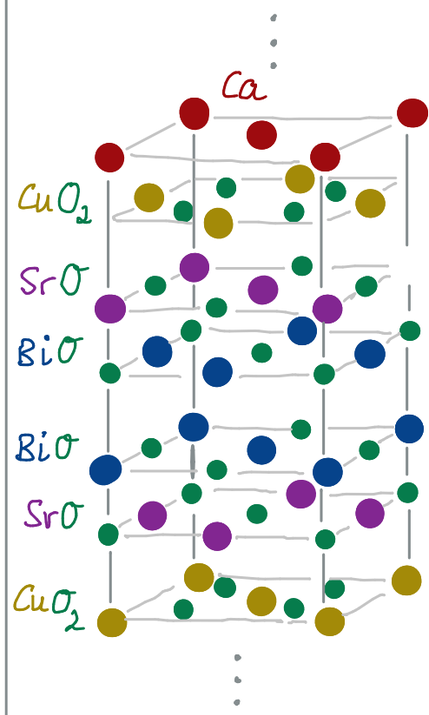

lattice length ~ Å

1.3.2. Cold atoms as quantum simulators of correlated materials

▷ alternative platform to study correlated materials

↳ Base - Einstein condensation in Rb cold atom gas (1995) (Nobel prize 2001)

↳ condensation of cold Fermi gases ⇝ superfluidity

▷ great progress in control and manipulation of ultracold atoms in optical lattices

↳ tune interactions precisely ⇝ tunable artificial correlated material #quantum-simulator

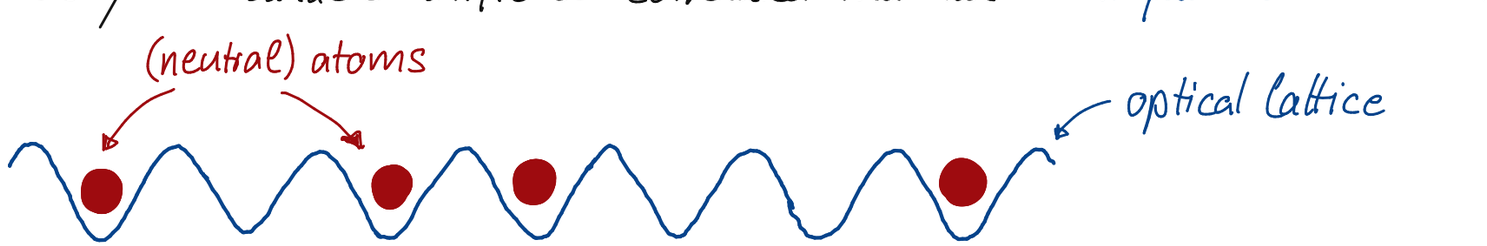

↳ realizations in 1D, 2D, 3D

↳ example. cold-atom Fermi-Hubbard antiferromagnet Mazurenko et al., Nature 545, 462 (2017)

▷ technical limitations in reaching low temperatures for superconductivity ($T \sim 1nK$)

1.3.3. Moiré quantum materials

▷ graphene ⇝ flat single layer of Carbon atoms on honeycomb lattice

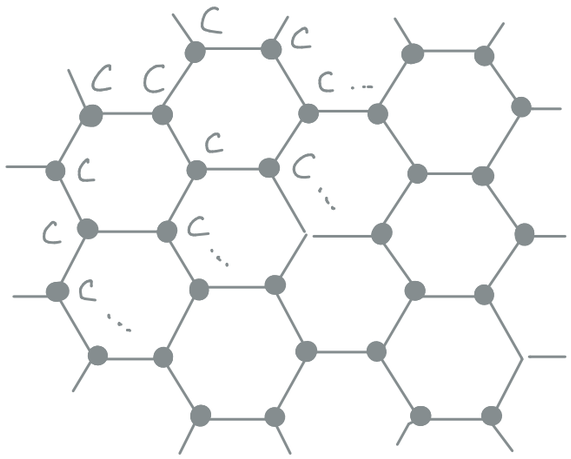

↳ excellent conductor, mechanically strong (Nobel prize 2010)

↳ band theory works ⇝ no sign of strong correlations

▷ after graphene ⇝ more 2D materials isolated and characterized

↳ hexagonal boron nitride ⇝ insulator

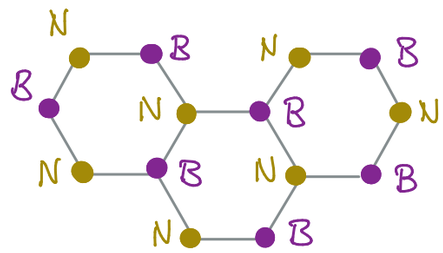

↳ MoS_2 ⇝ semi-conductor

↳ WSe_2 ⇝ semi-conductor

↳ fluorographene ⇝ insulator

▷ 2D materials can be stacked like Legos, but also at arbitrary angles!

▷ what happens when two periodic patterns with slight mismatch are brought together?

↳ rotational mismatch by <u>small</u> relative twist angle θ

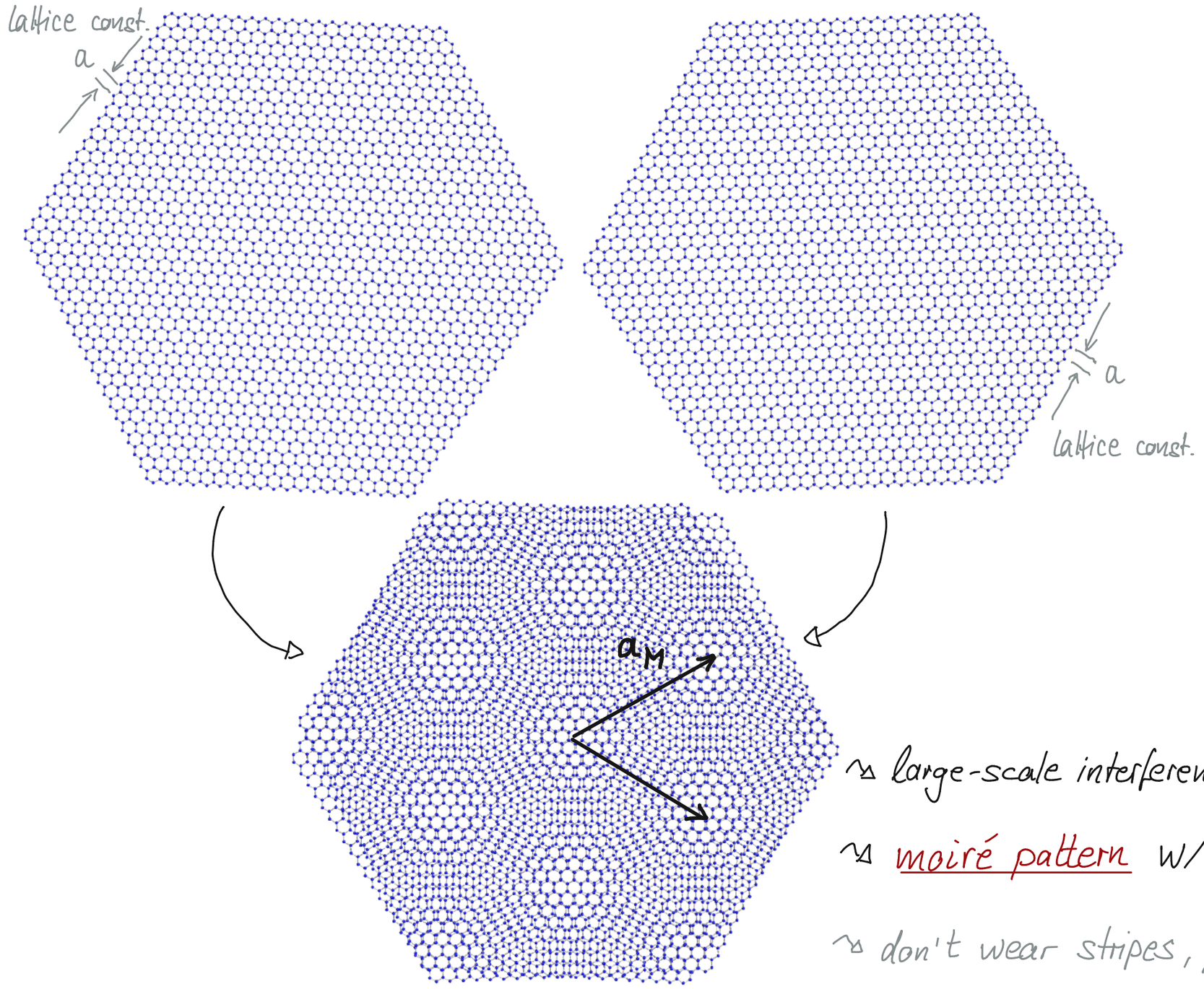

↘ large-scale interference effect

↘ <u>moiré pattern</u> w/ $a_M \gg a$

↘ don't wear stripes, you'll moiré!

▷ <u>twisted bilayer graphene (TBG) at magic angle $\theta \approx 1.1°$</u>

↳ huge moiré periodicity

↳ moiré lattice length $a_M \sim 10\,nm$

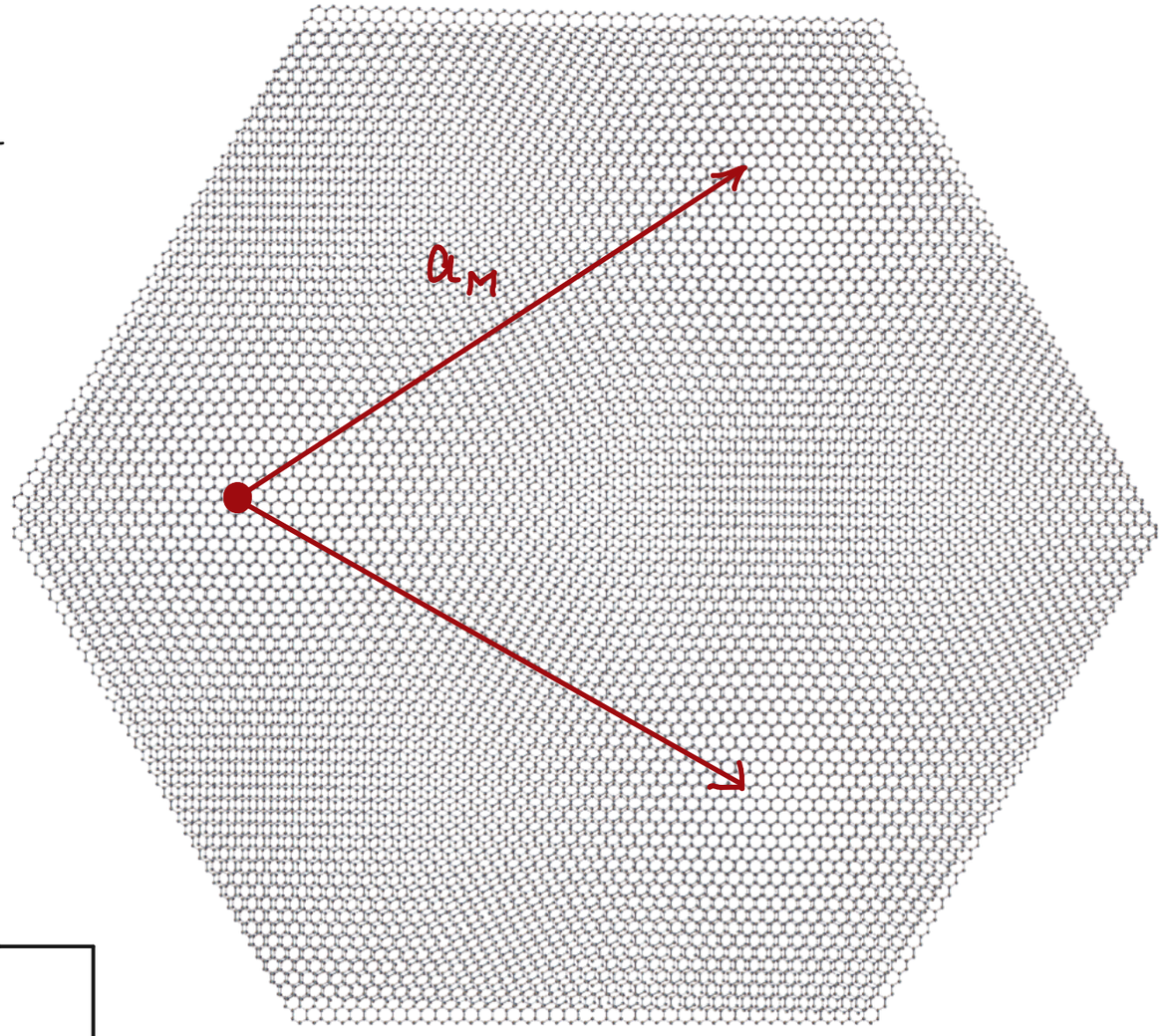

↳ experimental setup :

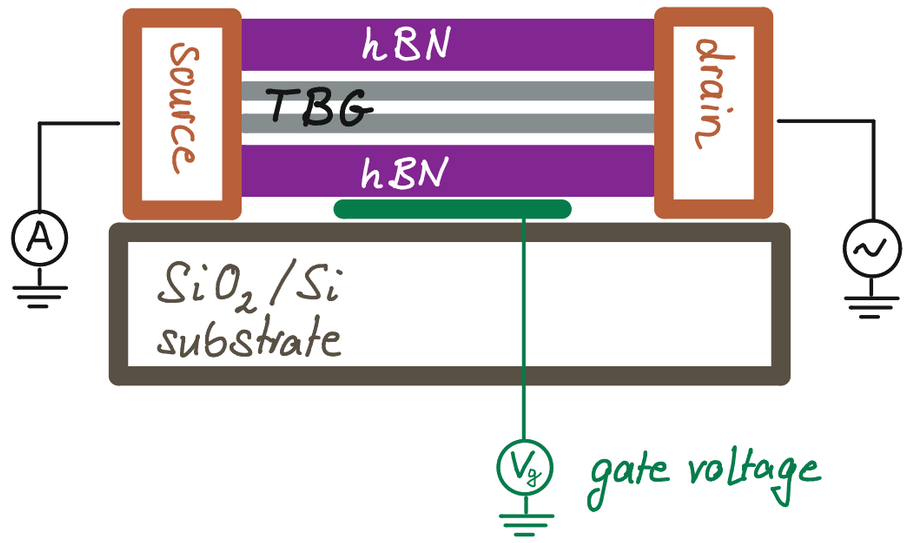

▷ phase diagram of magic-angle twisted bilayer graphene

↳▷ resistance measurements

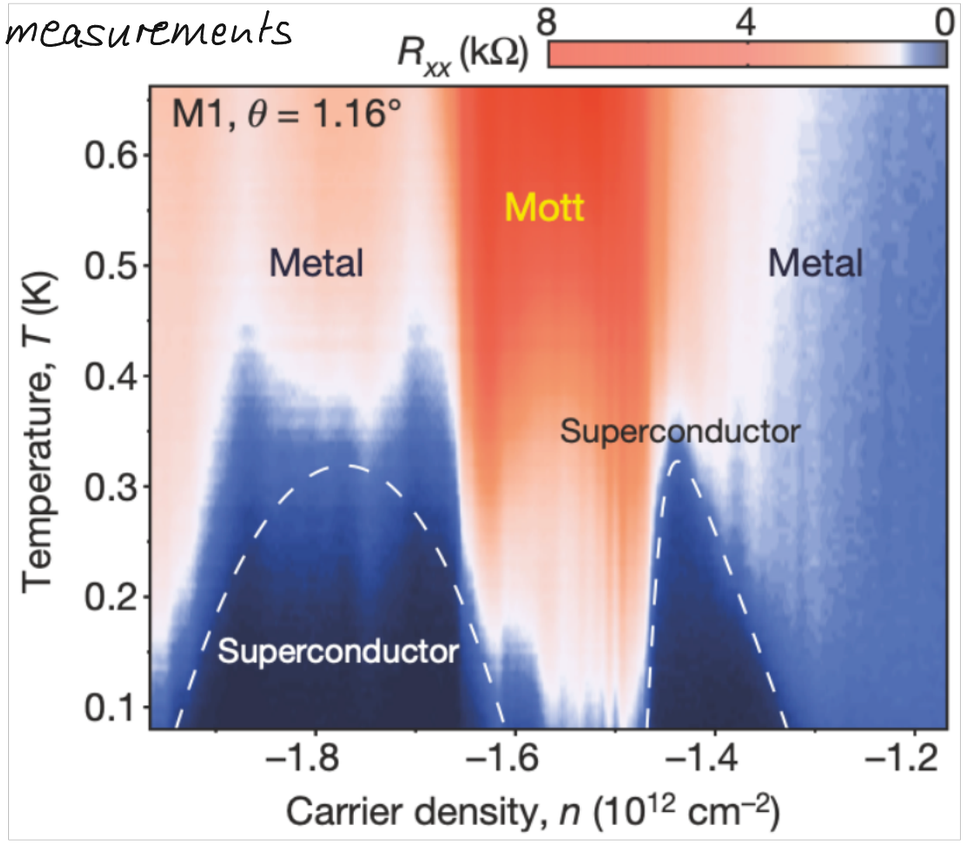

Cao et al., Nature 556, 43 (2018)

↳▷ tune carrier density *in situ* by tuning gate voltage

↳▷ insulating behavior for some carrier densities

↝ not expected within band theory ↝ induced by interactions ↝ "Mott" insulator

↳▷ superconducting domes adjacent to insulating state ($T_c \lesssim 1K$)

↳▷ striking similarity to cuprate / high-T_c superconductor phase diagram!

▷ features of magic-angle TBG

- high control of twist angle θ
- low level of disorder
- in situ tuning of carrier density (in contrast to chemical doping)
- correlated insulators and superconductivity
- other 2D materials available to stack and twist #moiré-materials
- new platform for correlated electrons

  ↳ why do we see correlated physics in TBG but not in graphene?

  ↳ what is the nature/origin of the correlated states

- promising for electronic applications
- brings together two worlds: ① graphene and ② correlated electrons

2. Crystal structure of graphene and moiré materials

2.1. Carbon atom and hybridizations

▷ C has 6 electrons in configuration $1s^2 \underbrace{2s^2 2p^2}_{\text{4 electrons in outer shell}}$

↳ excited state with 4 quantum mechanical states $|2s\rangle, |2p_x\rangle, |2p_y\rangle, |2p_z\rangle$

↳ superposition of 2s and two 2p orbitals ⇝ planar sp^2 hybridization:

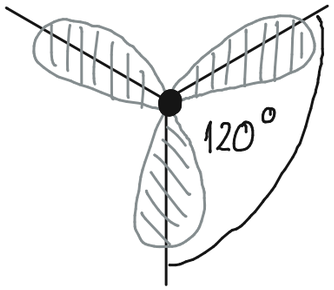

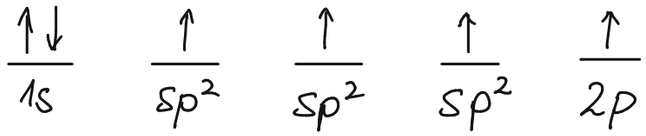

↳ formation of <u>σ bonds</u> with sp^2 orbitals from other C atoms

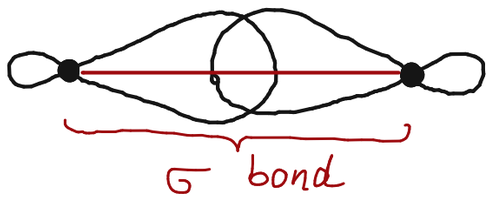

⇝ honeycomb lattice:

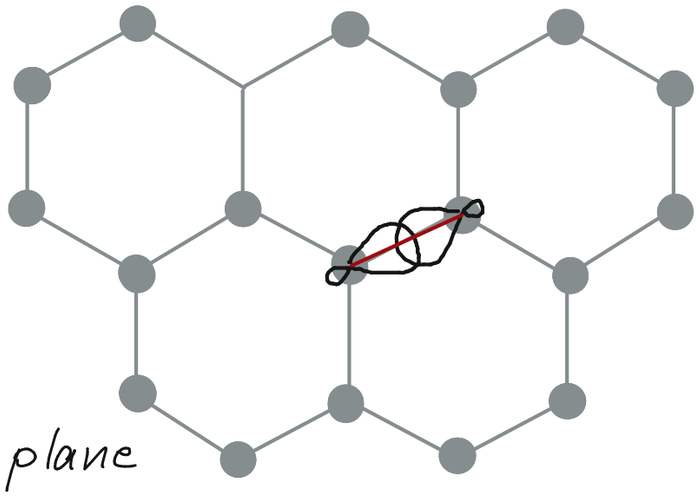

▷ remaining unhybridized p_z orbital is perpendicular to plane

↳ $2p_z$ orbitals form π bonds ⇝ delocalized over whole structure

2.2. Graphene

▷ flat single layer of C atoms arranged in 2D honeycomb lattice

↳ one-atom thick layer of graphite (1mm graphite ≈ 3,000,000 layers of graphene)

↳ basic building block of graphitic materials:

- 3D graphite
- 2D graphene
- 1D nanotubes
- 0D fullerenes

▷ properties

↳ density:
- thinnest material ever ↝ $\rho = 0.77\ mg/m^2$
- so dense that even He cannot pass through

↳ strength:
- breaking strength ~ 42 N/m
  - ↝ cf. steel ~ $10^9 N/m^2$ ⇒ 0.335nm film has 2D breaking strength ~ 0.3 N/m
- also flexible ↝ can be stretched

↳ optically transparent ↝ absorbs only 2.3% of visible light intensity

↳ thermal conductivity ↝ at room temperature conducts heat 10× better than copper

2.3. Graphene's honeycomb lattice

▷ honeycomb lattice is not Bravais lattice (i.e. two neighboring sites are not equivalent)

↳ triangular Bravais lattice with 2-atom (bipartite) basis (A and B)

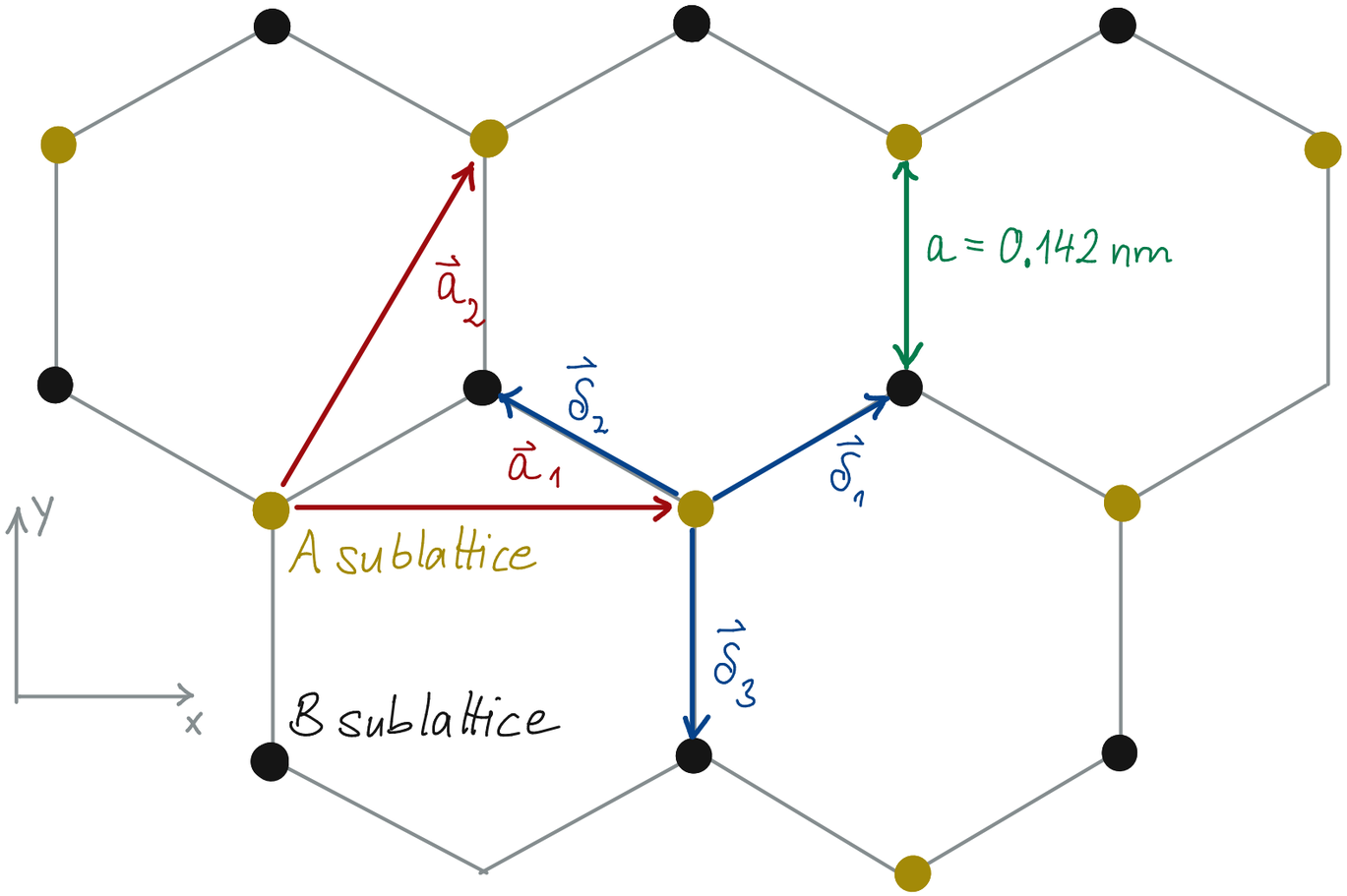

• Bravais lattice spanned by

$$\vec{a}_1 = \sqrt{3}\,a\,\vec{e}_x = a'\begin{pmatrix}1\\0\end{pmatrix} \qquad (2\text{-}3A)$$

$$\vec{a}_2 = \frac{\sqrt{3}\,a}{2}\left(\vec{e}_x + \sqrt{3}\,\vec{e}_y\right) = \frac{a'}{2}\begin{pmatrix}1\\\sqrt{3}\end{pmatrix} \qquad (2\text{-}3B)$$

• nearest-neighbor bond vectors

$$\vec{\delta}_1 = \frac{a}{2}\left(\sqrt{3}\,\vec{e}_x + \vec{e}_y\right) \qquad (2\text{-}3C)$$

$$\vec{\delta}_2 = \frac{a}{2}\left(-\sqrt{3}\,\vec{e}_x + \vec{e}_y\right) \qquad (2\text{-}3D)$$

$$\vec{\delta}_3 = -a\,\vec{e}_y \qquad (2\text{-}3E)$$

▷ lattice constant $a' = \sqrt{3}\,a = 0.246\,\text{nm}$ (2-3F)

↳ unit cell area $A_{uc} = 0.051\,\text{nm}^2$

↳ one π electron per C site ↝ density $n_\pi = 3.9 \cdot 10^{15}\,\text{cm}^{-2}$ ≠ carrier density (later!)

2.4. Graphene's reciprocal lattice

▷ reciprocal lattice is defined w.r.t. triangular Bravais lattice

↳ relation $\vec{a}_i \cdot \vec{a}_j^{\,*} = 2\pi\delta_{ij}$ where $i,j \in \{1,2\}$

↳ spanned by basis vectors

$$\vec{a}_1^{\,*} = \frac{2\pi}{\sqrt{3}a}\left(\vec{e}_x - \frac{1}{\sqrt{3}}\vec{e}_y\right) \qquad (2\text{-}4A)$$

$$\vec{a}_2^{\,*} = \frac{4\pi}{3a}\vec{e}_y \qquad (2\text{-}4B)$$

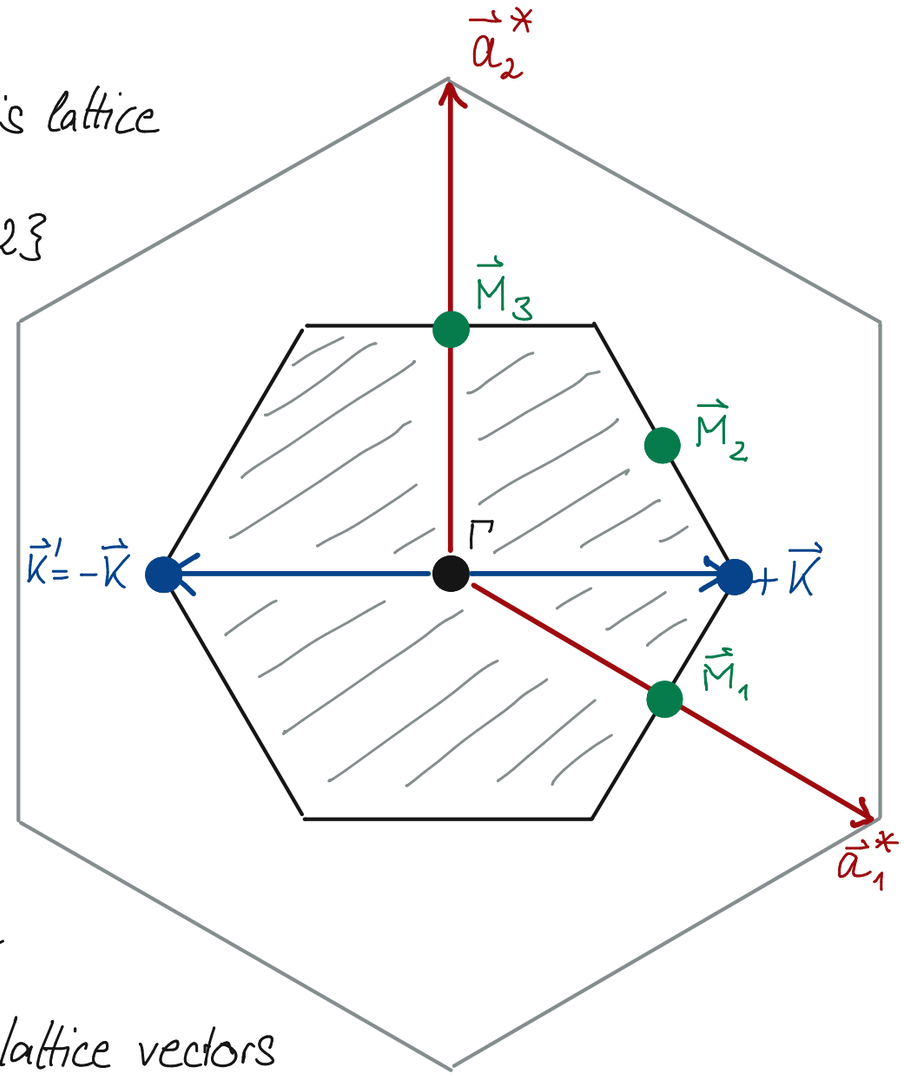

▷ 1st Brillouin zone (BZ, shaded area)

↳ set of inequivalent points in reciprocal space

↳ points which are not connected by reciprocal lattice vectors

↳ 6 corners of BZ consist of inequivalent points K, K': $\pm\vec{K} = \pm\frac{4\pi}{3\sqrt{3}a}\vec{e}_x$ (2-4C)

- 4 remaining corners connected to K, K' by reciprocal lattice vector

↳ further crystallographic points: M_1, M_2, M_3

2.5. Bilayer stacks of graphene

▷ AA stacking

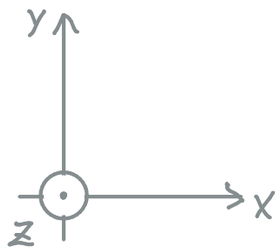

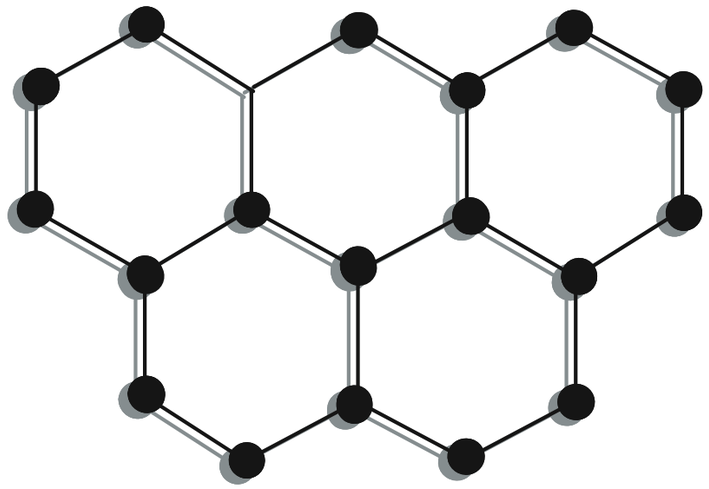

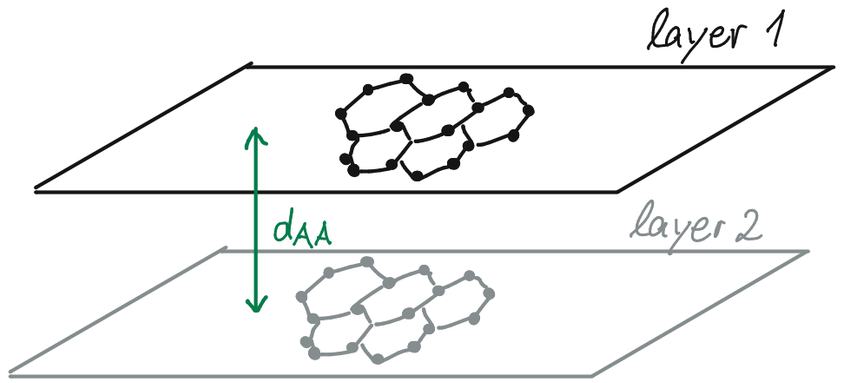

↳ interlayer distance $d_{AA} = 0.360\,nm$ (2-5A)

▷ AB stacking

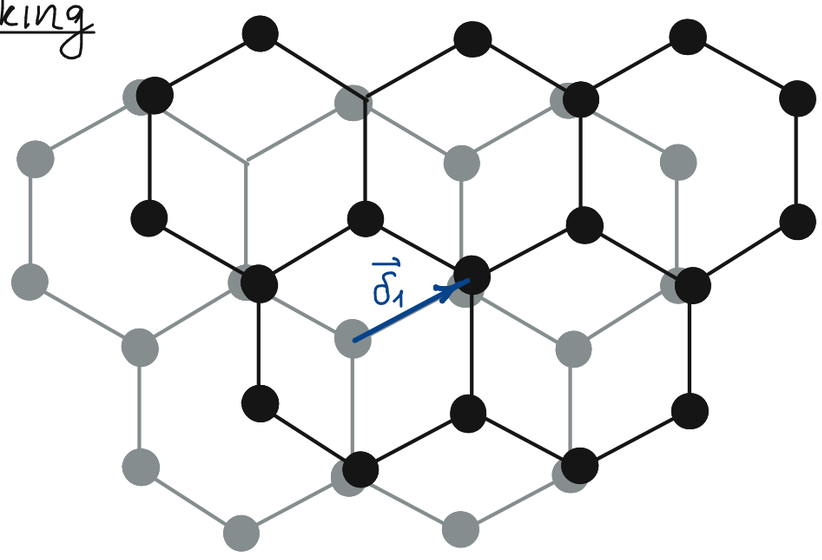

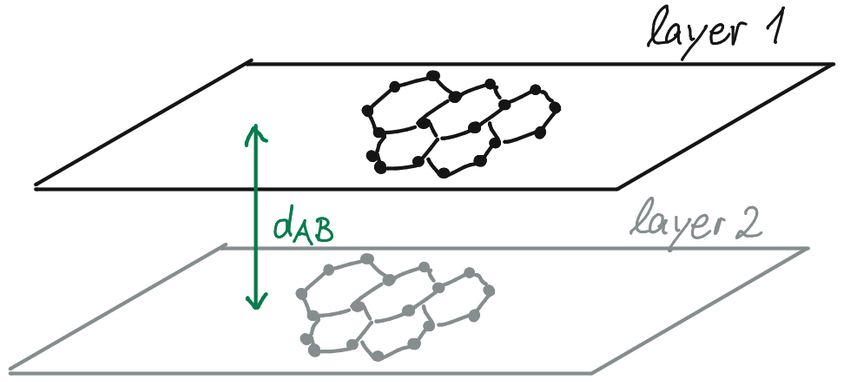

↳ interlayer distance $d_{AB} = 0.335\,nm$ (2-5B)

▷ AA stacking

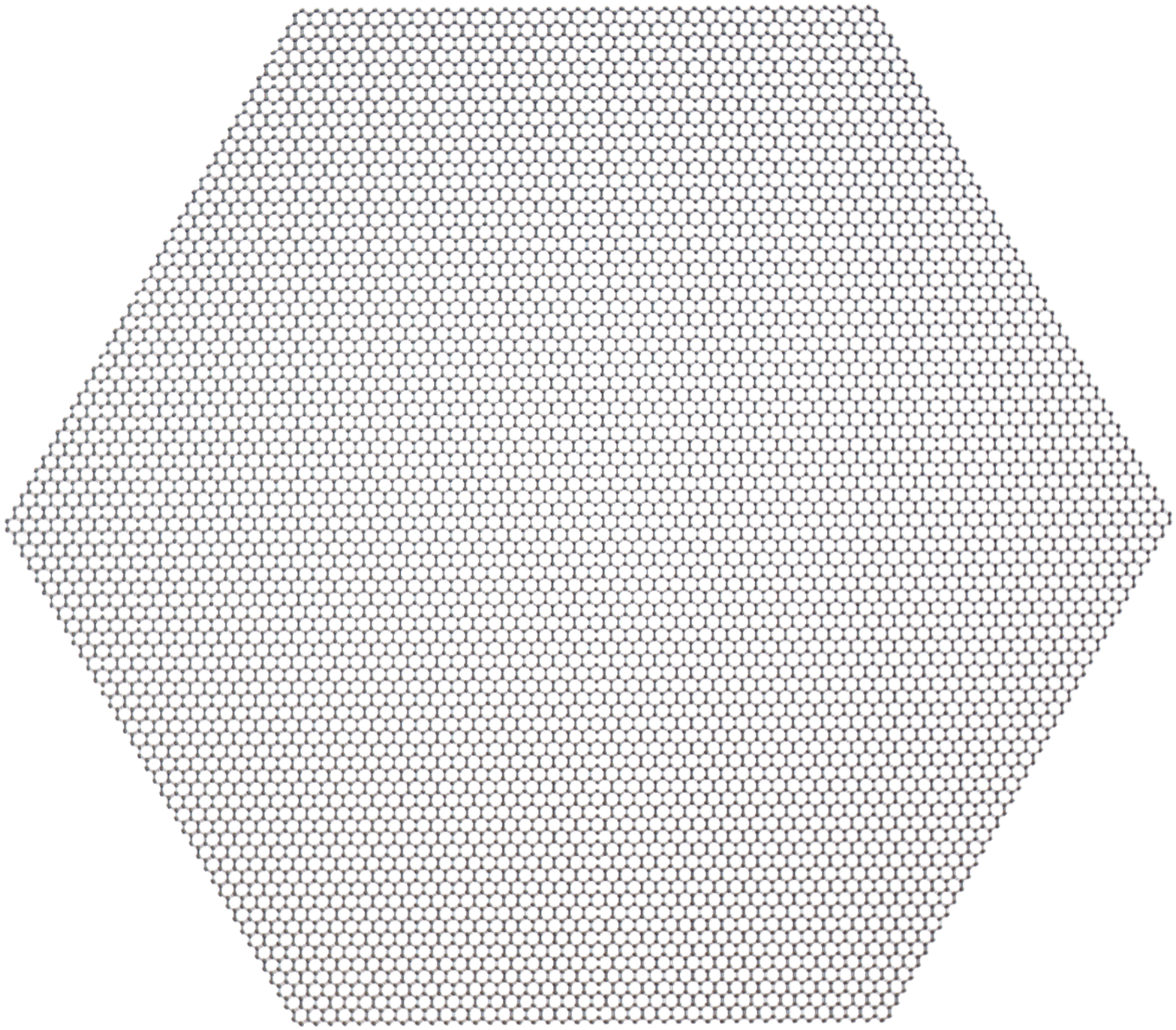

▷ <u>AB stacking</u> (from rotation by 60°)

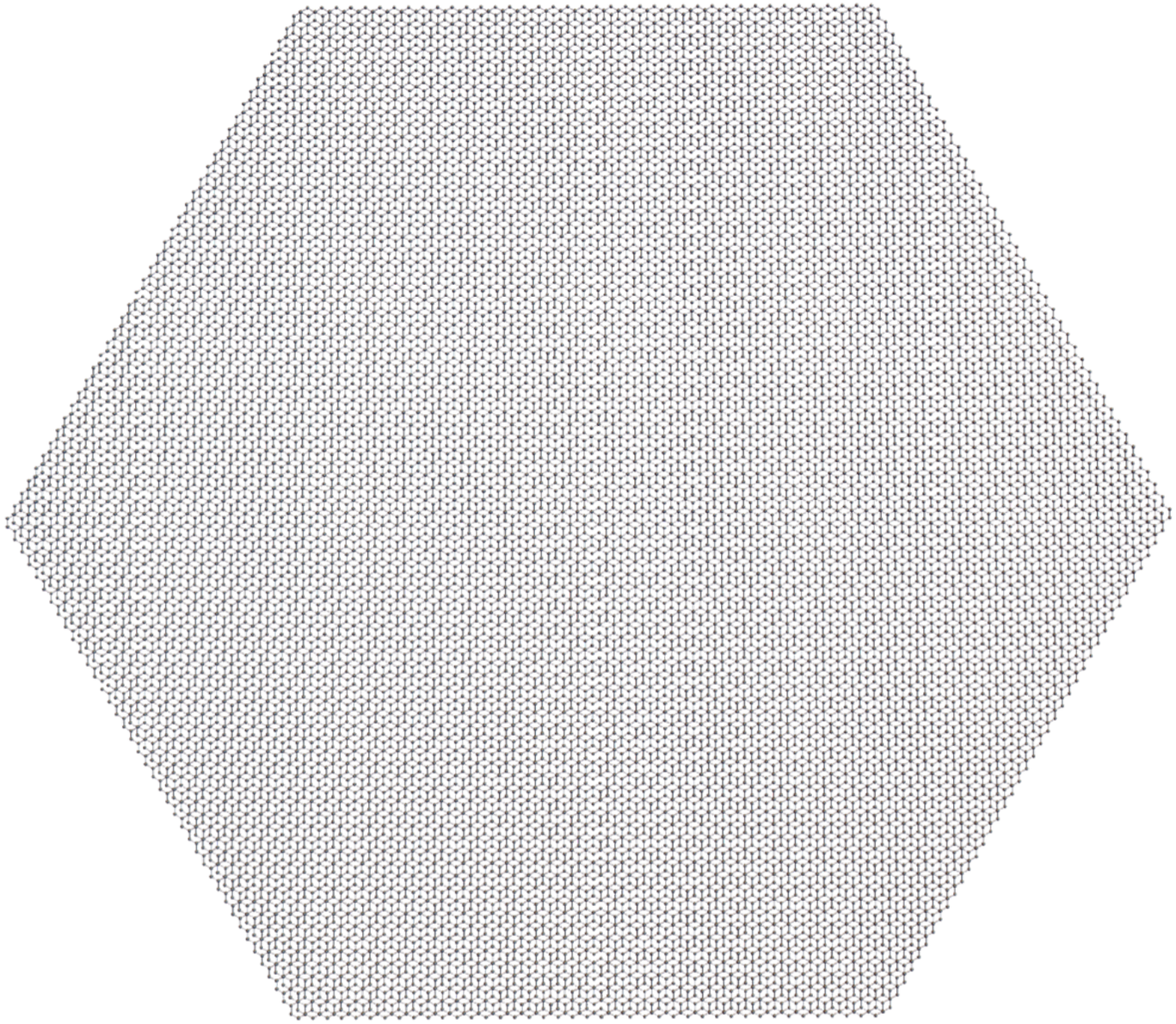

▷ rotation by 30°

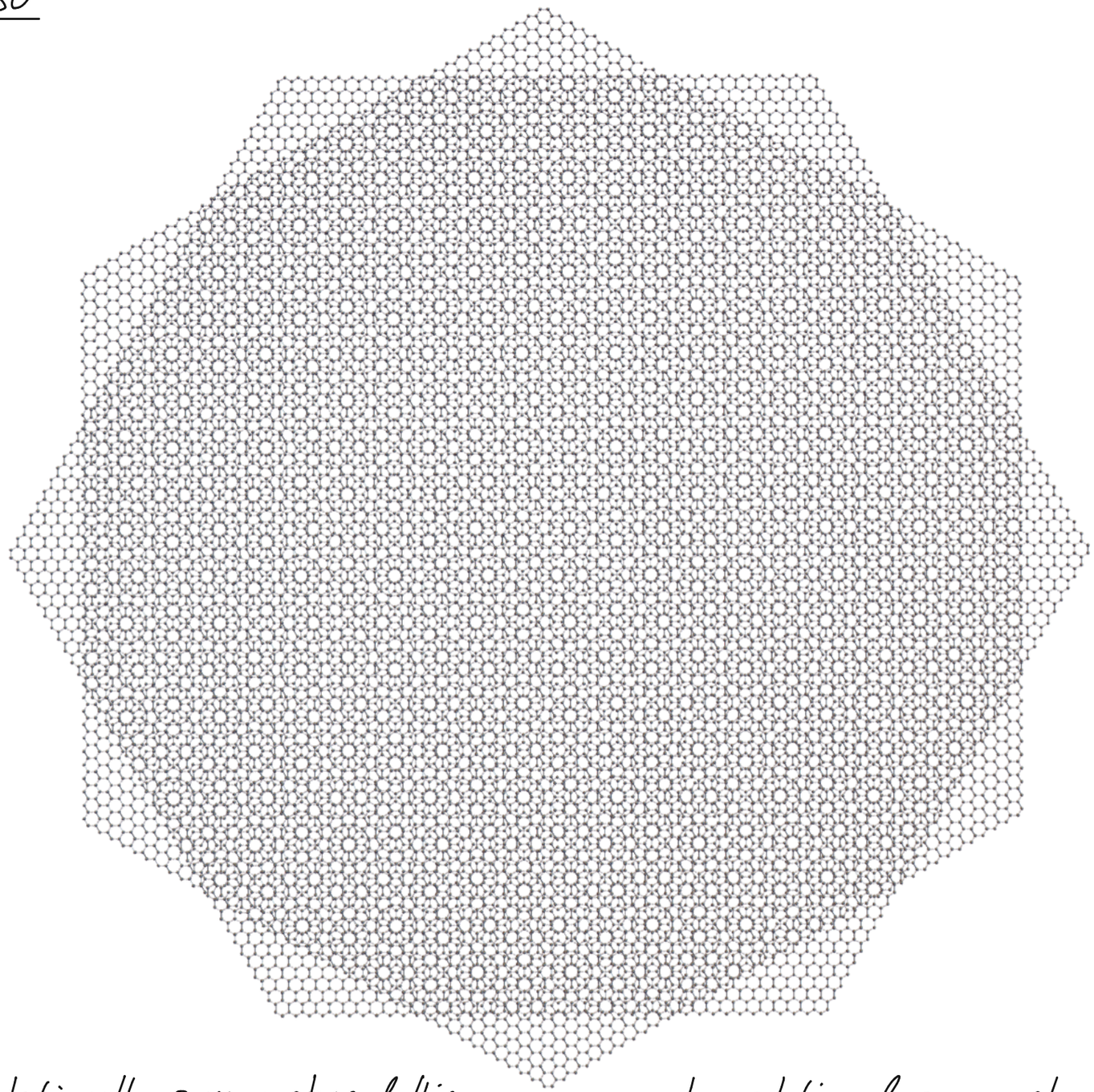

↳▷ 12-fold rotationally symmetric lattice ⇝ no translational symmetry (quasicrystal)

↳▷ very challenging problem of electron motion in quasiperiodic potential!

2.6. Moiré patterns

▷ rotation by $\theta = 5°$

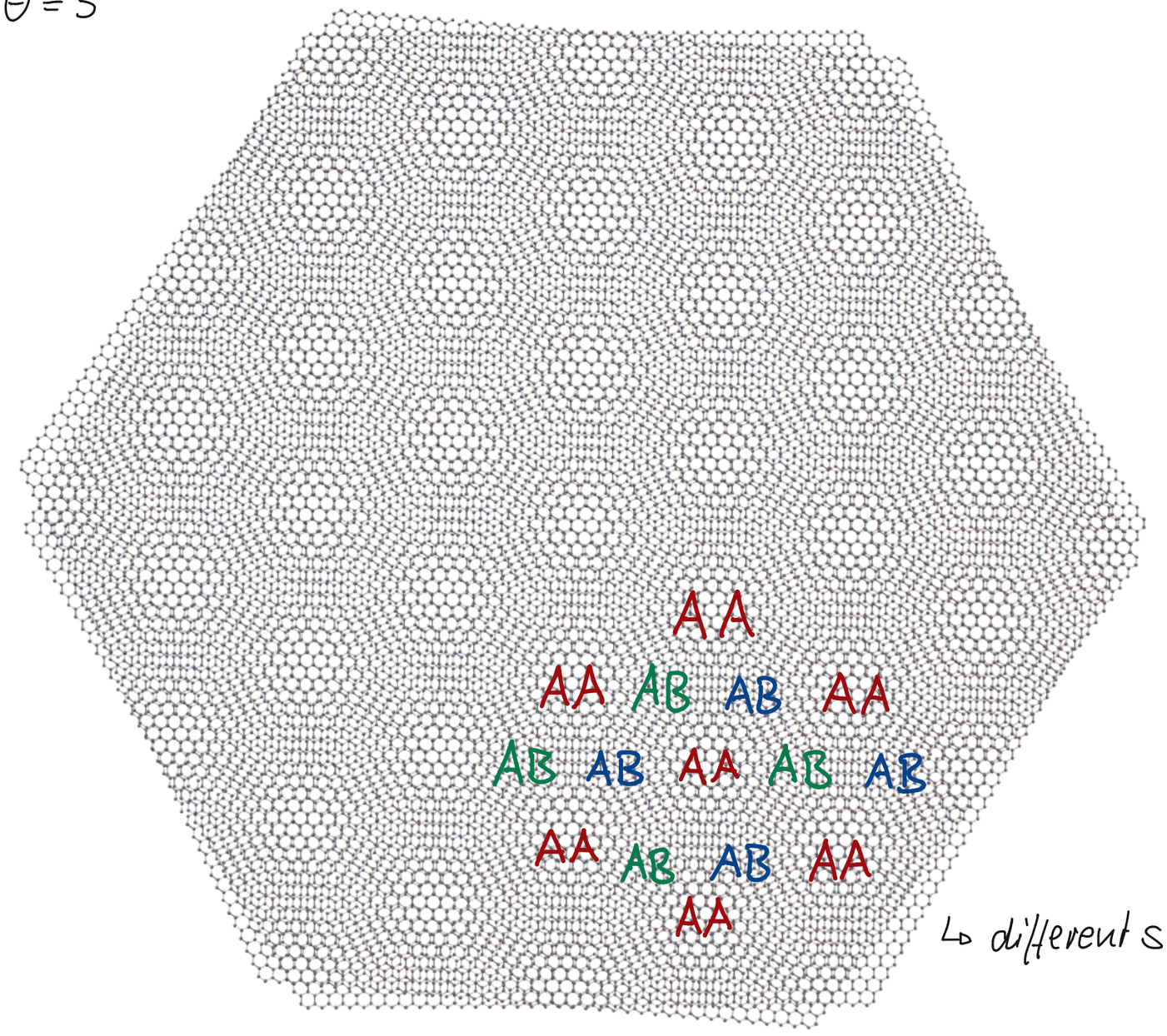

↳ different stacking regions

↳ small twist angle ↘ large-scale <u>moiré lattice</u> ↘ generally <u>aperiodic</u>

↳ carbon ions at lattice sites generate crystal potential for electrons ↘ <u>moiré potential</u>

▷ Geometric theory of 2D moiré patterns

↳ consider bilayer of two identical honeycomb lattices starting from AA stacking

↳ rotate layers 1 and 2 around pair of B sites by $\pm \theta/2$

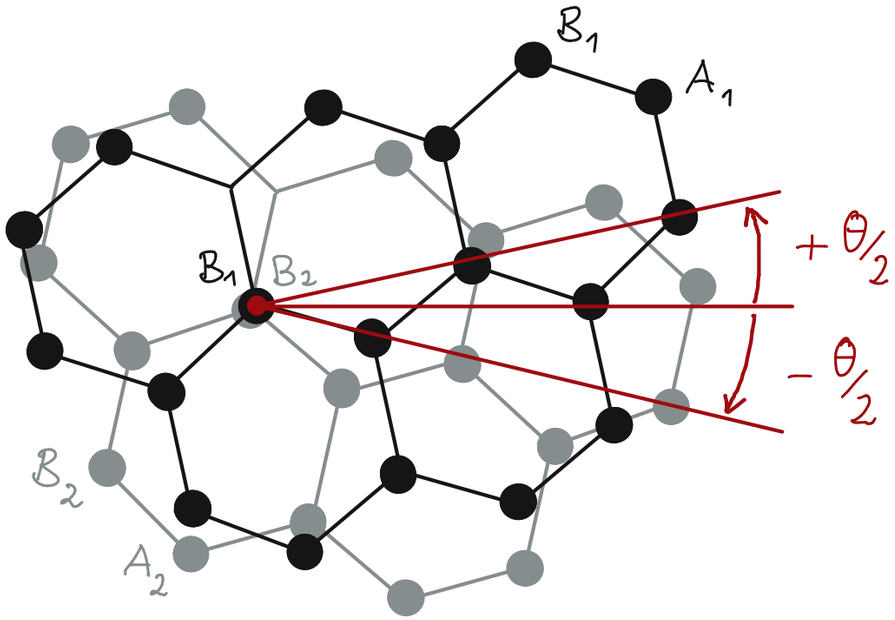

↳ Bravais lattice vectors of layer ℓ after rotation:

- $\vec{a}_i^{(\ell)} = R(\mp\theta/2)\,\vec{a}_i$ with rotational matrix $R(\varphi) = \begin{pmatrix} \cos\varphi & -\sin\varphi \\ \sin\varphi & \cos\varphi \end{pmatrix}$ (2-10A)

↳ likewise the reciprocal lattice vectors become $\vec{a}_i^{*(\ell)} = R(\mp\theta/2)\,\vec{a}_i^{*}$ (2-10B)

↳ crystal/moiré potential $V(\vec{r})$ of bilayer structure

- superposition of crystal potentials of the two individual layers
- can be represented as a sum of two Fourier expansions

$$V(\vec{r}) = \sum_{m,n} \left[u_{mn} e^{i m \vec{a}_1^{*(1)} \cdot \vec{r} + i n \vec{a}_2^{*(1)} \cdot \vec{r}} + w_{mn} e^{i m \vec{a}_1^{*(2)} \cdot \vec{r} + i n \vec{a}_2^{*(2)} \cdot \vec{r}} \right], \; m,n \in \mathbb{Z}$$

$$= \sum_{m,n} u_{mn} \underbrace{e^{i m \vec{a}_1^{*(1)} \cdot \vec{r} + i n \vec{a}_2^{*(1)} \cdot \vec{r}}}_{\text{modulation on scale of graphene lattice constant}} \left[1 + \frac{w_{mn}}{u_{mn}} \underbrace{e^{i m \vec{G}_1^{M} \cdot \vec{r} + i n \vec{G}_2 \cdot \vec{r}}}_{\text{(moiré) interference effect}} \right] \qquad (2\text{-}11A)$$

- where $\vec{G}_i^{M} = \vec{a}_i^{*(2)} - \vec{a}_i^{*(1)}$ (2-11B)

$$= \left[R(-\theta/2) - R(+\theta/2) \right] \vec{a}_i^{*} = \begin{pmatrix} 0 & 2\sin\theta/2 \\ -2\sin\theta/2 & 0 \end{pmatrix} \vec{a}_i^{*}, \; i \in \{1,2\}$$

↘ can be seen as reciprocal lattice vectors of moiré lattice

↘ real-space moiré lattice vectors $\vec{L}_j^{M}$ are obtained from $\vec{G}_i^{M} \cdot \vec{L}_j^{M} = 2\pi\delta_{ij}$

↘ length of moiré unit vectors: $L^{M} = |\vec{L}_j^{M}| = \frac{a'}{2|\sin\theta/2|} \Rightarrow L^{M} \gg a'$ (2-11C)

(for small θ)

↳ moiré superlattice structure of TBG is not periodic for general choice of θ

- reason: periods of two graphene layers are <u>incommensurate</u> for general θ
- for certain angles the two periods match (<u>commensurate</u> case)

  ↝ moiré superlattice structure becomes rigorously periodic

  ↝ <u>well-defined, finite unit cell</u>

  ↝ can use solid-state theory for crystals!

↳ <u>Commensurability condition</u>:

- twist angle θ coincides with the angle between

$$\vec{v}_1 = m\vec{a}_1 + n\vec{a}_2 \quad \text{and} \quad \vec{v}_2 = n\vec{a}_1 + m\vec{a}_2 \quad \text{with} \quad m,n \in \mathbb{Z} \qquad (2\text{-}12A)$$

- where $\vec{a}_1, \vec{a}_2$ are graphene's basis lattice vectors

↳ commensurability for example at $\theta \approx 3.89°$

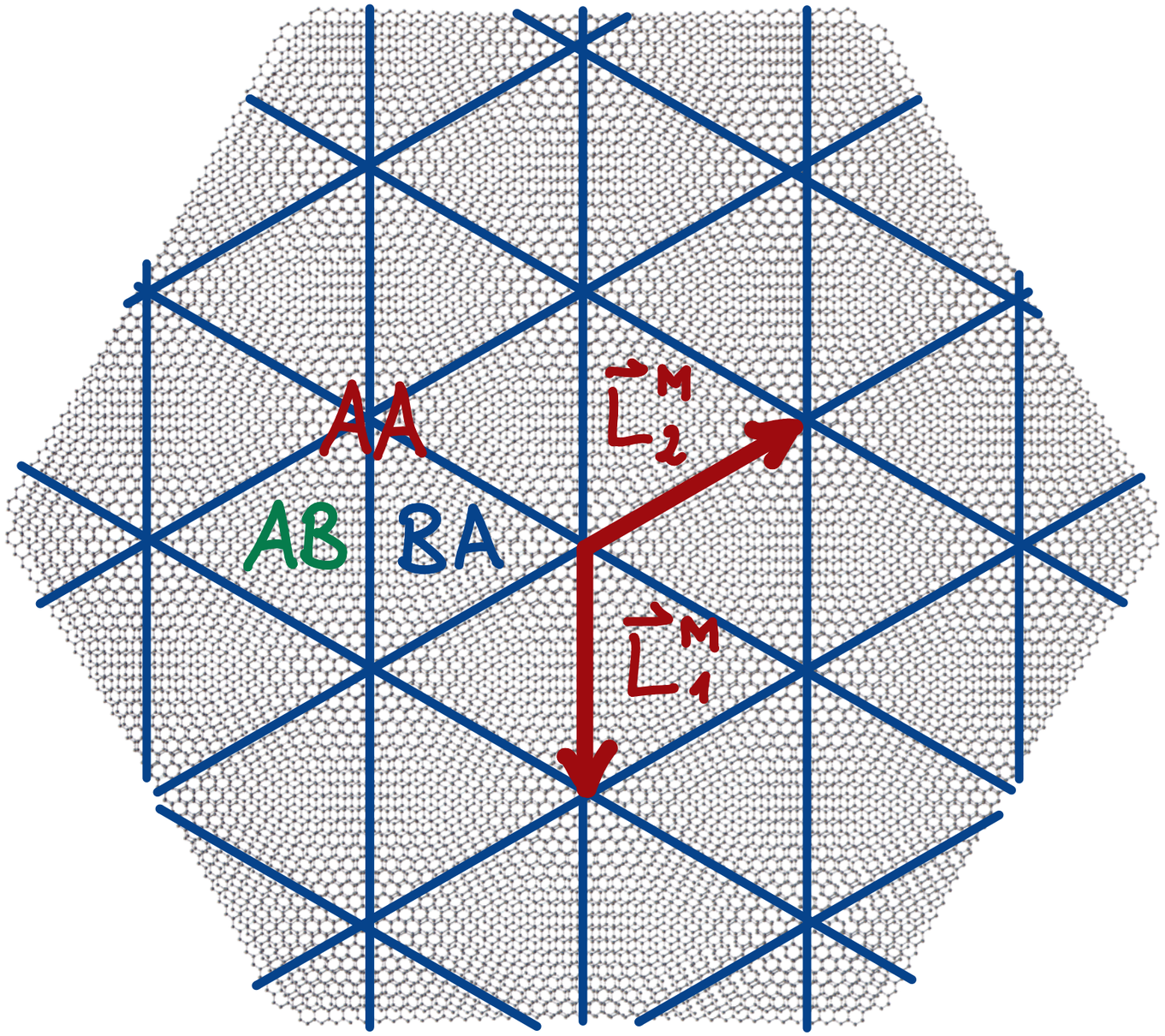

↳ atoms per unit cell: $N_M = 2 \times 2 \times (L^M/a')^2 = (\sin\theta/2)^{-2}$ ↘ here: $N_M(3.89°) \approx 868$

(2 ↑ layers, 2 ↑ sublattices, $(2-11C)$)

↘ exp. $N_M(1.05°) \approx 12{,}000$

▷ Commensurate twist angles

↳ start from AB stacking

↳ choose

$$\vec{a}_1 = \frac{a}{2}\begin{pmatrix} 1 \\ \sqrt{3} \end{pmatrix}$$

$$\vec{a}_2 = \frac{a}{2}\begin{pmatrix} -1 \\ \sqrt{3} \end{pmatrix}$$

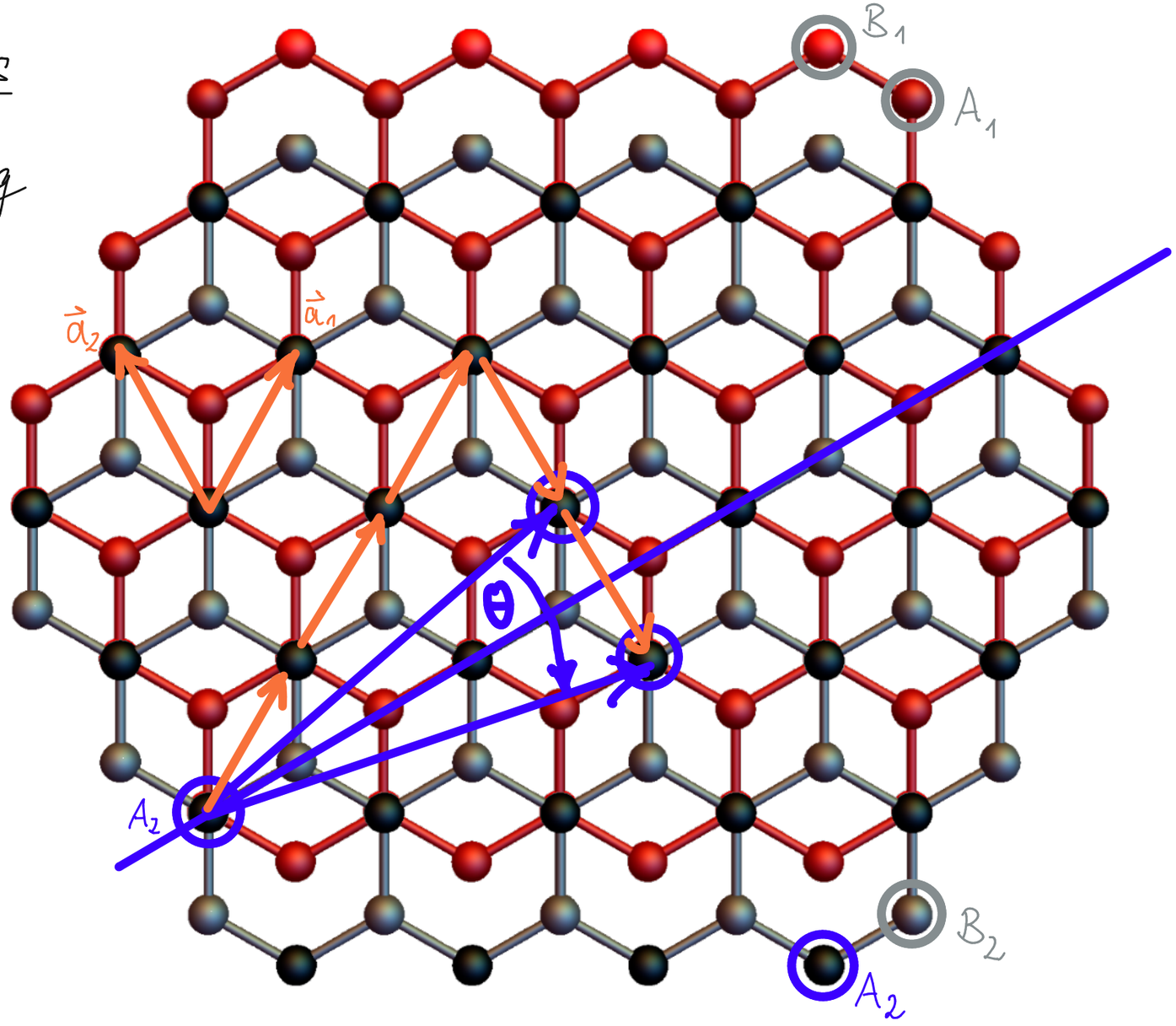

↳ commensurate structure when B_2 rotated to site formerly occupied by other B_2

↳ here twist angle between $\vec{v}_1 = 3\vec{a}_1 - \vec{a}_2$ and $\vec{v}_2 = 3\vec{a}_1 - 2\vec{a}_2$ $\rightsquigarrow \theta \approx 21.8°$

▷ <u>Commensurate twist angles</u> (example)

↳ start from AB stacking

↳ choose

$$\vec{a}_1 = \frac{a}{2}\begin{pmatrix} 1 \\ \sqrt{3} \end{pmatrix}$$

$$\vec{a}_2 = \frac{a}{2}\begin{pmatrix} -1 \\ \sqrt{3} \end{pmatrix}$$

↳ after rotation:

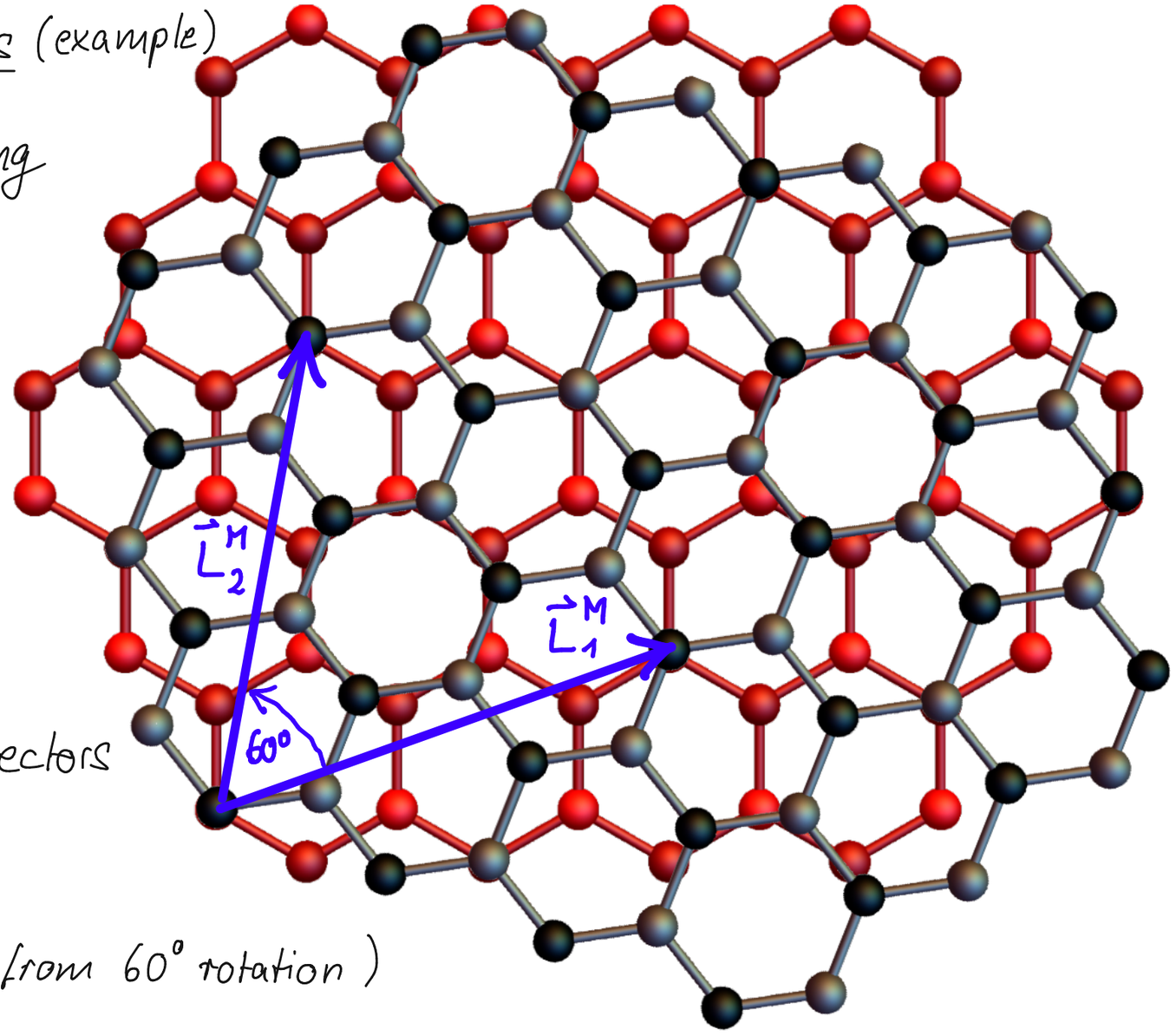

- moiré basis lattice vectors

$$\vec{L}^M_1 = 3\vec{a}_1 - 2\vec{a}_2$$

$$\vec{L}^M_2 = 2\vec{a}_1 + \vec{a}_2 \quad \text{(from } 60^\circ \text{ rotation)}$$

↳ generalize: $\vec{L}^M_1 = (2i+1)\vec{a}_1 - (i+1)\vec{a}_2$ and $\vec{L}^M_2 = (i+1)\vec{a}_1 + i\vec{a}_2$, $i \in \mathbb{N}_0$

↝ commensurability condition: $\cos(\theta_i) = \dfrac{3i^2 + 3i + \frac{1}{2}}{3i^2 + 3i + 1}$, $i \in \mathbb{N}_0$

↝ lattice constant: $L^M = |\vec{L}^M_i| = a\sqrt{3i^2 + 3i + 1}$ (experiment $i \approx 30$)

▷ Commensurate twist angles (reciprocal lattice)

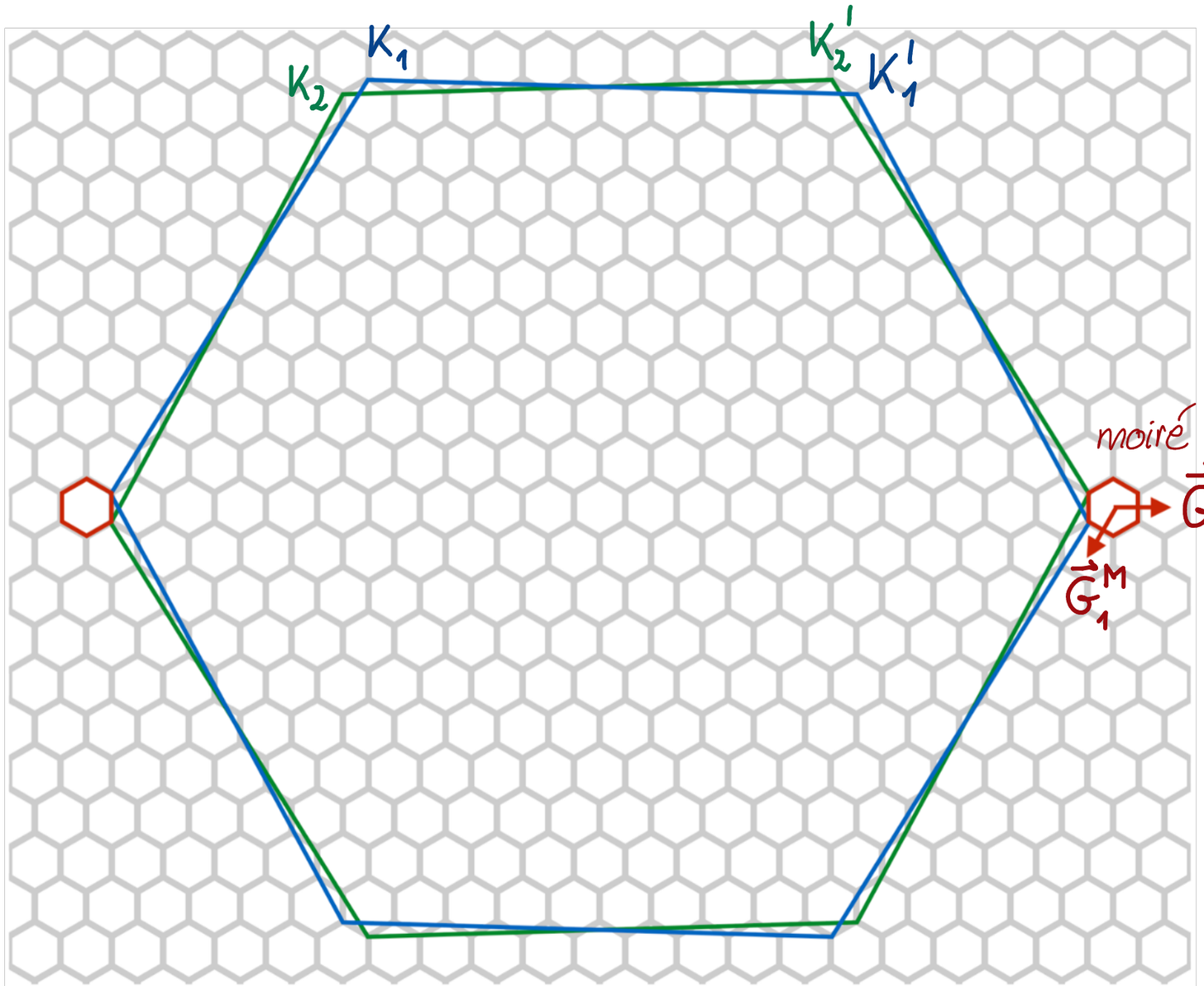

↳ for small twist angles ⇝ moiré Brillouin zone is tiny!

▷ <u>commensurate twist angles</u> (general case)

↳ commensurate twist angles : $\cos(\theta_{mn}) = \frac{1}{2}\frac{m^2+n^2+4mn}{m^2+n^2+mn}$, $m,n \in \mathbb{Z}$ (2-16A)

⇝ corresponding Bravais lattice vectors :

$$\vec{L}_1^M = m\vec{a}_1 + n\vec{a}_2 \;,\; \vec{L}_2^M = R(60°)\vec{L}_1^M \qquad (2\text{-}16B)$$

▷ <u>note</u> : moiré superlattice vectors can always be defined for any θ, see eq.(2-11B)

↳ also works for incommensurate angles

↳ for small angles ⇝ incommensuration effects are small

3. Electronic structure of graphene

3.1. Preparations

▷ 3 electrons per C atom ⇝ strong covalent σ bonds (energy bands far away from Fermi level)

▷ 1 electron / atom ⇝ π bonds (electronic properties at low energies)

↳ here: discuss energy bands of π electrons!

▷ we use the <u>tight-binding approximation</u> for the calculation of π energy bands

▷ <u>general idea</u> of tb approximation

↳ construct trial wave function for many-electron system

- use <u>orbital wave functions</u> $\phi^{(a)}(\vec{r} - \vec{R}_j)$ <u>of the atoms</u> forming the
- atoms form the crystal with Bravais lattice $\vec{R}_j = m_j \vec{a}_1 + n_j \vec{a}_2$, $m_j, n_j \in \mathbb{Z}$.
- trial wave function must reflect lattice symmetries (translation invariance)

↳ here: focus on 2D lattices!

▷ consider Bravais lattice with single atom per unit cell and $1e^-$ per atom (generalize later)

▷ Hamiltonian for e^- labelled by $\ell \in \mathbb{N}$: $H_\ell = -\frac{\hbar^2}{2m}\vec{\nabla}_\ell^2 + \sum_{j=1}^{N} V_{ion}(\vec{r}_\ell - \vec{R}_j)$ (3-2A)

↳ here: electron mass m, number of lattice sites N

↳ 2nd term: overall potential energy of the carbon lattice felt by electron ℓ

↘ for $N \to \infty$: $V(\vec{r}) = \sum_{j=1}^{\infty} V_{ion}(\vec{r} - \vec{R}_j) = V(\vec{r} + \vec{R})$ for any lattice vector $\vec{R}$

↘ periodic function w.r.t. translations by $\vec{R}_j$ by construction

▷ <u>total Hamiltonian</u> for all electrons: $H = \sum_{\ell=1}^{N} H_\ell$ (3-2B)

▷ <u>assumption</u>: electron ℓ is originally tightly bound to lattice site $\vec{R}_\ell$

↳ well-described by bound state $\phi^{(a)}(\vec{r})$ of atomic $H_\ell^a = -\frac{\hbar^2}{2m}\vec{\nabla}_\ell^2 + V_{ion}(\vec{r}_\ell - \vec{R}_\ell)$ (3-2C)

↳ potential energy contributions from other ions $\Delta V = \sum_{j \neq \ell} V_{ion}(\vec{r}_\ell - \vec{R}_j)$ (3-2D)

↘ can be treated perturbatively

3.2. Bloch's theorem

▷ trial wave function must respect discrete translational symmetry of the lattice (Bloch)

▷ translation operator for translation by lattice vector $\vec{R}$: $T_{\vec{R}}$ (3-3A)

↳ defined through: $T_{\vec{R}}\,|\vec{r}\rangle = |\vec{r}+\vec{R}\rangle$ and $\langle\vec{r}\,|\,T_{\vec{R}} = \langle\vec{r}-\vec{R}\,|$ (3-3B)

↳ described by $T_{\vec{R}} = \exp\left(\frac{i}{\hbar}\,\vec{p}\cdot\vec{R}\right)$ (3-3C)

"momentum operator" (see below)

▷ Hamiltonian H invariant under discrete set of lattice translations.

↳ translation operator commutes with H: $[T_{\vec{R}}, H] = 0$ (3-3D)

↳ eigenstates of H are simultaneously eigenstates of $T_{\vec{R}}$

▷ due to $\vec{a}_i \cdot \vec{a}_j^{\,*} = 2\pi\delta_{ij}$ ⇝ momentum only defined modulo reciprocal lattice vector:

$$\vec{G} = m^*\vec{a}_1^{\,*} + n^*\vec{a}_2 \quad , \quad m^*, n^* \in \mathbb{Z} \qquad (3\text{-}3E)$$

↳ shift $\vec{p}\,' = \vec{p} + \hbar\vec{G}$ only gives factor $e^{i\vec{G}\cdot\vec{R}} = e^{i2\pi n} = 1$ in $T_{\vec{R}}$ since $n \in \mathbb{Z}$

↳ identify all momenta which differ by $\vec{G}$ ⇝ <u>quasi-momentum</u> $\vec{p} = \hbar\vec{k}$ restricted to 1st BZ

▷ trial wave function: $\psi_{\vec{k}}(\vec{r}) = \sum_{\vec{R}_j} e^{i\vec{k}\cdot\vec{R}_j}\, \phi^{(a)}(\vec{r}-\vec{R}_j)$ (Bloch function) (3-4A)

(atomic orbitals)

↳ eigenstate of $T_{\vec{R}}$: $T_{\vec{R}}\,\psi_{\vec{k}}(\vec{r}) = \psi_{\vec{k}}(\vec{r}+\vec{R}) = \sum_{\vec{R}_j} e^{i\vec{k}\cdot\vec{R}_j}\, \phi^{(a)}(\vec{r}-(\vec{R}_j-\vec{R}))$

($\vec{R}_j' = \vec{R}_j - \vec{R}$)

$$= \sum_{\vec{R}_j'} e^{i\vec{k}\cdot(\vec{R}_j'+\vec{R})}\, \phi^{(a)}(\vec{r}-\vec{R}_j') = e^{i\vec{k}\cdot\vec{R}}\,\psi_{\vec{k}}(\vec{r}) \quad (3\text{-}4B)$$

▷ these Bloch functions are not orthogonal!

↳ alternative approach to tight-binding approx.: <u>Wannier functions/states</u>

- Fourier transforms of Bloch functions
- constructed to obey orthogonality relations
- centered/"localized" on real-space lattice sites

▷ here: continue with Bloch functions ...

3.3. Bipartite lattices

▷ honeycomb lattice has two atoms per unit cell ↝ adapt previous description

▷ translation by $\vec{\delta}$ relating different sublattices is <u>not</u> symmetry op.: $[T_{\vec{\delta}}, H] \neq 0$ (3-5A)

↳ need to treat different sublattices A and B separately

↳ trial wave function: $\psi_{\vec{k}}(\vec{r}) = a_{\vec{k}}\, \psi_{\vec{k}}^{(A)}(\vec{r}) + b_{\vec{k}}\, \psi_{\vec{k}}^{(B)}(\vec{r})$ (3-5B)

- here $a_{\vec{k}}, b_{\vec{k}}$ are complex functions of quasi-momentum $\vec{k}$

- Bloch fcts. $\psi_{\vec{k}}^{(A/B)}(\vec{r})$: $\psi_{\vec{k}}^{(i)}(\vec{r}) = \sum_{\vec{R}} e^{i\vec{k}\cdot\vec{R}}\, \phi^{(i)}(\vec{r} + \vec{\delta}_i - \vec{R})$, $i \in \{A, B\}$ (3-5C)

- $\vec{\delta}_i$ connects sites of Bravais lattice with site of atom i in unit cell

  ↝ example: $\vec{\delta}_A = 0$ and $\vec{\delta}_B = a(0, -1)$

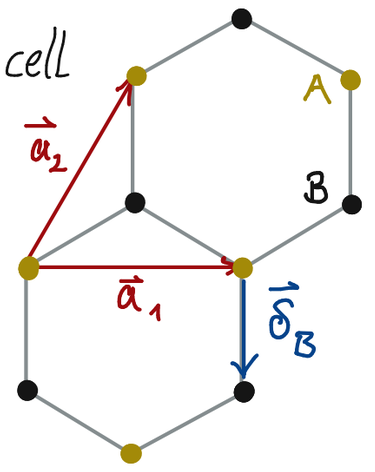

▷ use trial wave function to search for solutions of Schrödinger eq.: $H\Psi_{\vec{k}} = \varepsilon_{\vec{k}}\Psi_{\vec{k}}$ (3-6A)

↳ multiply with $\Psi_{\vec{k}}^*$ from the left ⇝ $\Psi_{\vec{k}}^* H \Psi_{\vec{k}} = \varepsilon_{\vec{k}} \Psi_{\vec{k}}^* \Psi_{\vec{k}}$ (3-6B)

↳ rewrite in matrix form: $(a_{\vec{k}}^*, b_{\vec{k}}^*)\, \mathcal{H}_{\vec{k}} \begin{pmatrix} a_{\vec{k}} \\ b_{\vec{k}} \end{pmatrix} = \varepsilon_{\vec{k}} (a_{\vec{k}}^*, b_{\vec{k}}^*) S_{\vec{k}} \begin{pmatrix} a_{\vec{k}} \\ b_{\vec{k}} \end{pmatrix}$ (3-6C)

- with Hamiltonian matrix $\mathcal{H}_{\vec{k}} = \begin{pmatrix} \Psi_{\vec{k}}^{(A)*} H \Psi_{\vec{k}}^{(A)} & \Psi_{\vec{k}}^{(A)*} H \Psi_{\vec{k}}^{(B)} \\ \Psi_{\vec{k}}^{(B)*} H \Psi_{\vec{k}}^{(A)} & \Psi_{\vec{k}}^{(B)*} H \Psi_{\vec{k}}^{(B)} \end{pmatrix} = \mathcal{H}_{\vec{k}}^\dagger$ (3-6D)

- and overlap matrix $S_{\vec{k}} = \begin{pmatrix} \Psi_{\vec{k}}^{(A)*} \Psi_{\vec{k}}^{(A)} & \Psi_{\vec{k}}^{(A)*} \Psi_{\vec{k}}^{(B)} \\ \Psi_{\vec{k}}^{(B)*} \Psi_{\vec{k}}^{(A)} & \Psi_{\vec{k}}^{(B)*} \Psi_{\vec{k}}^{(B)} \end{pmatrix} = S_{\vec{k}}^\dagger$ (3-6E)

- includes integration over 2D coord., $S_{\vec{k}}$ from non-orthogonality of trial wavefcts.

▷ eigenvalues of Schrödinger eq. ⇝ energy dispersion/bands

↳ obtained from secular equation: $\det\left(\mathcal{H}_{\vec{k}} - \varepsilon_{\vec{k}}^\lambda S_{\vec{k}}\right) = 0$ (3-6F)

↳ band index λ (2 bands from 2 sublattices)

↳ straightforward generalization to n atoms per unit cell ⇝ n energy bands

3.4. Formal solution of secular eq.

▷ arbitrary lattice with n atoms per unit cell: $\mathcal{H}_{\vec{k}}^{ij} = \psi_{\vec{k}}^{(i)*} H \psi_{\vec{k}}^{(j)}$, $i,j \in \{1,\dots,n\}$ (3-7A)

↳ use eq. (3-5C):

$$\mathcal{H}_{\vec{k}}^{ij} = \sum_{\vec{R}_\ell, \vec{R}_m} e^{i\vec{k}\cdot(\vec{R}_\ell - \vec{R}_m)} \int_{\vec{r}} \phi^{(i)*}(\vec{r} + \vec{\delta}_i - \vec{R}_\ell) \underbrace{H}_{H^a + \Delta V} \phi^{(j)}(\vec{r} + \vec{\delta}_j - \vec{R}_m) \qquad (3\text{-}7B)$$

$$= N \sum_{\vec{R}_\ell} e^{i\vec{k}\cdot\vec{R}_\ell} \int_{\vec{r}} \phi^{(i)*}(\vec{r} + \vec{\delta}_i)[H^a + \Delta V] \phi^{(j)}(\vec{r} + \vec{\delta}_j - \vec{R}_\ell)$$

$$= N(\underbrace{\varepsilon^{(j)}}_{\text{atomic wavefcts. are eigenfcts. of } H^a \text{ with atomic orbital energy } \varepsilon^{(i)}} S_{\vec{k}}^{ij} + t_{\vec{k}}^{ij}) \qquad (3\text{-}7C)$$

- here $S_{\vec{k}}^{ij} = \sum_{\vec{R}_\ell} e^{i\vec{k}\cdot\vec{R}_\ell} \int_{\vec{r}} \phi^{(i)*}(\vec{r} + \vec{\delta}_i) \phi^{(j)}(\vec{r} + \vec{\delta}_j - \vec{R}_\ell) = S^{ij}/N$ (3-7D)

- <u>hopping matrix</u> $t_{\vec{k}}^{ij} = \sum_{\vec{R}_\ell} e^{i\vec{k}\cdot\vec{R}_\ell} \underbrace{\int_{\vec{r}} \phi^{(i)*}(\vec{r} + \vec{\delta}_i) \Delta V \phi^{(j)}(\vec{r} + \vec{\delta}_j - \vec{R}_\ell)}_{\tilde{t}(\vec{\delta}_i, \vec{\delta}_j, \vec{R}_\ell) \quad \text{(hopping amplitude)}}$ (3-7E)

$\Rightarrow$ secular eq.: $\det\left[t_{\vec{k}}^{ij} - (\varepsilon_{\vec{k}}^{\lambda} - \varepsilon^{(j)}) S_{\vec{k}}^{ij} \right] = 0$ (3-7F)

- graphene: $\varepsilon^{(j)} = \varepsilon_0$ since all C atoms contribute same orbital

3.5. Solution for graphene

▷ tb model on honeycomb lattice ↝ accurately yields π energy bands of graphene

▷ omit ε^0 because all atomic orbitals are p_z ↝ only constant energy shift

▷ choose Bravais lattice vectors to be those of A sublattice ($\vec{\delta}_A = 0$)

↳ equivalent site on B sublattice through displacement $\vec{\delta}_B = \vec{\delta}_3 = -a(0,1)$

▷ <u>hopping amplitudes</u> (overlap/transfer integrals)

(1) nearest neighbors (nn): $$t = t(\vec{\delta}_3) = \int_{\vec{r}} \phi^{(A)*}(\vec{r})\, \Delta V\, \phi^{(B)}(\vec{r}+\vec{\delta}_3) \qquad (3\text{-}8A)$$

(2) next-to-nearest neighbors (nnn): $\tilde{t}' = t(\vec{a}_1) = \int_{\vec{r}} \phi^{(A)*}(\vec{r})\, \Delta V\, \phi^{(A)}(\vec{r}+\vec{a}_1)$ (3-8B)

(3) overlap correction: $$s = \int_{\vec{r}} \phi^{(A)*}(\vec{r})\, \phi^{(B)}(\vec{r}+\vec{\delta}_3) \qquad (3\text{-}8C)$$

(4) atomic orbitals. $$\int_{\vec{r}} \phi^{(i)*}(\vec{r})\, \phi^{(i)}(\vec{r}) = 1 \qquad (3\text{-}8D)$$

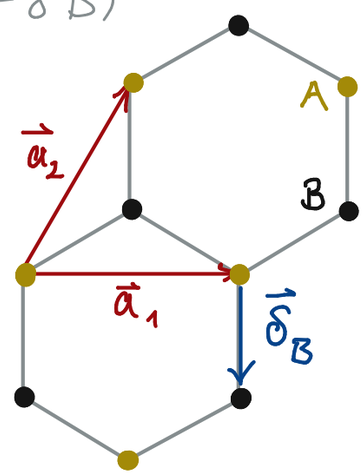

↳ neglect ovelap corrections between all other orbitals

↳ neglect hopping for larger distances than nnn (ok, bc. atomic orbitals are tightly bound!)

▷ hopping amplitude t is identical for three nn

↳ hopping matrix (3-7E) with nn sites gets contributions from neighboring Bravais sites

↘ nn: $$t_{\vec{k}}^{AB} = t\underbrace{\left(1 + e^{i\vec{k}\cdot\vec{a}_1} + e^{i\vec{k}\cdot(\vec{a}_2-\vec{a}_1)}\right)}_{=:\gamma_{\vec{k}}}{}^{*} = \left(t_{\vec{k}}^{BA}\right)^{*} \qquad (3\text{-}9A)$$

↘ further: $$s_{\vec{k}}^{AB} = s\gamma_{\vec{k}}^{*} = \left(s_{\vec{k}}^{BA}\right)^{*} \qquad (3\text{-}9B)$$

↘ nnn: $$t_{\vec{k}}^{AA} = t_{\vec{k}}^{BB} = \tilde{t}'\left(e^{i\vec{k}\cdot\vec{a}_1} + e^{-i\vec{k}\cdot\vec{a}_1} + e^{i\vec{k}\cdot\vec{a}_2} + e^{-i\vec{k}\cdot\vec{a}_2} + e^{i\vec{k}(\vec{a}_2-\vec{a}_1)} + e^{-i\vec{k}(\vec{a}_2-\vec{a}_1)}\right)$$

$$= \tilde{t}'\sum_{i=1}^{3}\cos(\vec{k}\cdot\vec{a}_i) = \tilde{t}'\left(|\gamma_{\vec{k}}|^2 - 3\right) \quad \text{with } \vec{a}_3 = \vec{a}_2 - \vec{a}_1 \qquad (3\text{-}9C)$$

▷ secular eq.: $$\det\left[\begin{pmatrix} t_{\vec{k}}^{AA} - \varepsilon_{\vec{k}} & (t - s\varepsilon_{\vec{k}})\gamma_{\vec{k}}^{*} \\ (t - s\varepsilon_{\vec{k}})\gamma_{\vec{k}} & t_{\vec{k}}^{AA} - \varepsilon_{\vec{k}} \end{pmatrix}\right] = 0 \qquad (3\text{-}9D)$$

↳ two solutions ($\lambda = \pm$): $$\varepsilon_{\vec{k},\pm} = \frac{t_{\vec{k}}^{AA} \pm t|\gamma_{\vec{k}}|}{1 \pm s|\gamma_{\vec{k}}|} \qquad (3\text{-}9E)$$

↳ for $s \ll 1$, $\tilde{t}' \ll 1 \Rightarrow$ $$\varepsilon_{\vec{k},\pm} \approx \pm t|\gamma_{\vec{k}}| + t_{\vec{k}}^{AA} - st|\gamma_{\vec{k}}|^2 \approx \pm t|\gamma_{\vec{k}}| + t'|\gamma_{\vec{k}}|^2 \qquad (3\text{-}9F)$$

- with $t' = \tilde{t}' - st$ and we dropped the unimportant constant $-3\tilde{t}'$ in last step
- t, t' can be determined by fitting (3-9F) to full band structure calculations.

3.6. Energy dispersion of π electrons in graphene

▷ $\varepsilon_{\vec{k},\pm} = \pm t|\gamma_{\vec{k}}| + t'|\gamma_{\vec{k}}|^2$ with $\gamma_{\vec{k}} = 1 + e^{i\vec{k}\cdot\vec{a}_1} + e^{i\vec{k}(\vec{a}_2-\vec{a}_1)}$ and $t \approx -2.7\,eV$, $t' \approx 0.1t$ (3-10A)

↳▷ for $t'=0$ ↝ energy dispersion is electron-hole symmetric: $\varepsilon_{\vec{k},\lambda} = -\varepsilon_{\vec{k},-\lambda}$

▷ Fermi level is situated at points where π band touches π^* band (Fermi points)

↳▷ for $t'=0$ this happens at $\vec{k}_D$ where $\varepsilon_{\vec{k}_D,\lambda} = 0 \Rightarrow \gamma_{\vec{k}_D} = 0$

↳▷ one finds: $\vec{k}_D = \pm\vec{K} = \left(\pm\frac{4\pi}{3\sqrt{3}a}, 0\right)$ (3-10B)

↝ Fermi points sit at crystallographic K, K'

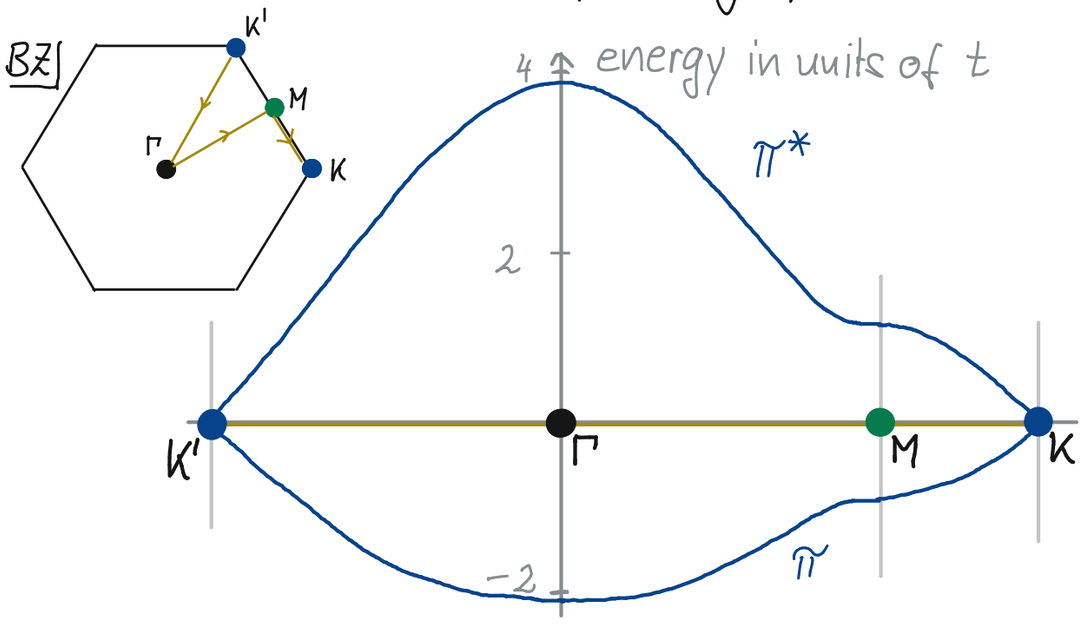

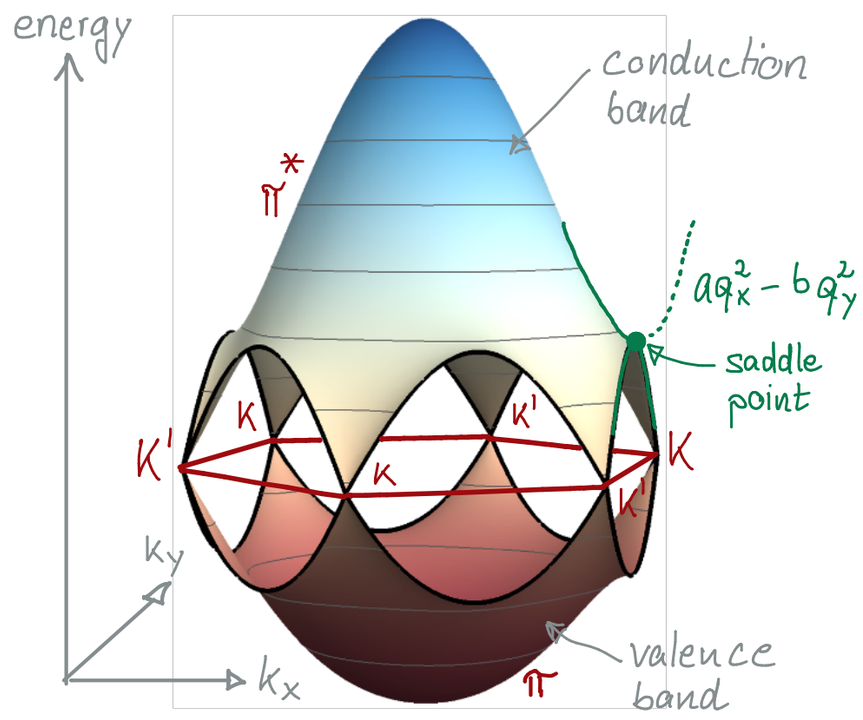

↳ symmetry $\varepsilon_{\vec{k},\pm} = \varepsilon_{-\vec{k},\pm}$ ⇒ if $\varepsilon_{\vec{K}} = 0$ ↝ $\varepsilon_{-\vec{K}} = 0$ ⇒ Fermi points come in pairs

▷ <u>density of states</u> (DOS)

↳ definition DOS: $g(E) = \sum_{\vec{k},\sigma} \delta(E - \varepsilon(\vec{k}))$ (3-10'A)

↳ determine number of states $g(E)dE$ in BZ located in $E \leq \varepsilon(\vec{k}) \leq E+dE$

↳ DOS in graphene ($t'=0$):

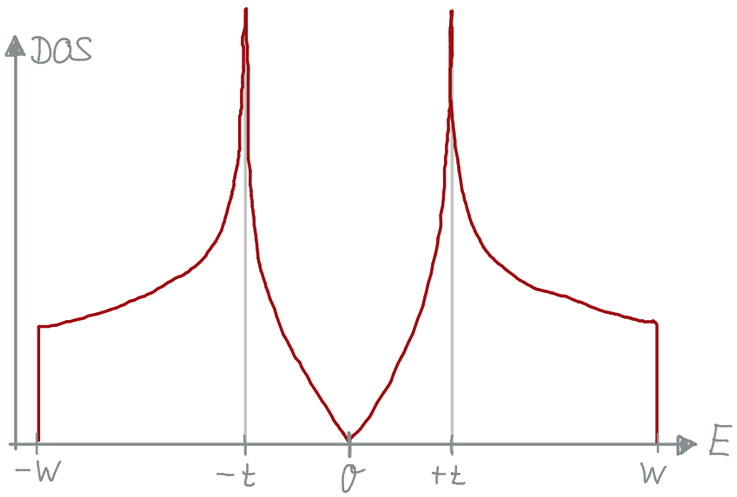

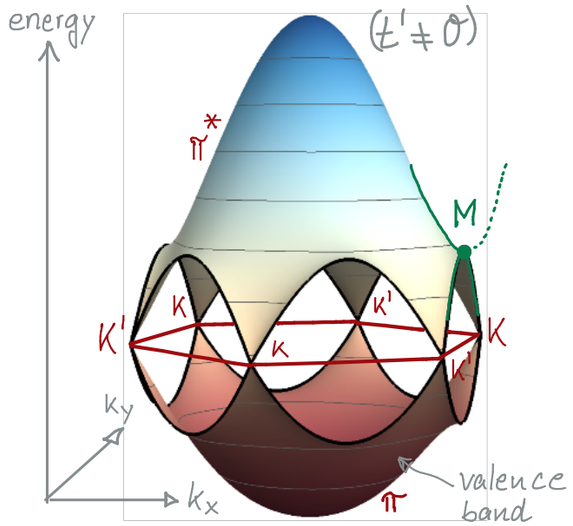

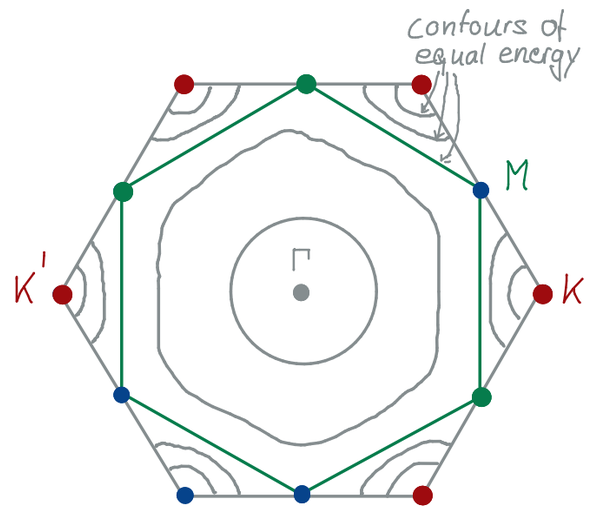

- vanishing DOS near band touching $E \to 0$: $g(E) \propto |E|$ (3-10'B)
- divergent <u>DOS near saddle points</u> $E_{VH} = \pm t$: $g(E) \propto -\ln|E - E_{VH}|$ (3-10'C)

  ↳ such a divergence in DOS is called <u>Van Hove Singularity</u> (VHS)
- VHS near Fermi surface ↳ large number of states which can be coupled by i.a.

3.7. Tight-binding models in 2nd quantization formulation

▷ tb formulation easily implemented in 2nd quantized language ⇝ intuitive interpretation!

↳ introduce fermionic operators.

- $\hat{c}^{(\dagger)}_{j\sigma}$ creates/annihilates e^- on site $\vec{R}_j$ with spin $\sigma \in \{\uparrow,\downarrow\}$ (in corresp. Wannier state $|\vec{R}_j\rangle$)

▷ <u>tb Hamiltonian</u>:

$$H = \sum_{j\sigma} \varepsilon_0 \hat{c}^{\dagger}_{j\sigma} \hat{c}_{j\sigma} + \sum_{ij\sigma} t_{ij} \hat{c}^{\dagger}_{i\sigma} c_{j\sigma} \qquad (3\text{-}11A)$$

↳ <u>hopping matrix elements</u> $t_{ij} = t(\vec{R}_i - \vec{R}_j)$ from overlap/transfer integrals

↳ represents kinetic energy of e^- which hop from site i to j

▷ p_z atomic orbitals in graphene and graphite (<u>Slater-Koster form of hoppings</u>)

↳ $$t(\vec{R}) = -V_{pp\pi}(R)\left[1 - \left(\frac{\vec{R}\cdot\vec{e}_z}{R}\right)^2\right] - V_{pp\sigma}(R)\left(\frac{\vec{R}\cdot\vec{e}_z}{R}\right)^2 \qquad (3\text{-}11B)$$

↳ here
- $V_{pp\pi}(R) \approx 2.7\exp[-(R/a - 1)/0.184]\,eV \qquad (3\text{-}11C)$
- $V_{pp\sigma}(R) \approx 0.48\exp[-(R - d_{AB})/(0.184a)]\,eV \qquad (3\text{-}11D)$

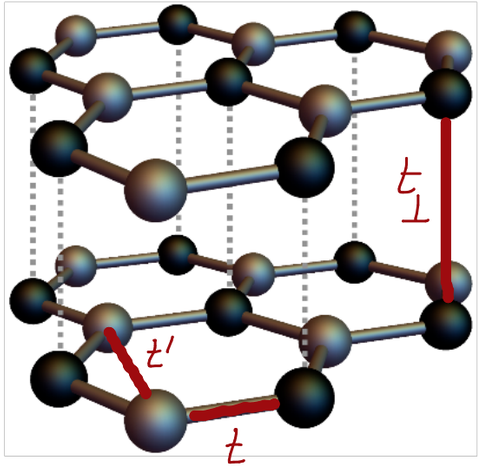

▷ 2nd quantized tb Hamiltonian can be diagonalized using Fourier trafo (cf. Bloch↔Wannier)

↳ $\hat{c}_{i\sigma} = \hat{c}_\sigma(\vec{r}_i) = \frac{1}{\sqrt{N}} \sum_{\vec{k}} \hat{c}_\sigma(\vec{k}) e^{-i\vec{k}\cdot\vec{r}_i}$ (3-12A)

↳ $\hat{c}^\dagger_{i\sigma} = \hat{c}^\dagger_\sigma(\vec{r}_i) = \frac{1}{\sqrt{N}} \sum_{\vec{k}} \hat{c}^\dagger_\sigma(\vec{k}) e^{+i\vec{k}\cdot\vec{r}_i}$ (3-12B)

▷ for graphene's bipartite lattice: $\hat{c}^{(\dagger)}(\vec{r}) = \begin{cases} a^{(\dagger)}(\vec{r}) & \text{for } \vec{r} \in A \text{ sublattice} \quad (3\text{-}12C) \\ b^{(\dagger)}(\vec{r}) & \text{for } \vec{r} \in B \text{ sublattice} \quad (3\text{-}12D) \end{cases}$

↳ dropped spin index for simplicity

↳ $H = t \sum_{\langle i,j \rangle} \hat{c}^\dagger(\vec{r}_i)\hat{c}(\vec{r}_j) + h.c. = t \sum_i \sum_{n=1}^{3} \hat{c}^\dagger(\vec{r}_i)\hat{c}(\vec{r}+\vec{\delta}_n) + h.c.$ (3-12E)

($\langle i,j \rangle$ ← sum over all nn)

$$= \frac{t}{N} \sum_{i,\vec{k},\vec{k}'} \sum_{n=1}^{3} a^\dagger(\vec{k}) b(\vec{k}') e^{i(\vec{k}-\vec{k}')\cdot\vec{R}_i} \cdot e^{i\vec{k}\cdot\vec{\delta}_n} + h.c.$$

$$= t \sum_{\vec{k}} a^\dagger(\vec{k}) b(\vec{k}) f(\vec{k}) + h.c. \quad \text{using} \quad \sum_{\vec{r}} e^{i(\vec{k}-\vec{k}')\cdot\vec{r}} = N\delta_{\vec{k},\vec{k}'}$$

↳ introduced $f(\vec{k}) = \sum_{n=1}^{3} \exp(i\vec{k}\cdot\vec{\delta}_n)$ (3-12F)

↳ rewrite in matrix form: $H = t \sum_{\vec{k}} (a^\dagger(\vec{k}), b^\dagger(\vec{k})) \underbrace{\begin{pmatrix} 0 & f(\vec{k}) \\ f^*(\vec{k}) & 0 \end{pmatrix}}_{H_{\vec{k}}} \begin{pmatrix} a(\vec{k}) \\ b(\vec{k}) \end{pmatrix}$ (3-12G)

↳ diagonalization of $H_{\vec{k}}$ ⇝ energy bands $\varepsilon_{\vec{k},\pm} = \pm t\,|f(\vec{k})| = \pm t\,|\gamma(\vec{k})|$ ✓ cf. (3-10A)

3.8. Low-energy effective Hamiltonian ($\hbar = 1$)

▷ band touching at K, K' points: $\vec{K}_\xi = \xi\left(\frac{4\pi}{3\sqrt{3}a}, 0\right)$ with valley index $\xi \in \{+,-\}$

▷ introduce momentum $\vec{q}$ measured from $\vec{K}_\xi$ point: $\vec{k} = \vec{K}_\xi + \vec{q}$ (3-13A)

↳ expand $f(\vec{k})$ near $\vec{K}_\xi$: $f(\vec{k}) \approx \frac{3at}{2}(\xi q_x - i q_y) + \mathcal{O}(q^2)$ (3-13B)

↳ near $\vec{K}_+$: $\mathcal{H}_q^+ = \frac{3at}{2}\begin{pmatrix} 0 & q_x - iq_y \\ q_x + iq_y & 0 \end{pmatrix} = \frac{3at}{2}\vec{\sigma}\cdot\vec{q}$ (3-13C)

↳ near $\vec{K}_-$: $\mathcal{H}_q^- = \frac{3at}{2}\begin{pmatrix} 0 & -q_x - iq_y \\ -q_x + iq_y & 0 \end{pmatrix} = -\frac{3at}{2}\vec{\sigma}^*\cdot\vec{q}$ (3-13D)

• with vector of Pauli matrices $\vec{\sigma} = (\sigma_x, \sigma_y)$

▷ 2D Weyl Hamiltonians $\mathcal{H}_q^{+/-}$

↳ conical dispersion $\mathcal{E}(\vec{q}) = \pm v_F |\vec{q}|$ (3-13E)

↳ with Fermi velocity $v_F = \frac{3at}{2} \sim \frac{c}{300}$ (3-13F)

speed of light

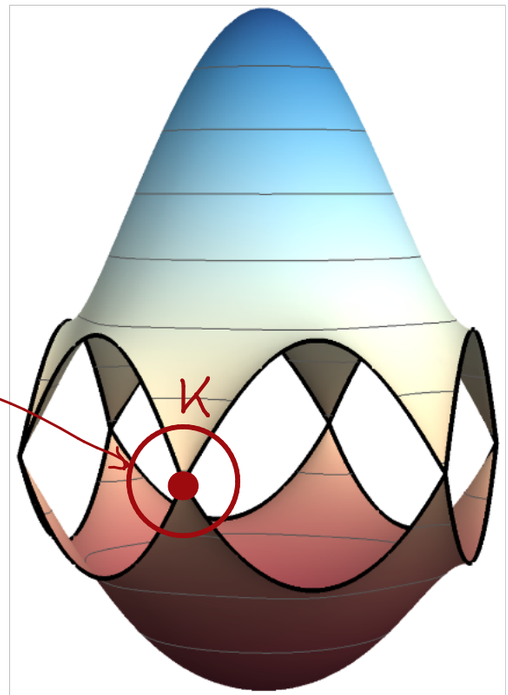

▷ low-energy Hamiltonian near $\vec{K}_\xi$ points

$$H = v_F \int_{\vec{k}=\vec{K}+\vec{q}} d^2\vec{q}\, (a^\dagger(\vec{k}), b^\dagger(\vec{k}))[\sigma_x q_x + \sigma_y q_y]\begin{pmatrix} a(\vec{k}) \\ b(\vec{k}) \end{pmatrix} + v_F \int_{\vec{k}=-\vec{K}+\vec{q}} d^2\vec{q}\, (a^\dagger(\vec{k}), b^\dagger(\vec{k}))[-\sigma_x q_x + \sigma_y q_y]\begin{pmatrix} a(\vec{k}) \\ b(\vec{k}) \end{pmatrix}$$

↳ introduce spinor $\Psi = \begin{pmatrix} \Psi_+(\vec{q}) \\ \Psi_-(\vec{q}) \end{pmatrix}$ with $\Psi_+ = \begin{pmatrix} a(\vec{K}+\vec{q}) \\ b(\vec{K}+\vec{q}) \end{pmatrix}$ and $\Psi_- = \begin{pmatrix} a(-\vec{K}+\vec{q}) \\ b(-\vec{K}+\vec{q}) \end{pmatrix}$ (3-14A)

↳ rewrite $H = v_F \int d^2\vec{q}\, \Psi^\dagger(\vec{q}) \left[\begin{pmatrix} \sigma_x & 0 \\ 0 & -\sigma_x \end{pmatrix} q_x + \begin{pmatrix} \sigma_y & 0 \\ 0 & \sigma_y \end{pmatrix} q_y \right] \Psi(\vec{q})$

$$\Rightarrow \quad H = v_F \int d^2\vec{q}\, \Psi^\dagger(\vec{q}) [\alpha_1 q_x + \alpha_2 q_y] \Psi(\vec{q}) \qquad \text{(2D Dirac-Weyl Hamiltonian)} \qquad (3\text{-}14B)$$

- here $\alpha_1 = \sigma_z \otimes \sigma_x$ and $\alpha_2 = \mathbb{1} \otimes \sigma_y$ (3-14C)

↳ Clifford algebra $\{\alpha_i, \alpha_j\} = 2\delta_{ij}\mathbb{1}_4$ (σ_x, σ_y : irreducible representation in 2D)

↳ alternatively $\alpha_1 = i\gamma_0\gamma_1$ and $\alpha_2 = i\gamma_0\gamma_2$ ⇝ $\{\gamma_\mu, \gamma_\nu\} = 2\delta_{\mu\nu}$ with $\mu \in \{0,1,2\}$

▷ <u>elections in graphene with low energy</u> are governed by <u>2D Dirac-Weyl Hamiltonian</u>

↳ therefore the 2 band touching points (<u>valleys</u>) at K, K' are called <u>Dirac points</u>

3.9. Massless Dirac fermions in graphene

▷ consider single Dirac point, no K-K' mixing and spin independence

↳ for example valley "+": $\mathcal{H}_q^+ = v_F(q_x\sigma_x + q_y\sigma_y)$ ⟶

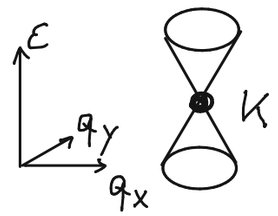

↳ resulted from tb model with only nn hopping ⇝ what happens for more realistic model?

↳ more generally: what happens to Dirac cone in presence of <u>perturbations</u>?

▷ <u>general 2×2 Hamiltonian</u> (for system with 2 energy bands):

$$\mathcal{H} = a(\vec{q})\mathbb{1} + b_x(\vec{q})\sigma_x + b_y(\vec{q})\sigma_y + b_z(\vec{q})\sigma_z \qquad (3\text{-}15A)$$

$$\Rightarrow \underline{\text{energy dispersion}}: \quad \mathcal{E}_\pm(\vec{q}) = a(\vec{q}) \pm \sqrt{b_x(\vec{q})^2 + b_y(\vec{q})^2 + b_z(\vec{q})^2} \qquad (3\text{-}15B)$$

↳ <u>band touching</u> (BT) of $\mathcal{E}_+(\vec{q}_0)$ and $\mathcal{E}_-(\vec{q}_0)$ for some $\vec{q}_0$ only if $b_i(\vec{q}_0) = 0 \quad \forall\, i \in \{x, y, z\}$

↳ for general $\vec{q}$: $b_i(\vec{q}) \neq 0$

▷ <u>BT generally works in 3D</u>: three components of $\vec{q}$ ⇝ find simultaneous zeros of three $b_i(\vec{q})$

▷ <u>2D case:</u> only two components of $\vec{q}=(q_x, q_y)$ that can be freely varied

↳ impossible to find simultaneous zeros of 3 fcts. $b_i(\vec{q})$ without additional tuning!

▷ <u>concretely</u> (2D): consider q independent, translationally invariant perturbation of $\mathcal{H}_q^+$ (3-13C):

$$\mathcal{H}_{pert.} = a\,\mathbb{1} + b_x\sigma_x + b_y\sigma_y + b_z\sigma_z \qquad (3\text{-}16A)$$

$$\Rightarrow\quad \mathcal{H}' = \mathcal{H}_q^+ + \mathcal{H}_{pert.} = \begin{pmatrix} a+b_z & v_F(q_x - iq_y)+b_x-ib_y \\ v_F(q_x+iq_y)+b_x+ib_y & a-b_z \end{pmatrix} \qquad (3\text{-}16B)$$

$$\Rightarrow\quad \varepsilon_\pm(\vec{q}) = a \pm \sqrt{\underbrace{(v_F q_x + b_x)^2 + (v_F q_y + b_y)^2}_{=0 \text{ for some } \vec{q}} + \underbrace{b_z^2}_{\text{splits degeneracy of bands}}} \qquad (3\text{-}16C)$$

↳ 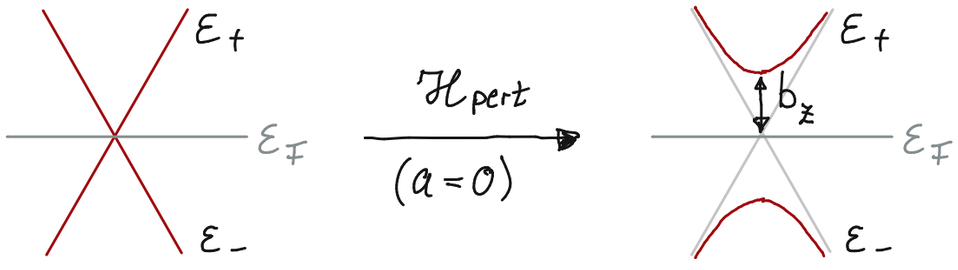

↝ <u>Dirac mass</u> $(b_z \to m)$ (3-16D)

↳ Fermi points for Dirac fermions are unstable w.r.t. perturbations in 2D*

* Hořava, Phys. Rev. Lett. 95, 016405 (2005)

▷ Fermi points for Dirac fermions can be <u>stabilized by symmetries</u>!

▷ <u>graphene</u>: complete low-energy Hamiltonian takes into account both valleys / K points

↳ 4×4 matrix: $\mathcal{H} = \begin{pmatrix} \mathcal{H}_q^+ & 0 \\ 0 & \mathcal{H}_q^- \end{pmatrix}$ with spinor basis $\Psi = (\Psi_+, \Psi_-)$ (3-17A)

↳ further: need to add spin ↑,↓ ⇝ 8×8 matrix (omitted here!)

▷ <u>symmetries</u>* * Mañes, Guinea, Vozmediano, Phys. Rev. B 75, 155424 (2007)

↳ <u>time reversal</u> $T: t \longrightarrow -t$ ⇝ reverses $\vec{K}$ (3-17B)

↳ <u>spatial inversion</u> $I: (x,y) \longrightarrow (-x,-y)$ ⇝ reverses $\vec{K}$ and exchanges A↔B (3-17C)

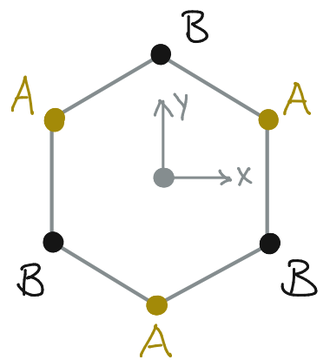

- point group operation around center of Wigner-Seitz cell
- operation exchanging sublattices: $\sigma_x \begin{pmatrix} c_{AA} & c_{AB} \\ c_{BA} & c_{BB} \end{pmatrix} \sigma_x = \begin{pmatrix} c_{BB} & c_{BA} \\ c_{AB} & c_{AA} \end{pmatrix}$

▷ graphene: both sublattices occupied by C ⇝ invariant under these symmetries

▷ symmetries put constraints on Hamiltonian:

$$\left.\begin{aligned} T: \quad & \mathcal{H}_q^+ = \mathcal{H}_{-q}^{-\,*} \\ I: \quad & \mathcal{H}_q^+ = \sigma_x \mathcal{H}_{-q}^- \sigma_x \end{aligned}\right\} \Longrightarrow \quad TI: \quad \mathcal{H}_q^+ = \sigma_x \mathcal{H}_q^{+\,*} \sigma_x \qquad (3\text{-}18A)$$

▷ eq. (3-18A) implies $\mathcal{H}^+_{q,11} = \mathcal{H}^+_{q,22} \xRightarrow{(3\text{-}16D)} m \overset{!}{=} 0$ (3-18B)

⇒ no mass gap opens in presence of <u>space-time inversion symmetry</u> TI

⇒ Dirac cones are protected by symmetries!

▷ case of inequivalent sublattices

↳ no inversion symmetry ⇝ $m \neq 0$ ⇝ gap opening

↳ this happens in hexagonal boron nitride (hBN)

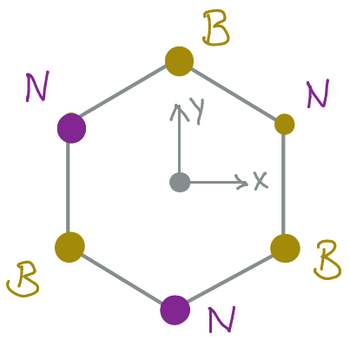

▷ note: similarly, C_3 symmetry fixes positions of Dirac cones to K, K'

▷ remark: mass contributions also have matrix form

↳ for Hamiltonian with both valleys, cf. (3-17A)

$$\mathcal{H}_{pert.} = M \otimes \sigma_z \quad \text{with} \quad M = \overbrace{m_0 \mathbb{1} + m_1 \sigma_z}^{\text{valley space}} \qquad (3\text{-}19A)$$

(σ_z: ↳ sublattice space)

- m_0 breaks inversion I, preserves time reversal T
- m_1 preserves inversion I, breaks time reversal T

↳ $m_0 > m_1$ ↝ charge density wave state (CDW)

↳ $m_1 > m_0$ ↝ quantum <u>anomalous</u> Hall effect (QAHE) ↝ QHE without magnetic field

↝ $\sigma_{xy} \propto \mathrm{sgn}(m_1) \frac{e^2}{h}$ ↝ Haldane model*

* F.D.M. Haldane, Phys. Rev. Lett. 61, 2015 (1988)

▷ various mass terms may be caused by

↳ <u>explicit</u> symmetry breaking or <u>spontaneous</u> symmetry breaking

↳ external fields, substrate, ... ↳ interactions (Coulomb, electron-phonon, ...)

3.10. Graphene in a magnetic field

▷ electrons in magnetic field ⇝ substitution $p_i \longrightarrow p_{oi} = p_i - \frac{e}{c} A_i$ (3-20A)

(vector potential)

↳ Hamiltonian near $\vec{K}$ (3-13C): $\mathcal{H}_q^+ \longrightarrow \mathcal{H}_{q_o}^+ = \begin{pmatrix} 0 & q_{ox} - iq_{oy} \\ q_{ox} + iq_{oy} & 0 \end{pmatrix}$ (3-20B)

↳ corresponding 2-component wavefunction $\Psi_+ = (\Psi_{A,+}, \Psi_{B,+})^T$ (3-20C)

↳ choose magnetic field perpendicular to graphene layer

• corresponding vector potential in Landau gauge $\vec{A} = (-By, 0, 0)^T$ (3-20D)

▷ Landau levels in graphene

↳ eigenvalue eqs.: $\left.\begin{aligned} \varepsilon \Psi_{A+} &= v_F (q_{ox} - iq_{oy}) \Psi_{B+} \\ \varepsilon \Psi_{B+} &= v_F (q_{ox} + iq_{oy}) \Psi_{A+} \end{aligned}\right\} \Longrightarrow$ (inserting one into the other)

$$\begin{cases} \varepsilon^2 \Psi_{A+} = (q_{ox} - iq_{oy})(q_{ox} + iq_{oy}) \Psi_{A+} & \text{(3-20E)} \\ \varepsilon^2 \Psi_{B+} = (q_{ox} + iq_{oy})(q_{ox} - iq_{oy}) \Psi_{B+} & \text{(3-20F)} \end{cases}$$

▷ find energy levels using eq. (3-20F)

$$\frac{\mathcal{E}^2}{v_F^2}\psi_{B+} = \left((q_x+\tfrac{e}{c}B_y) + iq_y\right)\cdot\left((q_x+\tfrac{e}{c}B_y) - iq_y\right)\psi_{B+} = \Big((q_x+\tfrac{e}{c}B_y)^2 - i\underbrace{(q_x+\tfrac{e}{c}B_y)q_y + iq_y(q_x+\tfrac{e}{c}B_y)}_{=[q_x+\frac{e}{c}B_y,\,q_y]} + q_y^2\Big)\psi_{B+}$$

$$= \left((q_x+\tfrac{e}{c}B_y)^2 - i[q_x+\tfrac{e}{c}B_y,\,q_y] + q_y^2\right)\psi_{B+} = \left((q_x+\tfrac{e}{c}B_y)^2 - i\tfrac{e}{c}B(+i\hbar) + q_y^2\right)\psi_{B+}$$

$$= \left((q_x+\tfrac{e}{c}B_y)^2 + \tfrac{\hbar e}{c}B + q_y^2\right)\psi_{B+} \qquad (3\text{-}21A)$$

$e=-e_0$

$$\Longleftrightarrow \quad \left(\frac{\mathcal{E}^2}{v_F^2} + \frac{\hbar e_0}{c}B\right)\psi_{B+} = \left(\left(\frac{e_0B}{c}\right)^2\left(y - \frac{q_x c}{e_0 B}\right)^2 + q_y^2\right)\psi_{B+} \qquad |\cdot\tfrac{1}{2m}$$

H': harmonic oscillator (oscillating around y_0)

$$\Longleftrightarrow \quad \frac{1}{2m}\left(\frac{\mathcal{E}^2}{v_F^2} + \frac{\hbar e_0}{c}B\right)\psi_{B+} = \left(\frac{\tilde{k}^2}{2}(y-y_0)^2 + \frac{q_y^2}{2m}\right)\psi_{B+} \quad \text{with } \tilde{k} = \frac{e_0B}{c\sqrt{m}},\ y_0 = \frac{q_x c}{e_0 B}$$

↳ if ψ_{B+} is eigenfct. of H' ⇝ eigenvalues: $\hbar\omega_c(n+\tfrac{1}{2})$ with $n\in\mathbb{N}$ and $\omega_c = \frac{\tilde{k}}{\sqrt{m}} = \frac{e_0B}{mc}$

▷ energy eigenvalues for Landau levels in graphene satisfy

$$\frac{1}{2m}\left(\frac{\mathcal{E}^2}{v_F^2} + \frac{\hbar e_0 B}{c}\right) = \hbar\omega_c\left(n+\tfrac{1}{2}\right) \Rightarrow \frac{\mathcal{E}^2}{v_F^2} = 2m\hbar\omega_c\left(n+\tfrac{1}{2}\right) - \frac{\hbar e_0 B}{c}$$

↳ $\mathcal{E}$ has positive and negative roots ⇝ extend domain of n to integers, i.e. $n\in\mathbb{Z}$

↳ <u>Landau levels (LL)</u> $\mathcal{E}_n = \hbar\omega_{Dirac}\,\mathrm{sgn}(n)\sqrt{|n|}$ with $\omega_{Dirac} = v_F\sqrt{\frac{2e_0B}{\hbar c}}$ (3-21B)

- recall: <u>usual</u> Landau levels $\mathcal{E}_n = (n+\tfrac{1}{2})\hbar\omega_c$ with $\omega_c = \frac{eB}{m}$ (3-21C)

▷ Comments:

↳ disregarded electron spin ⇝ additional 2-fold "degeneracy" (note: small Zeeman splitting!)

↳ additional 2-fold degeneracy from valley d.o.f.

↳ same procedure for Ψ_{A+} ⇝ $\varepsilon^2/v_F^2 = \frac{\hbar e_0 B}{c} 2(n+1)$, $n \in \mathbb{N}_0$ ⇝ no $\varepsilon = 0$ level!

- wavefcts at LL $n=0$ should have $\Psi_{A+} = 0$ (and $\Psi_{B+} \neq 0$) ⇝ $n=0$ level is special

▷ observation of level spacing $\propto \sqrt{|n|}$ (3-21B)

⇒ unusual sequence of LLs in contrast to (3-21C)

⇝ confirmation of Dirac electrons in graphene!

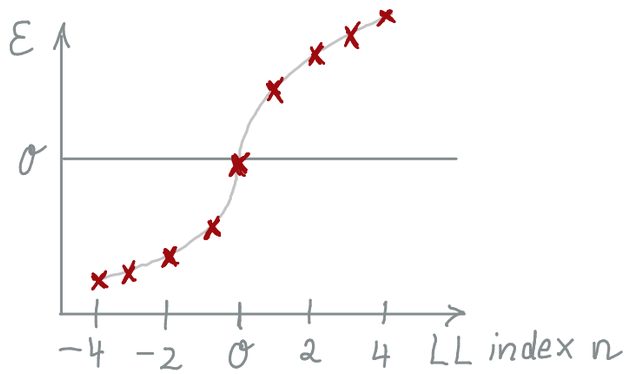

▷ large separation of lower Landau levels

↳ QHE at room temperature

↳ filling of 1LL changes Hall conductivity σ_{xy} by $2 \times 2 \times e^2/h$ (spin, valley)

3.11. Coulomb/Hubbard interaction

▷ electronic field operators $\Psi_\sigma(\vec{r})$ in many-body Hamiltonian:

$$H = \underbrace{\sum_\sigma \int_{\vec{r}} \Psi_\sigma^\dagger(\vec{r}) \left[-\frac{\vec{\nabla}^2}{2m} + U(\vec{r}) - \mu \right] \Psi_\sigma(\vec{r})}_{H_0} + \underbrace{\frac{e^2}{2} \sum_{\sigma\sigma'} \int_{\vec{r}} \int_{\vec{r}'} \frac{\Psi_\sigma^\dagger(\vec{r}) \Psi_\sigma(\vec{r}) \Psi_{\sigma'}^\dagger(\vec{r}') \Psi_{\sigma'}(\vec{r}')}{|\vec{r} - \vec{r}'|}}_{H_I}$$

↳ decompose $\Psi_\sigma(\vec{r})$ in Wannier fcts. $w_{n,\vec{R}}(\vec{r} - \vec{R})$ centered at sites $\vec{R}$: $\Psi_\sigma(\vec{r}) = \sum_{n\vec{R}} w_{n,\vec{R}}(\vec{r} - \vec{R}) c_{n\vec{R}\sigma}$

▷ interaction term: $H_I = \frac{1}{2} \sum_{\sigma\sigma'} \sum_{\substack{R_1 \dots R_4 \\ n_1 \dots n_4}} V_{n_1 \dots n_4}(R_1, \dots, R_4)\, c^\dagger_{n_1 R_1 \sigma} c_{n_2 R_2 \sigma} c^\dagger_{n_3 R_3 \sigma'} c_{n_4 R_4 \sigma'}$

↳ with $V_{n_1 \dots n_4}(R_1, \dots, R_4) = e^2 \int_{\vec{r}} \int_{\vec{r}'} \frac{w^*_{n_1}(r - R_1)\, w_{n_2}(r - R_2)\, w^*_{n_3}(r' - R_3)\, w_{n_4}(r' - R_4)}{|r - r'|}$

↳ onsite term ($R_1 = R_2 = R_3 = R_4$) is largest: $U := e^2 \int_r \int_{r'} \frac{|w(r)|^2 |w(r')|^2}{|r - r'|}$ (Hubbard U)

↳ must have $\sigma \neq \sigma'$ in H_I because of Pauli principle

▷ Hubbard model: combine nearest-neighbor hopping and onsite i.a.

$$H_{\text{Hubbard}} = -t \sum_{\langle R, R' \rangle} \left[c^\dagger_{R\sigma} c_{R'\sigma} + \text{h.c.} \right] + U \sum_R c^\dagger_{R\uparrow} c_{R\uparrow} c^\dagger_{R\downarrow} c_{R\downarrow}$$

3.12. Summary

▷ low-energy electrons in graphene behave like <u>2D massless Dirac electrons</u> with $v_F \sim c/300$

↳ symmetry protected Dirac cones

↳ characteristic Landau levels

▷ graphene: almost everything explainable as <u>single-particle physics</u>

↳ to correlate or localize electrons: need interaction $U >$ bandwidth W

↳ graphene has large bandwidth $W \sim 3t$ ↝ interactions don't rearrange e^- over whole band

▷ twisted bilayer graphene ↝ strongly reduced bandwidth

↝ next chapter ...

4. Electronic structure of twisted bilayer graphene

4.1. Preparations

▷ start with AA stacked bilayer of graphene ↝ rotate the layers by angle $\pm\theta/2$

↳ obtain new basic lattice vectors $\vec{a}_i^{(\ell)} = \mathcal{R}(\pm\theta/2)\,\vec{a}_i$ (4-1A)

(2-3A,B), (2-10A)

• layer index $\ell \in \{1,2\}$

↳ analoguously: reciprocal lattice spanned by $\vec{a}_i^{*(\ell)} = \mathcal{R}(\pm\theta/2)\,\vec{a}_i^{*}$ (4-1B)

(2-4A,B)

• position of K, K' points shifted: $\vec{K}_\xi^{(\ell)} = \vec{K}_\pm^{(\ell)} = \mp\frac{1}{3}(2\vec{a}_1^{*(\ell)} + \vec{a}_2^{*(\ell)})$ (4-1C)

ξ valley index

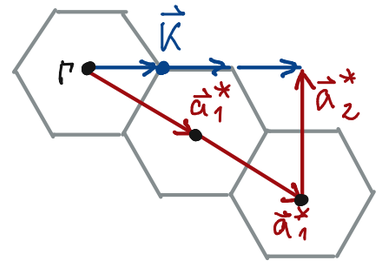

▷ low-energy Hamiltonians of rotated single layers

$$\mathcal{H}_\xi^{(\ell)}(\vec{k}) = v_F\left[\mathcal{R}(\pm\theta/2)(\vec{k} - \vec{K}_\xi^{(\ell)})\cdot(\xi\sigma_x, \sigma_y)\right] \quad (4\text{-}1D)$$

↳ from taking into account shift of K, K' points and Pauli matrices $e^{-i\frac{\theta}{4}\sigma_z}(\sigma_x,\sigma_y)e^{+i\frac{\theta}{4}\sigma_z}$

↳ ignore intervalley mixing between $\xi = \pm$ (ok for small θ)

↳ valley ξ of two rotated but uncoupled graphene layers:

$$\mathcal{H}_0^{(\xi)} = \begin{pmatrix} \mathcal{H}_\xi^{(1)}(\vec{k}) & 0 \\ 0 & \mathcal{H}_\xi^{(2)}(\vec{k}) \end{pmatrix} \text{ with basis } (A_1, B_1, A_2, B_2) \quad (4\text{-}1E)$$

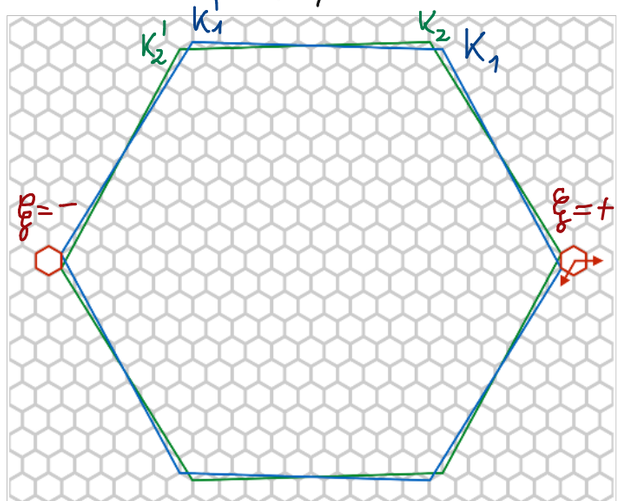

4.2. Interlayer coupling

▷ electrons can hop between the layers, cf. eq. (3-11B)

↳ Hamiltonian for valley ξ: $\mathcal{H}_{BM}^{(\xi)} = \begin{pmatrix} \mathcal{H}_\xi^{(1)}(k) & U^\dagger \\ U & \mathcal{H}_\xi^{(2)}(k) \end{pmatrix}$ with $U = \begin{pmatrix} u_{A_2A_1} & u_{A_2B_1} \\ u_{B_2A_1} & u_{B_2B_1} \end{pmatrix}$ (4-2A)

↳ U is an effective interlayer coupling matrix

- original work * Bistritzer and MacDonald, PNAS 108, 12233 (2011)
- here, I closely follow * Koshino et al, Phys. Rev. X 8, 031087 (2018)

▷ to determine U we start with $\theta = 0$ and constant in-plane displacement $\vec{\delta}$ from AA stacking

↳ real-space tight-binding contribution from Slater-Koster form, cf. eq. (3-11A)

$$H_{12} = -\sum_{ij} t(\vec{R}_i - \vec{R}_j)\, c_X^\dagger(\vec{R}_i)\, c_{X'}(\vec{R}_j) + \text{h.c.} \qquad (4\text{-}2B)$$

$$\text{"="} -\sum_{ij} t(\vec{R}_i - \vec{R}_j)\, |\vec{R}_i\rangle\langle\vec{R}_j| + \text{h.c.} \qquad (4\text{-}2C)$$

- X, X' denote sublattices A or B from layer 1 or 2, i.e. $X' \in \{A_1, B_1\}$ and $X \in \{A_2, B_2\}$

▷ lattice sites are then given as

↳ $$\vec{R}_j = \begin{cases} \vec{R}_{A_1} = n_1\vec{a}_1 + n_2\vec{a}_2 + \vec{\tau}_{A_1} \\ \vec{R}_{B_1} = n_1\vec{a}_1 + n_2\vec{a}_2 + \vec{\tau}_{B_1} \end{cases} \quad \text{where } n_1, n_2 \in \mathbb{Z} \qquad (4\text{-}3A),\ (4\text{-}3B)$$

in-plane displacement

↳ $$\vec{R}_i = \begin{cases} \vec{R}_{A_2} = n_1\vec{a}_1 + n_2\vec{a}_2 + \vec{\tau}_{A_1} + \vec{\delta} + d(\vec{\delta})\,\vec{e}_z \\ \vec{R}_{B_2} = n_1\vec{a}_1 + n_2\vec{a}_2 + \vec{\tau}_{B_1} + \vec{\delta} + d(\vec{\delta})\,\vec{e}_z \end{cases} \qquad (4\text{-}3C),\ (4\text{-}3D)$$

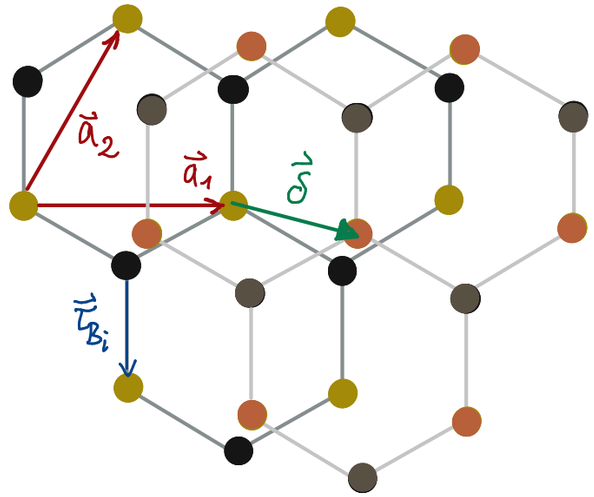

↳ we choose the sublattice basis vectors as $\vec{\tau}_{A_1} = \vec{\tau}_{A_2} = 0$ and $\vec{\tau}_{B_1} = \vec{\tau}_{B_2} = (0, -a)^T$

↳ $d(\vec{\delta})$ is the optimized interlayer distance ↝ depends on $\vec{\delta}$ (periodic in $\vec{a}_1$ and $\vec{a}_2$)

- $d(\vec{0}) = d_{AA}$ and $d(\vec{\tau}_{B_i}) = d_{AB}$
- interpolation for intermediate $\vec{\delta}$: $d(\vec{\delta}) = d_0 + 2d_1 \sum_{i=1}^{3} \cos(\vec{a}_i^{\,*} \cdot \vec{\delta})$ (4-3E)
- $\vec{a}_3^{\,*} = -\vec{a}_1^{\,*} - \vec{a}_2^{\,*}$ (4-3F)
- $d_0 = \frac{1}{3}(d_{AA} + 2d_{AB})$ and $d_1 = \frac{1}{9}(d_{AA} - d_{AB})$ (4-3G)

▷ we use the above definitions and go to Fourier space

using (4-2C)

↳ $$U_{x'x}(\vec{k},\vec{\delta}) \equiv \langle \vec{k},x' | H_{12} | \vec{k},x \rangle \tag{4-4A}$$

$$= -\sum_{n_1 n_2} t(n_1\vec{a}_1 + n_2\vec{a}_2 + \underbrace{(\vec{\tau}_{x'} - \vec{\tau}_x)}_{=\tau_{x'x}} + \vec{\delta} + d(\vec{\delta})\vec{e}_z)\, e^{-i\vec{k}\cdot(n_1\vec{a}_1 + n_2\vec{a}_2 + (\vec{\tau}_x - \vec{\tau}_{x'}) + \vec{\delta})} \tag{4-4B}$$

▷ $U_{x'x}(\vec{k},\vec{\delta})$ is periodic with periods $\vec{a}_1$ and $\vec{a}_2$ ↝ write it as Fourier expansion

↳ $$U_{x'x}(\vec{k},\vec{\delta}) = \sum_{m_1 m_2} \tilde{U}_{x'x}(m_1\vec{a}_1^* + m_2\vec{a}_2^* + \vec{k})\, e^{i(m_1\vec{a}_1^* + m_2\vec{a}_2^*)\cdot(\vec{\delta} + \vec{\tau}_{xx'})} \tag{4-4C}$$

- with $\tilde{U}_{x'x}(\vec{q}) := -\frac{1}{S_0}\int d^2\vec{R}\; t(\vec{R} + d(\vec{R} - \vec{\tau}_{x'x})\vec{e}_z)\, e^{-i\vec{q}\cdot\vec{R}}$ (4-4D)
- here $S_0 = \frac{\sqrt{3}}{2}a^2$ (unit area of singlelayer graphene)
- integration "$\int d^2\vec{R}$" is over infinite 2D space

▷ $t(\vec{R})$ decays exponentially in R with decay length $r_0 \sim 0.184\,a$, cf. eqs. (3-11B,C,D)

↳ Fourier transform $\tilde{U}_{x'x}(\vec{q})$ decays in $q \sim 1/r_0$

▷ now consider a rotation with <u>small relative twist angle</u> θ

↳▷ local lattice structure is approximately non-rotated bilayer with $\vec{\delta}$ slowly position dependent

$$\vec{\delta}(\vec{r}) = \left[R(\theta/2) - R(-\theta/2)\right]\vec{r} \qquad (4\text{-}5A)$$

($\vec{r}$: distance from center of rotation)

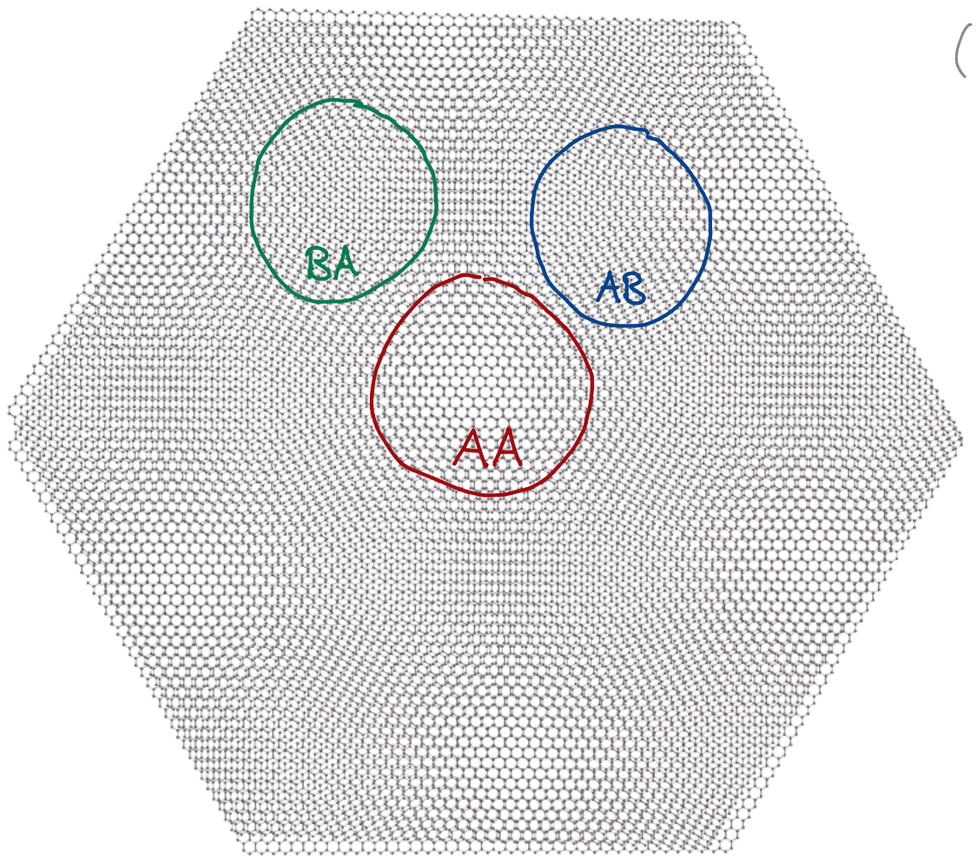

↳▷ can use previous expression with $U_{x'x}(\vec{K}_\xi, \vec{\delta}(\vec{r}))$ as approx. for interlayer coupling of valley ξ

(4-4C) & (4-5A)

$$\rightsquigarrow U_{x'x}(\vec{K}_\xi, \vec{\delta}(\vec{r})) = \sum_{m_1 m_2} \tilde{U}_{x'x}(m_1\vec{a}_1^{\,*} + m_2\vec{a}_2^{\,*} + \vec{K}_\xi)\, e^{i(m_1\vec{a}_1^{\,*} + m_2\vec{a}_2^{\,*})\cdot\vec{\tau}_{xx'}}\, e^{i(m_1\vec{G}_1^{\,M} + m_2\vec{G}_2^{\,M})\cdot\vec{r}} \qquad (4\text{-}5B)$$

• here we used $\vec{a}_i^{\,*}\cdot\delta(\vec{r}) = (a_i^{*(1)} - a_i^{*(2)})\cdot\vec{r} = \vec{G}_i^{\,M}\cdot\vec{r}$, cf. eqs. (2-11B)

▷ eq. (4-5B) is periodic in $\vec{r}$ with moiré reciprocal vectors $\vec{G}_i^M$

↳ $\tilde{U}_{x'x}(\vec{q})$ decays rapidly in q ⇝ only retain few Fourier components

↳ use the largest three terms $(m_1, m_2) = (0,0), \xi(1,0), \xi(1,1)$ in (4-5B)

⇝ $U = \begin{pmatrix} U_{A_2A_1} & U_{A_2B_2} \\ U_{B_2A_1} & U_{B_2B_1} \end{pmatrix}$ (cf. eq. (4-2A))

$$= \begin{pmatrix} u & u' \\ u' & u \end{pmatrix} + \begin{pmatrix} u & u'\omega^{-\xi} \\ u'\omega^{\xi} & u \end{pmatrix} e^{i\xi\vec{G}_1^M\cdot\vec{r}} + \begin{pmatrix} u & u'\omega^{\xi} \\ u'\omega^{-\xi} & u \end{pmatrix} e^{i\xi(\vec{G}_1^M+\vec{G}_2^M)\cdot\vec{r}} \quad (4\text{-}6A)$$

- here $\omega = \exp(2\pi i/3)$
- $u = -\frac{1}{S_0}\int d^2\vec{R}\; t(\vec{R}+d(\vec{R})\vec{e}_z)\, e^{-i\vec{K}_\xi\cdot\vec{R}} \approx 0.0797\,\text{eV}$ (4-6B)

  use Slater-Koster parameters
- $u' = -\frac{1}{S_0}\int d^2\vec{R}\; t(\vec{R}+d(\vec{R}-\vec{\tau}_{B_1})\vec{e}_z)\, e^{-i\vec{K}_\xi\cdot\vec{R}} \approx 0.0975\,\text{eV}$ (4-6C)

↳ $u < u'$ reflects that $d_{AA} > d_{AB}$ ⇝ corrugation in out-of-plane direction

- this difference introduces energy gaps between lowest bands and excited bands (see below)

4.3. Calculation of energy bands of TBG

▷ we use the <u>effective Hamiltonian</u> $\mathcal{H}_{BM}^{(\xi)}$, cf. eq. (4-2A) with (4-1D) and (4-6A)

↳ calculate eigenstates and eigenvalues in $\vec{k}$ space, with $\vec{k} \in$ moiré BZ

↳ moiré interlayer coupling hybridizes graphene's eigenstates at $\vec{q} = \vec{k} + \vec{G}$

- here $\vec{G} = m_1 \vec{G}_1^M + m_2 \vec{G}_2^M$, $m_1, m_2 \in \mathbb{Z}$

↳ the eigenstates can then be written as $\psi_{n\vec{k}}^X(\vec{r}) = \sum_{\vec{G}} C_{n\vec{k}}^X(\vec{G})\, e^{i(\vec{k}+\vec{G})\cdot\vec{r}}$ (4-7A)

- here $X \in \{A_1, B_1, A_2, B_2\}$ (sublattice index)
- n is the band index

▷ we're interested in the <u>low-energy states</u>

↳ dominated by states near graphene's Dirac points

↳ restrict $\vec{q}$ to values inside <u>cutoff</u> with $|\vec{q} - \vec{q}_0| < q_c$

- here $\vec{q}_0$ is midpoint between $K_\xi^{(1)}$ and $K_\xi^{(2)}$
- q_c is chosen as $q_c \sim 4|\vec{G}_1^M|$

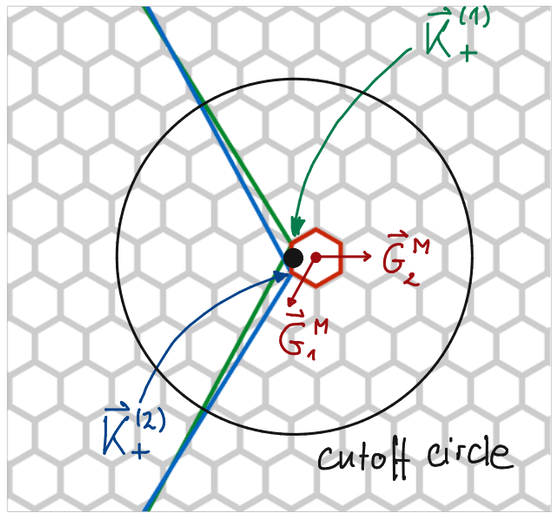

▷ we use $\mathcal{H}_{BM}^{(\xi)}$ to solve a Schrödinger-type eq. in momentum space w/ ansatz $\Psi_{n\vec{k}}^{X}(\vec{r})$

↳ intervalley coupling can be neglected ↝ independent calculation for each valley ξ

↳ $\mathcal{H}_{BM}^{(\xi)} \Psi_{n\vec{k}}^{X}(\vec{r}) = E\, \Psi_{n\vec{k}}^{X}(\vec{r})$ (4-8A)

↳ we separate $\mathcal{H}_{BM}^{(\xi)}$ as $\mathcal{H}_{BM}^{(\xi)} = \mathcal{H}_0^{(\xi)} + V$ with $V = \begin{pmatrix} 0 & u^\dagger \\ u & 0 \end{pmatrix}$ (4-8B)

- we have the Fourier expansion: $V = \sum_{\vec{G}''}{}' V_{\vec{G}''} e^{i\vec{G}''\cdot\vec{r}}$, cf. eq. (4-7A)

$$\overset{(4\text{-}7A)}{\rightsquigarrow} \sum_{\vec{G}} \mathcal{H}_0^{(\xi)} C_{n\vec{k}}^{X}(\vec{G}) e^{i(\vec{k}+\vec{G})\cdot\vec{r}} + \sum_{\vec{G},\vec{G}''}{}' V_{\vec{G}''} C_{n\vec{k}}^{X}(\vec{G}) e^{i(\vec{k}+\vec{G}+\vec{G}'')\cdot\vec{r}} = E \sum_{\vec{G}} C_{n\vec{k}}^{X} e^{i(\vec{k}+\vec{G})\cdot\vec{r}}$$

$$\Rightarrow \sum_{\vec{G}} \mathcal{H}_0^{(\xi)} \delta_{\vec{G},\vec{G}'} C_{n\vec{k}}^{X}(\vec{G}) + \sum_{\vec{G},\vec{G}''}{}' V_{\vec{G}''} \delta_{\vec{G}'-\vec{G},\vec{G}''} C_{n\vec{k}}^{X}(\vec{G}) = E \sum_{\vec{G}} C_{n\vec{k}}^{X}(\vec{G}) \delta_{\vec{G},\vec{G}'} \quad (4\text{-}8C)$$

▷ <u>eigenvalue eq.</u> (4-8C) yields matrix $\mathcal{H}_{\vec{G}\vec{G}'}$ to diagonalize w/ $\vec{G},\vec{G}'$ limited by cutoff q_c

- $\mathcal{H}_{\vec{G}\vec{G}'} = \begin{pmatrix} \mathcal{H}_\xi^{(1)}(\vec{k}+\vec{G}) & 0 \\ 0 & \mathcal{H}_\xi^{(2)}(\vec{k}+\vec{G}) \end{pmatrix} \delta_{\vec{G},\vec{G}'} + \begin{pmatrix} 0 & U_- \\ U_+ & 0 \end{pmatrix}$, (4-8D)

- $U_\lambda = \begin{pmatrix} u & u' \\ u' & u \end{pmatrix} \delta_{\vec{G},\vec{G}'} + \begin{pmatrix} u & u'\omega^{-\xi} \\ u'\omega^{\xi} & u \end{pmatrix} \delta_{\vec{G}'-\vec{G},\lambda\xi\vec{G}_1^M} + \begin{pmatrix} u & u'\omega^{\xi} \\ u'\omega^{-\xi} & u \end{pmatrix} \delta_{\vec{G}'-\vec{G},\lambda\xi(\vec{G}_1^M+\vec{G}_2^M)}$ (4-8E)

▷ <u>numerical diagonalization</u> of matrix (4-8D)

↳ tBG_BistritzerMacDonald.nb (Mathematica)
↝ for code, see appendix!

↳ diagonalizes $\mathcal{H}_{\vec{G}\vec{G}'}$ for chosen $\vec{k} \in$ moiré BZ

↳ choose $\vec{k}$ along path $K^M - \Gamma^M - M^M - K'^M$

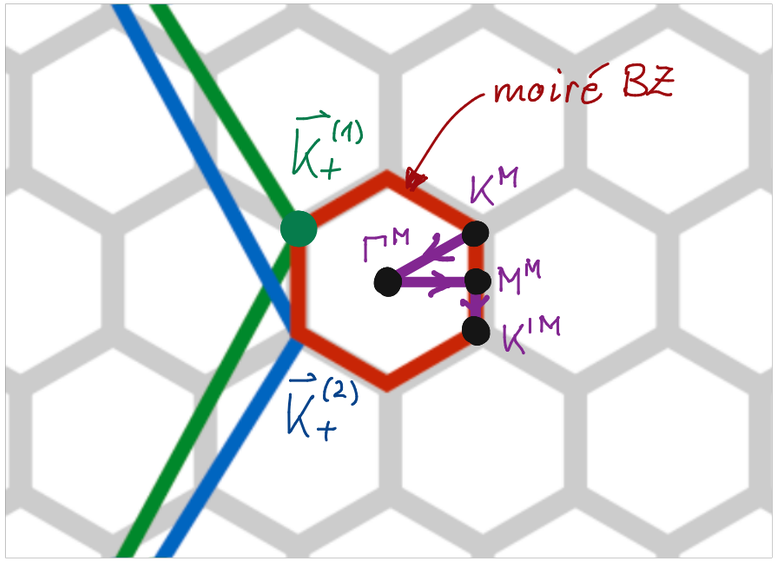

▷ evaluate for <u>different twist angles θ</u> for valley $\xi = +$

$\theta = 5°$ $\theta = 2°$ $\theta = 1.05°$

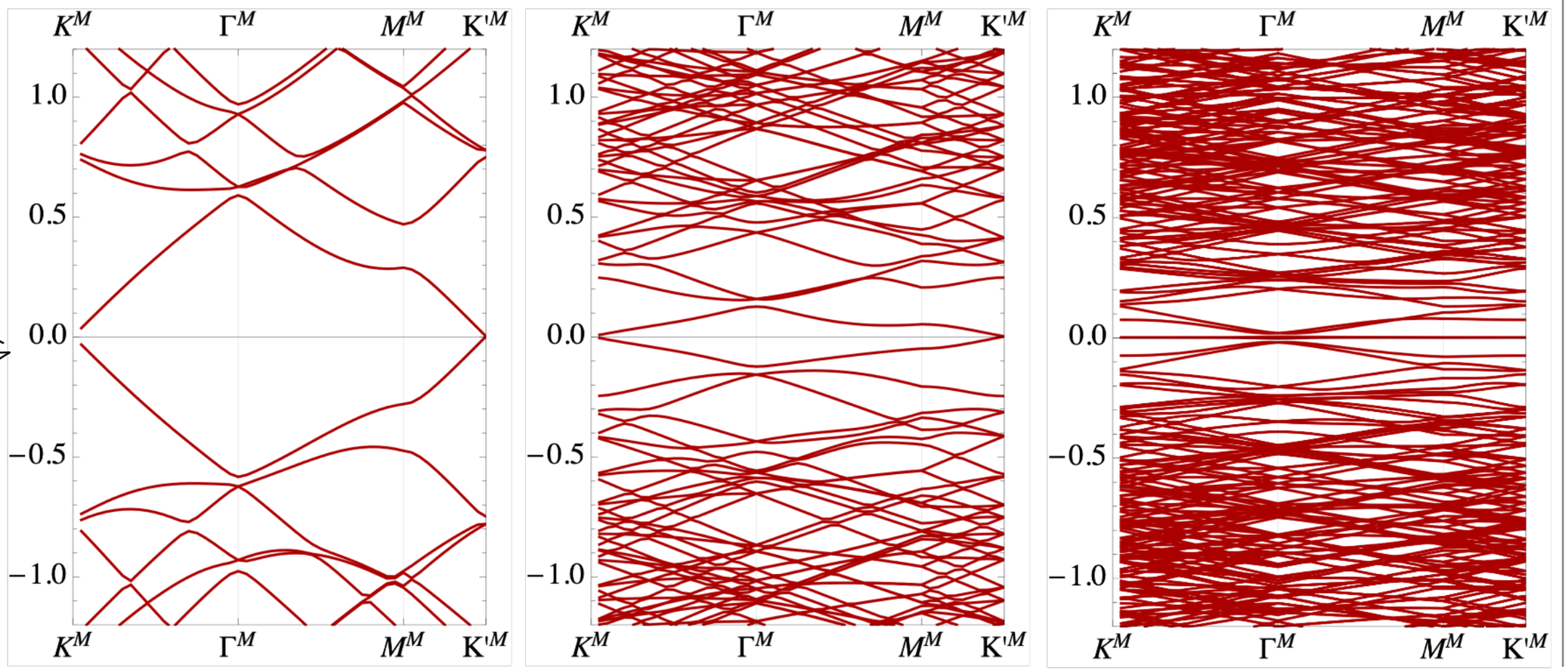

4.4. Properties of moiré bands in TBG

▷ for small angles : 2 bands/valley in middle of spectrum ("charge neutrality")

↳▷ these 2 bands are separated from all other bands by band gap

↳▷ bandwidth of the two separated bands decreases for decreasing angle

⇝ monotonic decrease expected because moiré BZ shrinks (4-10A)

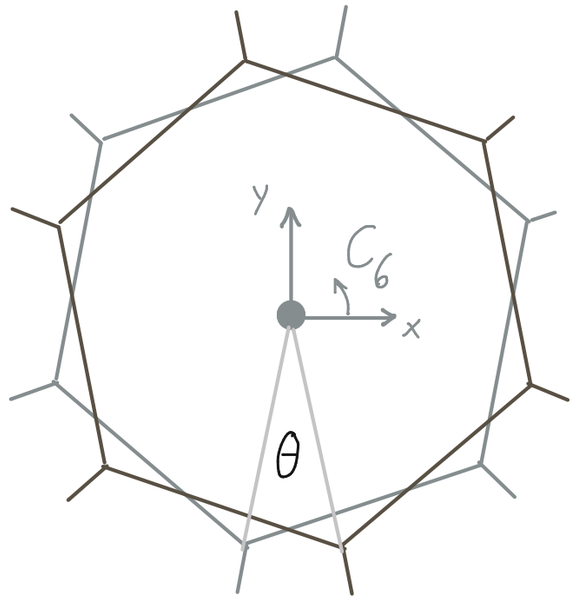

▷ TBG and the effective $\mathcal{H}_{BM}^{(\xi)}$

↳▷ preserve C_6, C_3, C_2 and time reversal symmetry T

↳▷ symmetry-protected Dirac points at K^M, K'^M:

⇝ energy dispersion : $\mathcal{E}_\theta(\vec{q}) = \pm v_F(\theta)|\vec{q}|$ (4-10B)

↳▷ due to (4-10A):

⇝ expect $v_F(\theta)$ to decrease monotonically w/ decreasing θ

⇝ instead one finds: $v_F(\theta)$ vanishes at $\theta_0 \approx 1.05°$

⇝ θ_0 is called the (first) magic angle

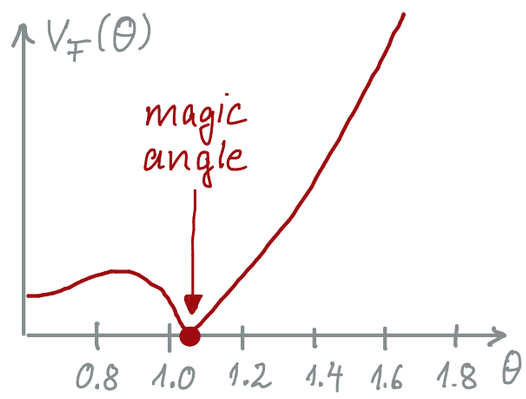

4.5. Flat bands near the magic angle

▷ near θ_0: Dirac points attached to 2 extremely flat bands ⇝ small band width

↳ flat bands are separated by band gap from other bands

↳ $\theta_0 \approx 1.05°$:

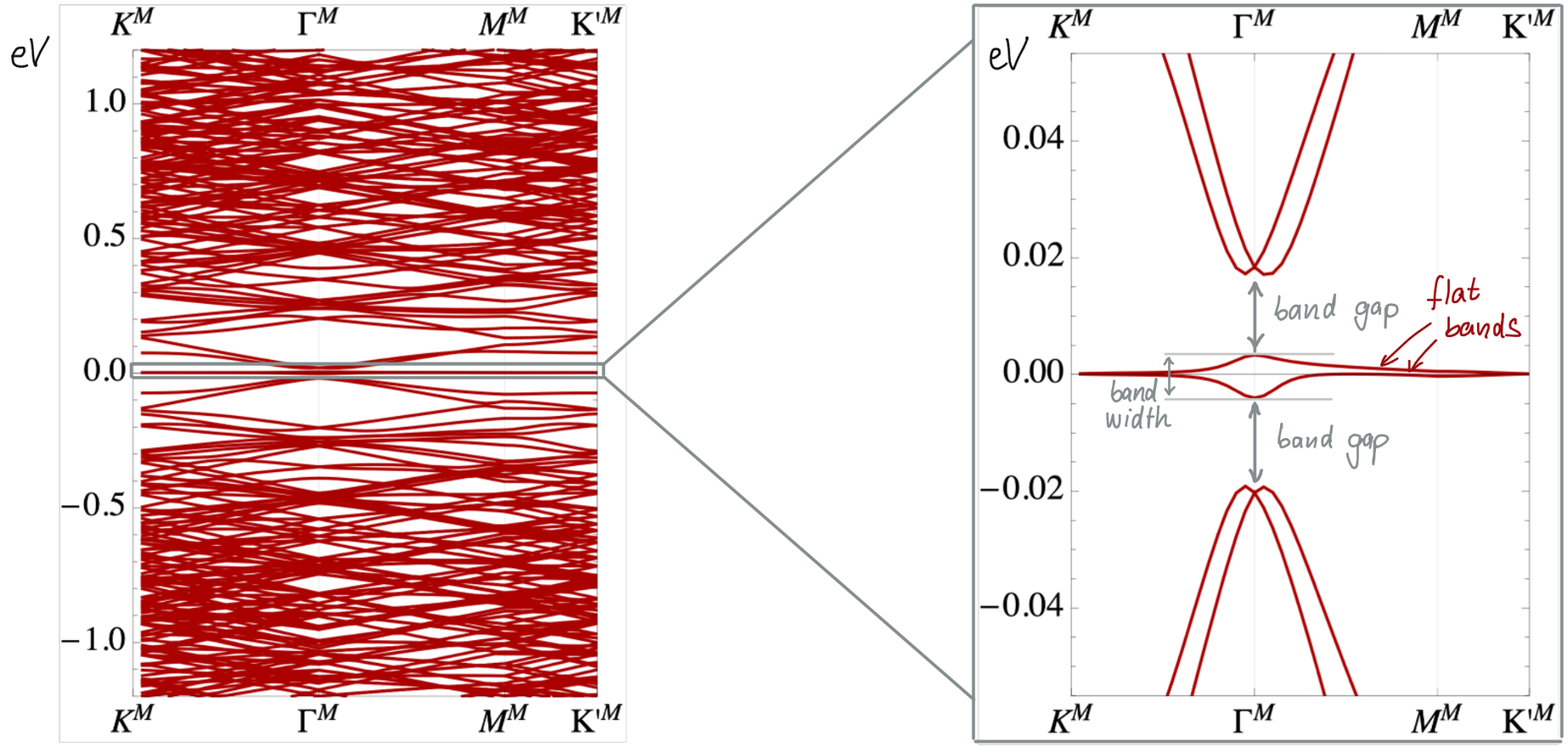

↳ flat bands weakly dispersive ⇝ saddle points in energy dispersion ⇝ van Hove singularities

↳ many aspects depend on details of the model Hamiltonian!

4.6. Band filling

▷ flat bands in magic-angle TBG : 4 spin-degenerate (topological) bands

↳ 2 bands for valley $\xi = +$ and 2 bands for valley $\xi = -$

↳ bandwidth $W_{TBG} \sim \mathcal{O}(10\,meV)$ in contrast to graphene where $W \sim \mathcal{O}(10\,eV)$

↳ band filling can be adjusted experimentally with electrical gates

↳ can study full range of fillings without chemical doping (in contrast to cuprates, ...)

▷ <u>flat band filling factor ν</u>: number of charge carriers (electrons/holes) per moiré cell

↳ $\nu = -4$: all bands are empty

↳ $\nu = 0$: half of the bands are filled (charge neutrality)

↳ $\nu = +4$: all bands are filled

↳ $\nu = \pm 1, \pm 2, \pm 3$: 1, 2, and 3 electrons (+) or holes (-) per moiré unit cell

} integer fillings

↳ fractional fillings : everything else for ν between -4 and $+4$

▷ flat bands and Fermi surfaces for both valleys $\xi = \pm$

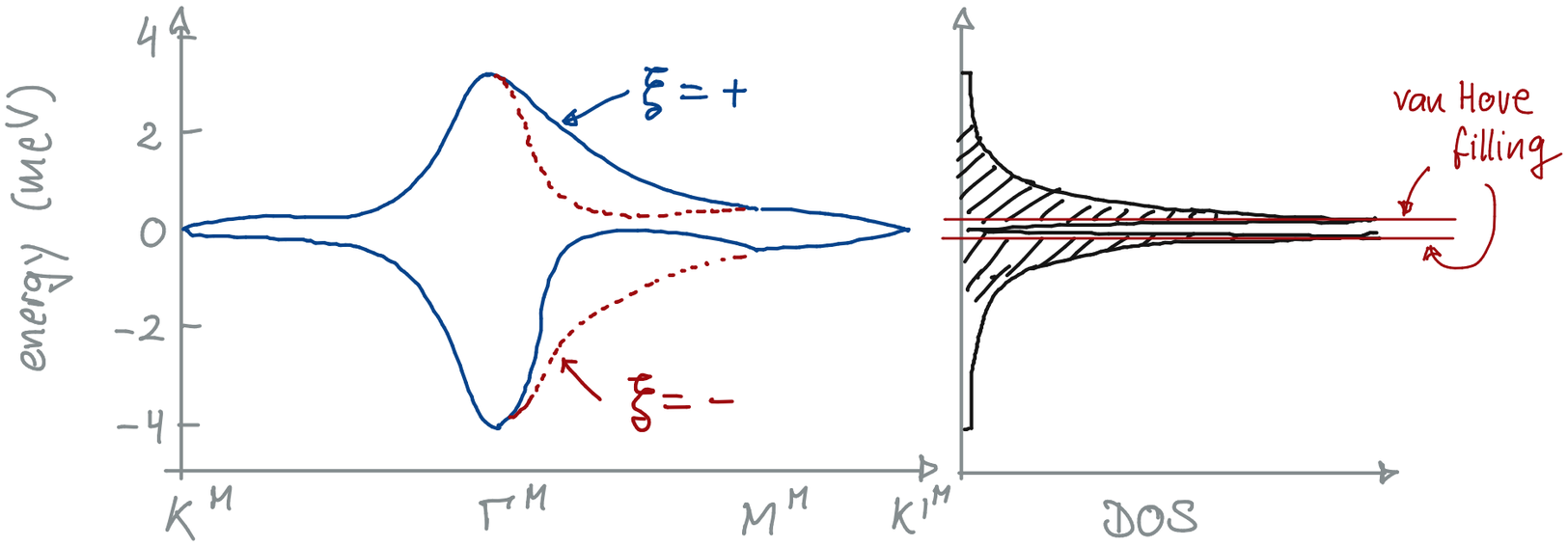

↳ energy contours for valley $\xi = +$ for filling of $+2e^-$ per moiré cell

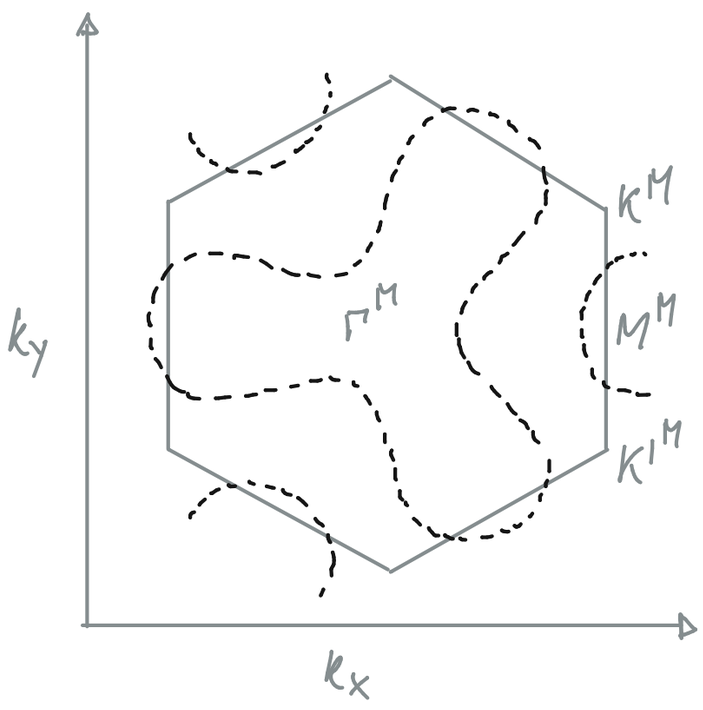

[• note: add discussion of Chern number of the flat bands in v2 of lecture notes.]

▷ Fermi surfaces at van Hove filling

↳ $\xi = +$ and $\xi = -$

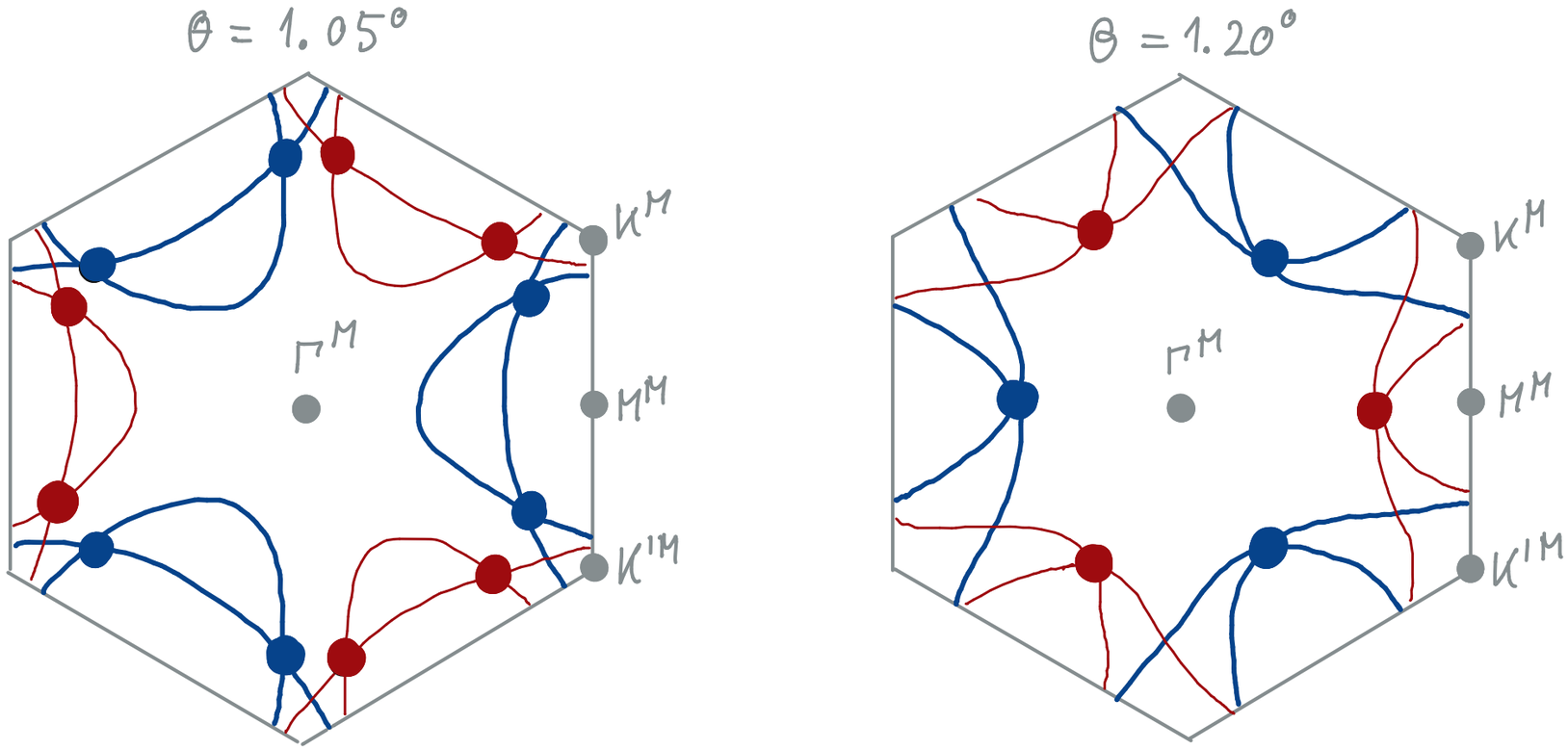

↳ saddle points marked by blue / red dots ⇝ Van Hove singularities in DOS

↳ depending on twist angle and details :

(1) 6 saddle points per valley in band intersecting FS

or (2) 3 saddle points per valley in band intersecting FS

↳ Van Hove points : hot spots for electronic interaction

4.7. Comments

▷ "fragile topology":

↳ flat bands for one valley contain two Dirac points (one from each layer)

↳ both Dirac points have same winding (come from same graphene K point)

↳ hard to write down simple tight-binding model for flat bands

* Po, Zou, Senthil, Vishwanath, Phys. Rev. B 99, 195455 (2019)

▷ mathematical origin of flat bands:

↳ interference of inter- and intralayer tunnelling

↳ rigorous treatment possible by setting $u=0$ in (4-6B) ("chiral limit")

↝ pair of perfectly flat isolated bands for discrete set of "magic" angles

↝ their wavefunctions are reminiscent of LL wavefunctions on torus

*Tarnopolsky, Kruchkov, Vishwanath, PRL 122, 106405 (2019)

5. Correlated phase diagram of twisted bilayer graphene

5.1. Phenomenology of magic-angle twisted bilayer graphene (MATBG)

▷ chapter 4: MATBG is metal for band filling factors $\nu \in [-4, 4]$

↳ but: bandwidth W_{TBG} is extremely small near magic angle

↝ suggests that interactions can play major role ↝ many-body ground states?

▷ MATBG phase diagram in full range of flat band fillings * Lu et al., Nature 574, 653 (2019)

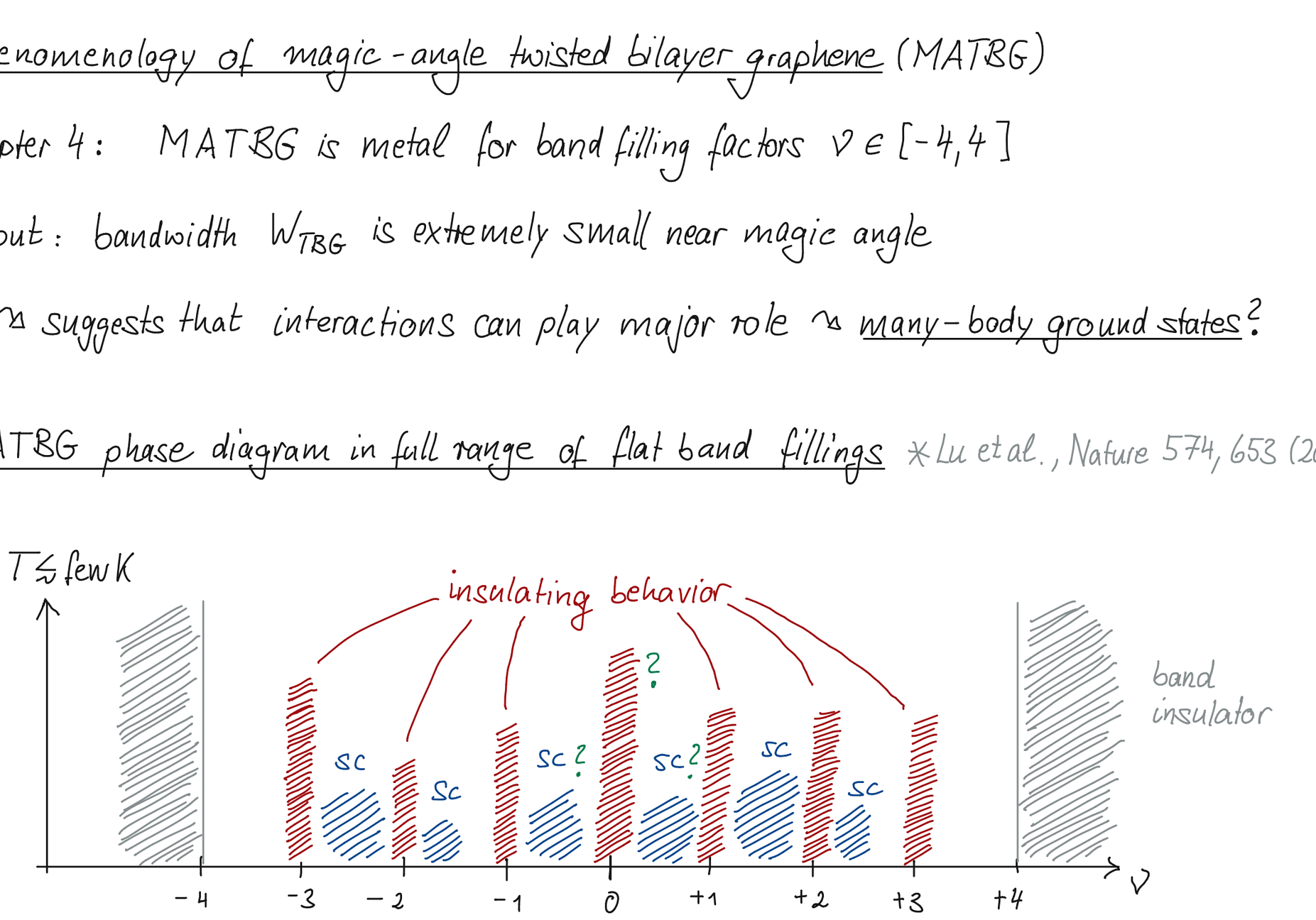

↳ insulating behavior at integer filling factors ν (some ferromagnetic)

↳ superconducting (SC) behavior between some insulators ($T_c \sim \mathcal{O}(1K)$)

} induced by interactions!

5.2. Similarities to other strongly-correlated materials (Sept. 2021)

▷ interaction-induced insulators and superconducting domes, see ρ 5-1 (cf. cuprates, pnictides,...)

▷ "large" $T_c/T_F \sim 0.1$:

↳ exceeds expected range at which standard weak-coupling theory of SC can be used

↳ similar to T_c/T_F of other materials near metal-insulator transition (cf. cuprates, pnictides,...)

▷ pseudogap state above SC dome (cf. cuprates, pnictides,...)

↳ density of states suppressed without being fully gapped

↳ pseudogap opens at Fermi energy in partially filled band

▷ strange metal phase (cf. cuprates, pnictides,...)

↳ high-T metallic state is "strange" ↝ cannot be described w/ coherent quasiparticles

↳ manifestation: resistivity $\rho \propto T$ down to temperatures below Debye scale

↝ seems in conflict with Fermi liquid theory, $\rho \propto T^2$

↝ alternative explanation of $\rho \propto T$: phonon scattering?

▷ broken symmetry states in pseudogap and SC phase (cf. cuprates, pnictides,...)

↳ global nematic charge order in partially filled band up to $T \sim 35\,K$ and $B \sim 8\,T$

↝ spontaneously broken lattice rotational symmetry

↝ precursor of (nematic?) SC at lower T?

↳ cf. high-T_c SCs: often hosts nematic/CDW/... states coexisting/competing with SC

5.3. Quantum anomalous Hall effect in MATBG

▷ at $\nu = 3$ ↝ spin- and valley-polarized ferromagnetic Chern insulator

↳▷ *quantum anomalous Hall effect ...*

↳▷ basic phenomenology of quatum Hall effect

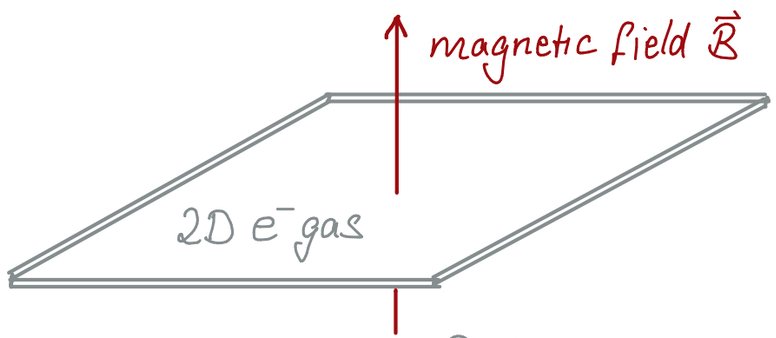

Peierls substitution

- free e^-: $H = \frac{\vec{p}^2}{2m} \rightsquigarrow \frac{(\vec{p} - e\vec{A})^2}{2m}$

  ↝ Landau levels: $E_n = \frac{eB}{m}(n + \frac{1}{2})$

  ↝ "normal" quantum Hall effect (QHE)

- transverse resistivity $\varrho_{xy} = \frac{h}{e^2}\nu, \nu \in \mathbb{N}$
- longitudinal conductivity $\sigma_{xx} = \varrho_{xx} / (\varrho_{xx}^2 + \varrho_{xy}^2)$

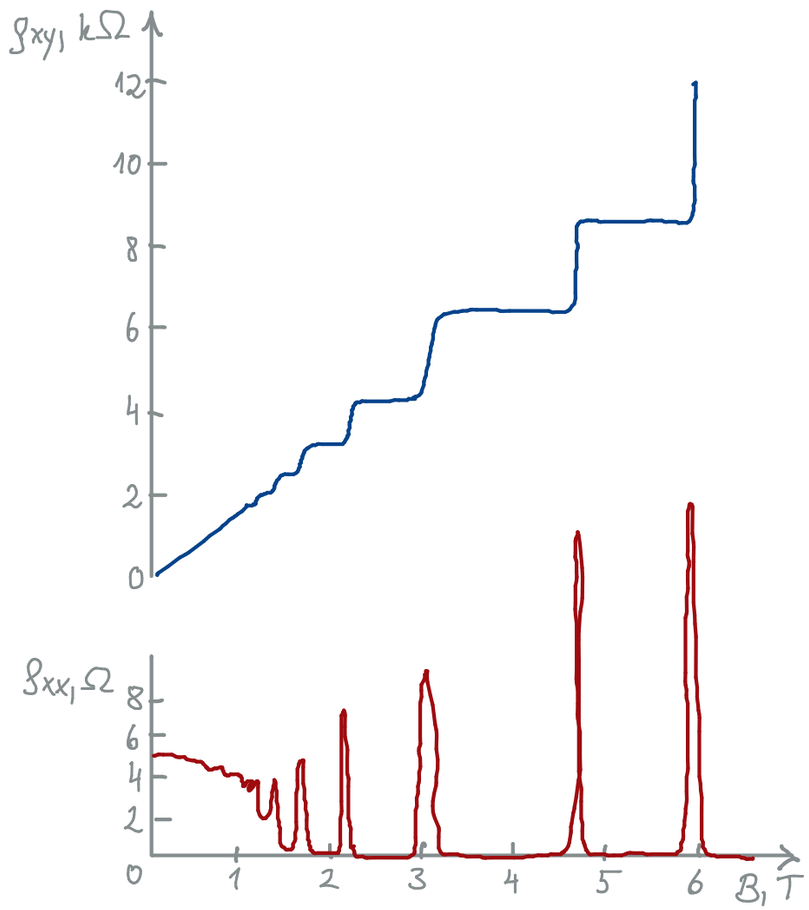

▷ observation in TBG at $\theta \sim 1.15°$, $\nu = 3$, $T \sim 1.6\,K$ *Serlin et al., Science 367, 900 (2020)

↳ spin- and valley-polarized <u>ferromagnetic</u> Chern insulator

↳ hysteretic transversal resistivity

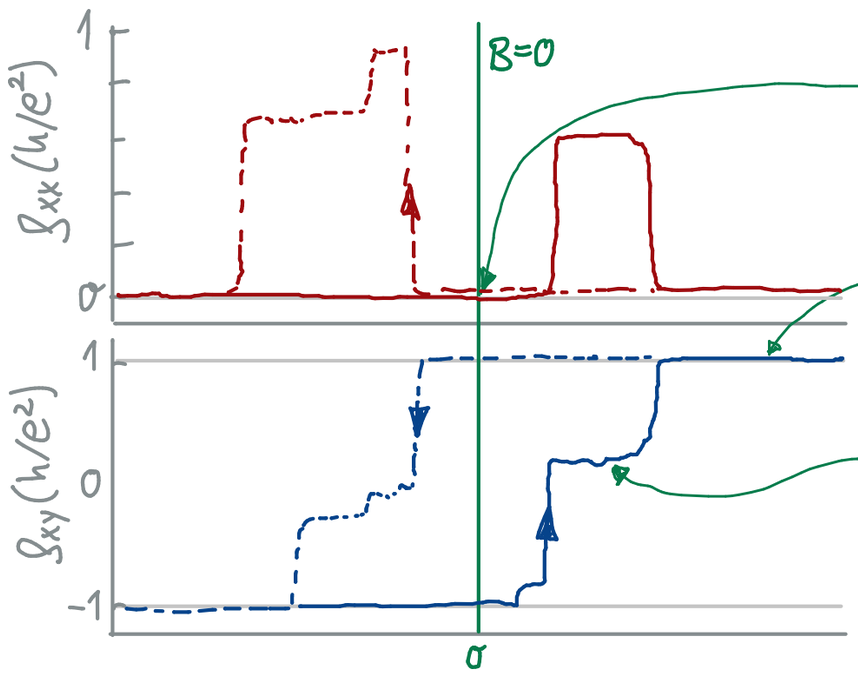

really insulating (not conducting) at $B = 0$

quantized to within 0.1% of h/e^2

steps from ferromagnetic domains

↘ time reversal symmetry is spontaneously broken

↳ not all samples show QAHE ↘ role of (mis-)aligned hBN substrate (sublattice-sym breaking)!

▷ Chern insulators w/ quantized Hall resistance plateaus at $\nu = \pm 3, \pm 2 \pm 1$

▷ magnetization is dominantly orbital (and not spin) (unique to MATBG)

▷ origin of (Chern) insulating states at integer ν? *Serlin et al., Science 367, 900 (2020)

↳ reduction of interaction energy by breaking spin/valley flavor symmetries ✓

↳ i.a.-induced insulators formed in flat bands at non-zero integer ν ✓

↳ flavor projected bands are topological ↝ quantum anomalous Hall effect ✓

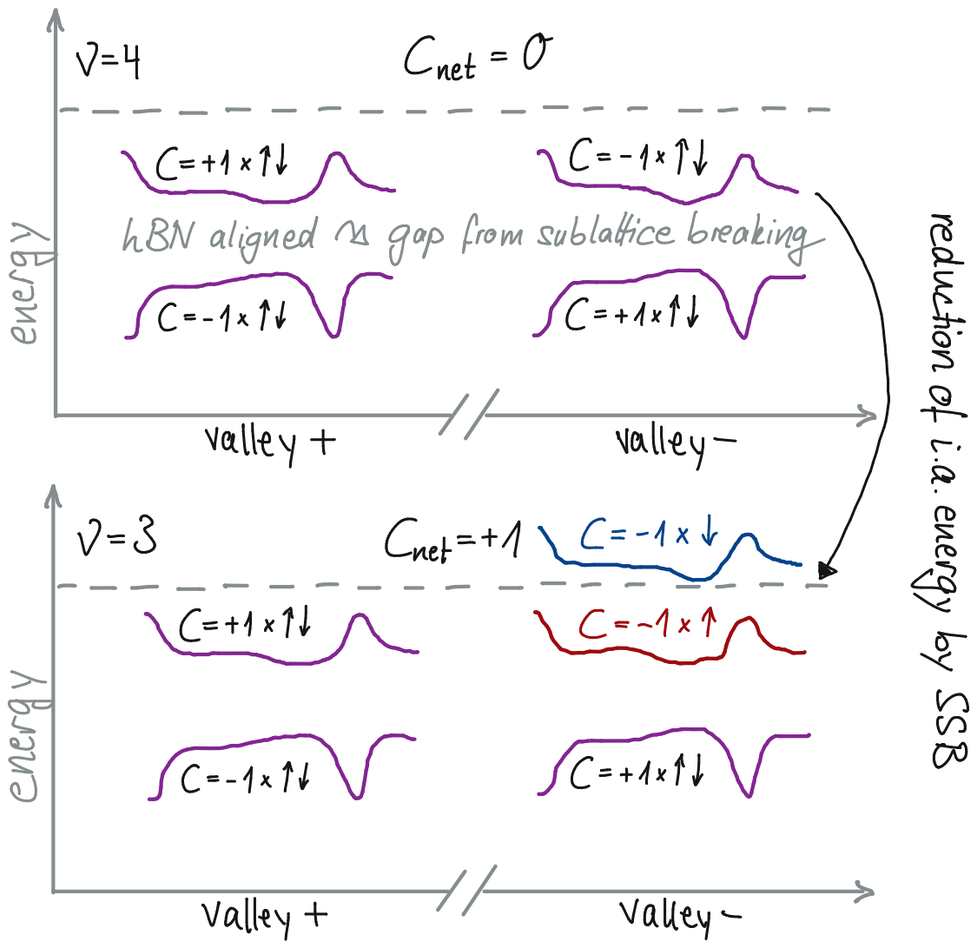

• spin-/valley polarization from i.a.

• non-zero Chern number

• breaking of time reversal symmetry

↝ quantum anomalous Hall effect!

5.4. Comment on superconductivity

▷ superconductivity: screening of magnetic field ↝ Meissner effect ↝ persistent electrical currents

↳ ordered state occurring below critical temp. T_c ↝ breaking of global U(1) symmetry

↳ microscopic theory by Bardeen, Cooper, & Schrieffer ↝ coherent state of e^- (Cooper) pairs

↳ needs effective attractive interaction between electrons ↝ "pairing"

▷ question: origin and nature of superconducting states in MATBG ?

↳ electrons require "pairing glue" (attractive i.a.)

↳ BCS theory: electron-phonon i.a. ↝ attractive electron-electron i.a. ?

- works for "conventional" SC (e.g. Pb, ...), but not for high-T_c SC (cuprates, ...)

↳ SC pairing mechanism from repulsive Coulomb i.a. ?

↝ what happens in MATBG? ?

▷ <u>conventional BCS theory in a nutshell</u>

↳ start with: $H = \sum_{\vec{k},\sigma} \varepsilon(\vec{k}) c^\dagger_{\vec{k}\sigma} c_{\vec{k}\sigma} + g \sum_{\vec{k},\vec{k}'} c^\dagger_{\vec{k}\uparrow} c^\dagger_{\vec{k}'\downarrow} c_{\vec{k}'\downarrow} c_{\vec{k}\uparrow}$, $g < 0$ (attractive i.a.) (5-5A)

↳ introduce "gap" from Cooper pairs: $\Delta = -g \sum_{\vec{k}} \langle c_{-\vec{k}\downarrow} c_{\vec{k}\uparrow} \rangle$ w/ $\langle A \rangle = \frac{tr(Ae^{-\beta H})}{tr(e^{-\beta H})}$ (5-5B)

↳ meanfield decoupling: $H = \sum_{\vec{k},\sigma} \varepsilon(\vec{k}) c^\dagger_{\vec{k}\sigma} c_{\vec{k}\sigma} - \sum_{\vec{k}} \left(\Delta^* c_{-\vec{k}\downarrow} c_{\vec{k}\uparrow} + \Delta c^\dagger_{\vec{k}\uparrow} c^\dagger_{-\vec{k}\downarrow} \right) + \ldots$ (5-5C)

↝ quasiparticle energy $E(\vec{k}) = \sqrt{\varepsilon(\vec{k})^2 + |\Delta|^2}$ ← energy gap at Fermi surface (5-5D)

↳ Δ from self-consistent <u>gap equation</u>: $\Delta = -g \sum_{\vec{k}} \frac{\Delta}{2E(\vec{k})} \tanh\left(\frac{E(\vec{k})}{k_B T} \right)$ (5-5E)

↳ T_c from <u>linearized gap eq.</u> ($\Delta \to 0$): $1 = -g \int_0^{\varepsilon_c} d\varepsilon \frac{\rho(\varepsilon)}{2\varepsilon} \tanh\left(\varepsilon / k_B T_c \right)$ (5-5F)

• with DOS $\rho(\varepsilon)$

▷ <u>additional symmetries</u> of normal-state Hamiltonian <u>may be broken</u> ↝ <u>unconventional SC</u>

↳ additional broken symmetries can include:

(1) crystal lattice (2) spin rotation (3) time reversal

▷ general analysis of possible SC states ↝ <u>group theory</u>

* Sigrist & Ueda, Rev. Mod. Phys. 63, 239 (1991)

▷ <u>ansatz</u>: effective Hamiltonian with attractive interaction between pairs of electrons

$$H = \sum_{\vec{k}\sigma} \underbrace{\varepsilon(\vec{k})}_{\text{band energy}} c^{\dagger}_{\vec{k}\sigma} c_{\vec{k}\sigma} + \frac{1}{4} \sum_{\vec{k}\vec{k}'} \sum_{\sigma_1 \ldots \sigma_4} \underbrace{V_{\sigma_1\sigma_2\sigma_3\sigma_4}(\vec{k},\vec{k}')}_{\text{effective attractive } e^- \text{-} e^- \text{ i.a.}} \underbrace{c^{\dagger}_{-\vec{k}\sigma_1} c^{\dagger}_{\vec{k}\sigma_2} c_{\vec{k}'\sigma_3} c_{-\vec{k}'\sigma_4}}_{\text{zero total momentum}} \qquad (5\text{-}6A)$$

↳ mean-field approach ↝ define superconducting order parameter ("gap function")

$$\Delta_{\sigma\sigma'}(\vec{k}) = -\frac{1}{2} \sum_{\vec{k}'\sigma_3\sigma_4} V_{\sigma'\sigma\sigma_3\sigma_4}(\vec{k},\vec{k}') \langle c_{\vec{k}'\sigma_3} c_{-\vec{k}'\sigma_4} \rangle \qquad (5\text{-}6B)$$

↳ use to decouple ↝ general quadratic BCS Hamiltonian H_{BCS}

↝ self-consistent gap eq. ↝ close to T_c ↝ gap function $\Delta(\vec{k})$ is small ↝ linearize

$$V_c \Delta_{\sigma_1\sigma_2}(\vec{k}) = -\frac{1}{2} \sum_{\sigma_3\sigma_4} \langle V_{\sigma_2\sigma_1,\sigma_3\sigma_4}(\vec{k},\vec{k}') \Delta_{\sigma_3\sigma_4}(\vec{k}') \rangle_{\vec{k}'} \qquad (5\text{-}7A)$$

- prefactor $V_c = [\ln(1.14\varepsilon_c / k_B T_c)]^{-1}$ with cutoff energy ε_c (5-7B)

- (6-2C) is eigenvalue eq. ↝ largest eigenvalue V_c determines T_c and symmetry of $\Delta(\vec{k})$!

- quasiparticle energy (w/ unitary pairing): $E(\vec{k}) = \sqrt{\varepsilon(\vec{k})^2 + |\Delta(\vec{k})|^2}$ (5-7C)

▷ momentum dependence of gap function $\Delta(k)$ in BZ

↳ analyze w.r.t. set of basis functions ⇝ <u>classification</u>:

- irreducible representations (irreps) of symmetry group of normal-state Hamiltonian

▷ for 2D honeycomb lattice (graphene) ⇝ crystal symmetry group C_{6v} ⇝ irreps.

irrep	simple basis functions	BZ symmetry
A_{1g}	$1,\ k_x^2+k_y^2$	
A_{2g}	$k_x k_y(k_x^2-3k_y^2)(k_y^2-3k_x^2)$	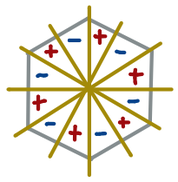
E_{2g}	$(k_x^2-k_y^2,\ 2k_x k_y)$	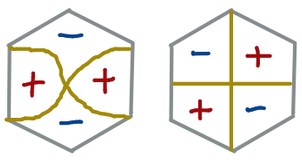

irrep	simple basis functions	BZ symmetry
B_{1u}	$k_x(k_x^2-3k_y^2)$	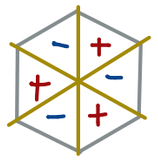
B_{2u}	$k_y(k_y^2-3k_x^2)$	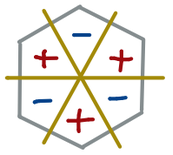
E_{1u}	$(k_x,\ k_y)$	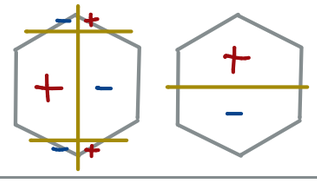

▷ A_{1g} is fully isotropic ⇝ s-wave symmetry (following notation from atomic orbitals)

↳ does not break additional symmetries ⇝ <u>conventional SC</u>

▷ quasiparticle energy $E(\vec{k})$ (5-7C) energetically favors $\Delta(\vec{k})$ with as few nodes as possible

↳ preference towards fully gapped spectrum (no nodes!)

↳ full gap for (k-space) isotropic A_{1g} state

↝ but: A_{1g} energetically disfavored by strong onsite Coulomb repulsion

↝ Coulomb repulsion also favors spin-singlet pairing (excludes E_{1u})

↝ next-lowest no. of nodes: E_{2g}

▷ <u>irrep E_{2g} is 2D</u>:

↳ linearized gap eq. (5-7A) gives same T_c for any basis function belonging to E_{2g}

↳ gap function can be (complex-valued) superposition of basis fcts. in E_{2g}

- <u>example</u>: $(k_x \pm i k_y)^2 = k_x^2 - k_y^2 \pm 2i k_x k_y$ ("$d_{x^2-y^2} \pm i d_{xy}$" / "chiral d-wave" state)

↝ this superposition has full gap (no nodes on FS) ↝ <u>minimizes free energy</u>!

↝ breaks time-reversal K: $K\Delta(\vec{k}) = \Delta^*(-\vec{k}) \neq e^{i\theta}\Delta(\vec{k})$ for fixed θ

▷ materials with 2D hexagonal symmetry and strong Coulomb repulsion

↳ previous symmetry + energetic arguments suggest: <u>chiral d-wave SC state</u>

↳ <u>problem</u>: starting assumption needed <u>effective attractive i.a.</u>

• but: Coulomb i.a. is repulsive and can be strong (↝ jams e^--ph interaction)

▷ <u>question</u>: where could <u>pairing glue</u> for (5-7A) come from?

↳ spin-/charge fluctuation mechanisms

↝ not easily included in meanfield approach

↝ naturally included in <u>(functional) renormalization group framework</u>

... lecture notes to be continued... (or check my notes on "Interacting Fermi Systems")

↝ application of RG to MATBG, e.g. * Isobe, Yuan, Fu, PRX 8, 041041 (2018)

↝ phonons may be relevant, e.g. * Wu, MacDonald, Martin, PRL, 257001 (2018)

Appendix

▷ Mathematica code to numerically calculate TBG's band structure

Parameters

```
θ = 1.05 °; (* twist angle in degrees *)
a = 0.246; v = 2.1354 a; (* lattice constant in nm and Fermi velocity of graphene in eV *)
u = 0.0797; up = 0.0975; (* interlayer couplings in eV *)
cut = 3; (* size of cutoff circle near the original graphene Dirac points *)
```

Geometry

```
a1ast0 = (2 π / a) {1, -1 / Sqrt[3]}; a2ast0 = (2 π / a) {0, 2 / Sqrt[3]}; (* graphene reciprocal lattice vectors before rotation *)
a1ast[l_] := RotationMatrix[(-1)^l θ/2].a1ast0 (* rotated graphene reciprocal lattice vector 1 *)
a2ast[l_] := RotationMatrix[(-1)^l θ/2].a2ast0 (* rotated graphene reciprocal lattice vector 2 *)
Klxi[l_, ξ_] := -ξ (2 a1ast[l] + a2ast[l]) / 3 (* Graphene's Dirac points for layer l=1,2 and valley ξ=+1,-1 *)
GM1 = a1ast[1] - a1ast[2]; GM2 = a2ast[1] - a2ast[2]; (* reciprocal lattice vectors for moire pattern *)
GMlattice = Select[Flatten[Table[m GM1 + n GM2, {n, -5, 5}, {m, -5, 5}], 1], Norm[#] ≤ cut Norm[GM1] &]; (* list of reciprocal lattice vectors within cutoff circle *)
GM[i_] := GMlattice[[i]] (* array of reciprocal lattice vectors within cutoff circle *)
```

Hamiltonian

```
HDirac[l_, ξ_, k_] := - v (RotationMatrix[(-1)^(l+1) θ/2].(k - (Klxi[l, ξ]))).{ξ PauliMatrix[1], PauliMatrix[2]} (* Dirac Hamiltonians of individual rotated layers l=1,2 *)
HDirac12[i_, j_, k_, ξ_] := ( HDirac[1, ξ, k + GM[i]]   0
                              0                         HDirac[2, ξ, k + GM[i]] ) * KroneckerDelta[i, j]; (* Dirac Hamiltonian for both layers with selection rule G[i]=G[j] *)
U12[i_, j_, ξ_, λ_] := ( u          up
                         up         u ) KroneckerDelta[i, j] + ( u                                up * Exp[2 π I / 3.]^(-ξ)
                                                                 up * Exp[2 π I / 3.]^(+ξ)       u ) KroneckerDelta[GM[i] - GM[j], λ ξ GM1] + ( u                                up * Exp[2 π I / 3.]^(+ξ)
                                                                                                                                                up * Exp[2 π I / 3.]^(-ξ)       u ) KroneckerDelta[GM[i] - GM[j], λ ξ (GM1 + GM2)]
U[i_, j_, ξ_] := ( 0                 U12[i, j, ξ, -1]
                   U12[i, j, ξ, +1]  0 ) (* interlayer coupling Hamiltonian *)
H[i_, j_, k_, ξ_] := ArrayFlatten[HDirac12[i, j, k, ξ] + U[i, j, ξ]] (* full Hamiltonian matrix *)
```

Diagonalization in moiré BZ along path K - Γ - M - K'

```
mmax = 20; (* number of wavevectors to plot along K-Γ-M-K' divided by 2.5 *)
k0[ξ_] := (Klxi[1, ξ] + Klxi[2, ξ]) / 2; (* high-symmetry point M in moire BZ of valley ξ *)
kgen[m_, ξ_] := Klxi[2^(1-ξ), ξ] + (GM1 - GM2) / 3 * m / mmax /; m < mmax (* definition of path from K to Γ *)
kgen[m_, ξ_] := k0[ξ] - GM2 / 2 (1 - (m - mmax) / mmax) /; m ≥ mmax && m < (2 mmax) (* definition of path from Γ to M *)
kgen[m_, ξ_] := k0[ξ] + ξ (Klxi[2, ξ] - Klxi[1, ξ]) / 2 (m - (2 mmax)) / (mmax / 2) /; m ≥ (2 mmax) && m ≤ (2.5 mmax) (* definition of path M to K' *)

bandsxipls = ParallelTable[Hmatrix = ArrayFlatten[Table[H[i, j, kgen[m, +1], +1], {i, 1, Length[GMlattice]}, {j, 1, Length[GMlattice]}]];
   locallist = Sort[Re[Eigenvalues[Hmatrix]]];
   locallist, {m, 1, 2.5 mmax}]; (* Diagonalization of full Hamiltonian along path of wavevectors for + valley *)
```

```
ListPlot[Table[bandsxipls[[All, k]] - 0.00155, {k, 1, 4 Length[GMlattice]}], Joined → True, PlotStyle → Darker[Red], PlotRange → {{0, 2.5 mmax}, {-0.7, 0.7}}, AspectRatio → 7 / 5, GridLines → {{mmax, 2 mmax}, {}}, Frame → True,
 FrameTicks → {{{0, "K^M"}, {mmax, "Γ^M"}, {2 mmax, "M^M"}, {2.5 mmax, "K'^M"}}, Automatic}, BaseStyle → {FontFamily → "Times", FontSize → 18}, ImageSize → 300]
```